Exceptional service in the national interest

SAND2018-1903PE

Sandia National Laboratories


https://en.wikipedia.org/wiki/Sandia_Mountains

Digital Image Correlation at Sandia National Laboratories:

Emphasizing material characterization and finite-element model validation

Elizabeth M. C. Jones, Ph.D.

Diagnostic Science and Engineering

U.S. DEPARTMENT OF ENERGY

NNSA National Nuclear Security Administration

Sandia National Labs and Engineering Science

- SNL is a federally-funded research and development center:
  - Nuclear Weapons
  - Defense Systems and Assessments
  - Energy and Climate
  - Global Security

- Engineering Science, Center 1500
  - Revolutionizing the fundamental understanding of complex engineered systems
    - solid mechanics
    - fluid mechanics
    - structural dynamics
    - thermal and combustion sciences
    - aerodynamics
    - shock physics and energetics
    - electromagnetic sciences

  - https://www.youtube.com/watch?v=o1qAjLSEv0A

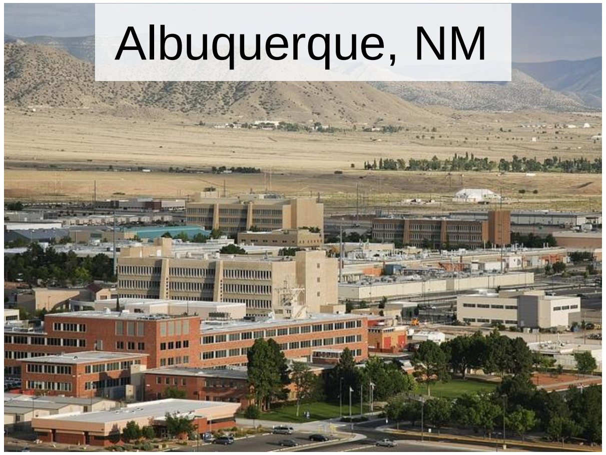

Outline

- Digital Image Correlation
  - Fundamentals
  - International DIC Society (iDICs)
  - Applications at Sandia
- Material Characterization
  - Background
  - Viscoplastic Material Model
  - Traditional Calibration Technique
  - Advanced, Full-Field Calibration Technique
- Finite-Element Model Validation
  - Global Data
  - Full-Field Data
  - Boundary Conditions
- Conclusions and Future Work

Outline

- Digital Image Correlation
  - Fundamentals
  - International DIC Society (iDICs)
  - Applications at Sandia
- Material Characterization
  - Background
  - Viscoplastic Material Model
  - Traditional Calibration Technique
  - Advanced, Full-Field Calibration Technique
- Finite-Element Model Validation
  - Global Data
  - Full-Field Data
  - Boundary Conditions
- Conclusions and Future Work

Digital Image Correlation (DIC)

- Diagnostic technique providing full-field shape, displacement and strain measurements on the surface of a solid specimen
- Optical (non-contact)
- Length scale independent
- “Keep the dots in the box”* (Prof. Samantha Daly)

Digital Image Correlation (DIC)

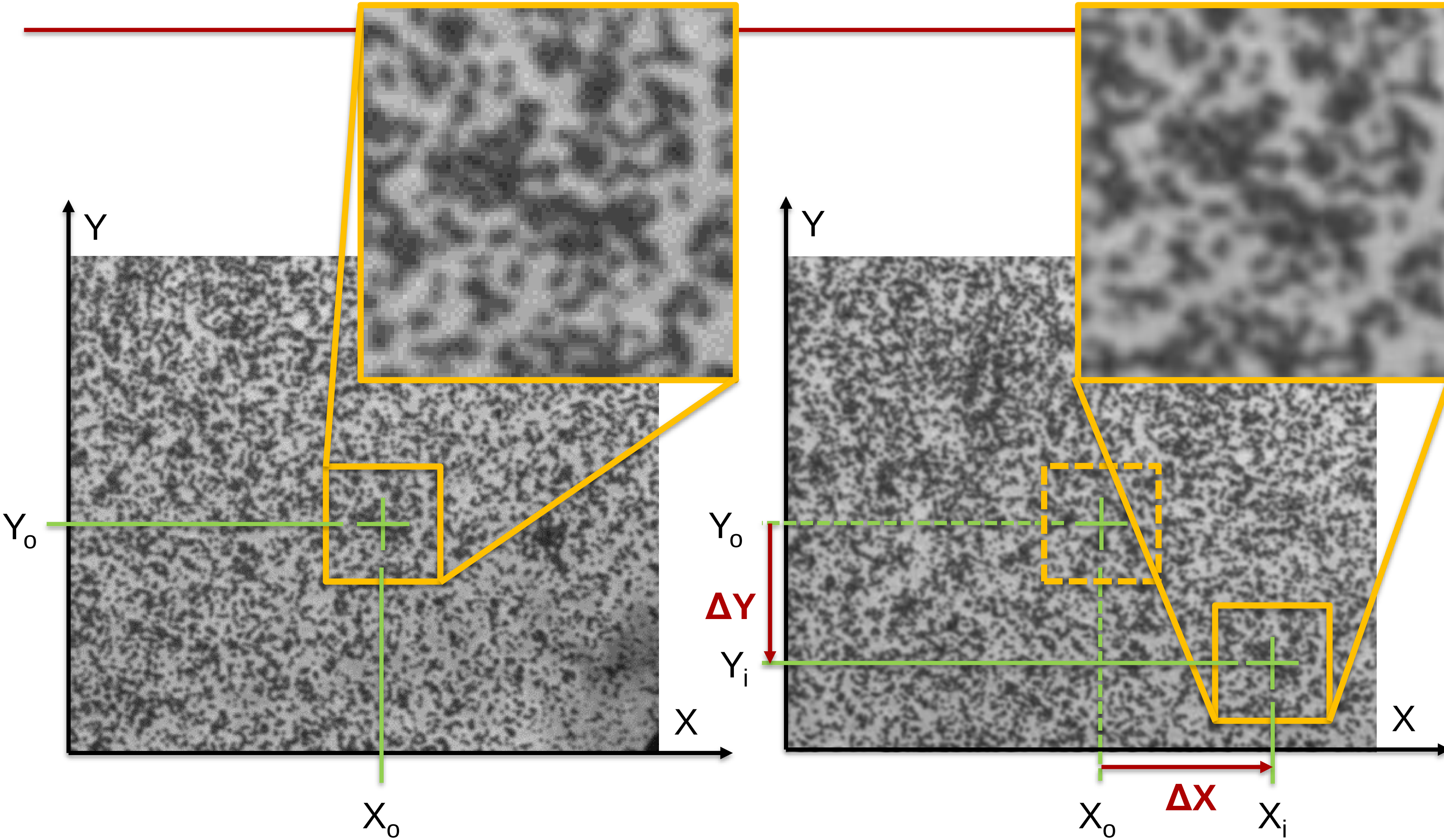

Reference (undeformed) image **Deformed image**

Stereo DIC provides locations and displacements in three dimensions.

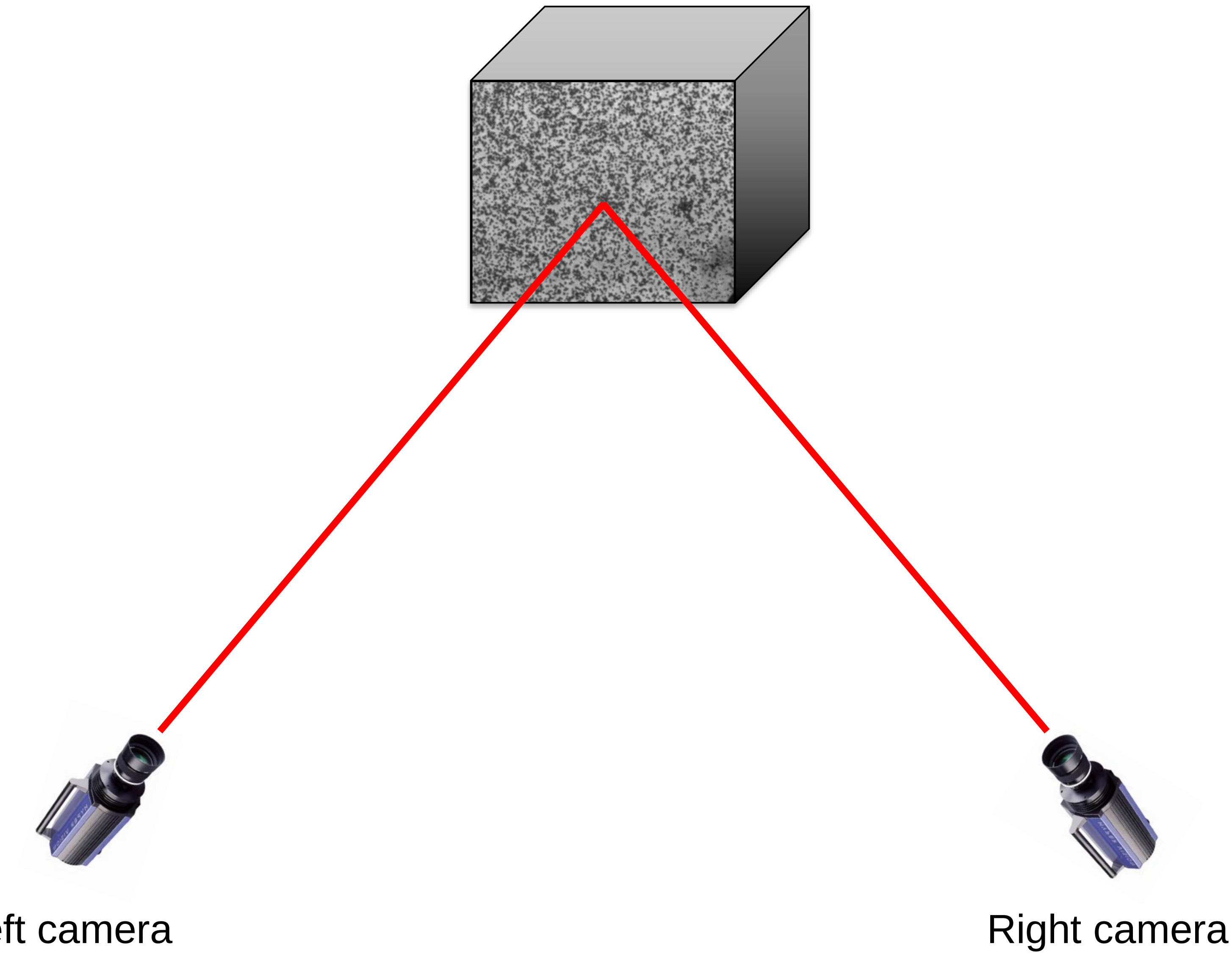

Stereo DIC provides locations and displacements in three dimensions.

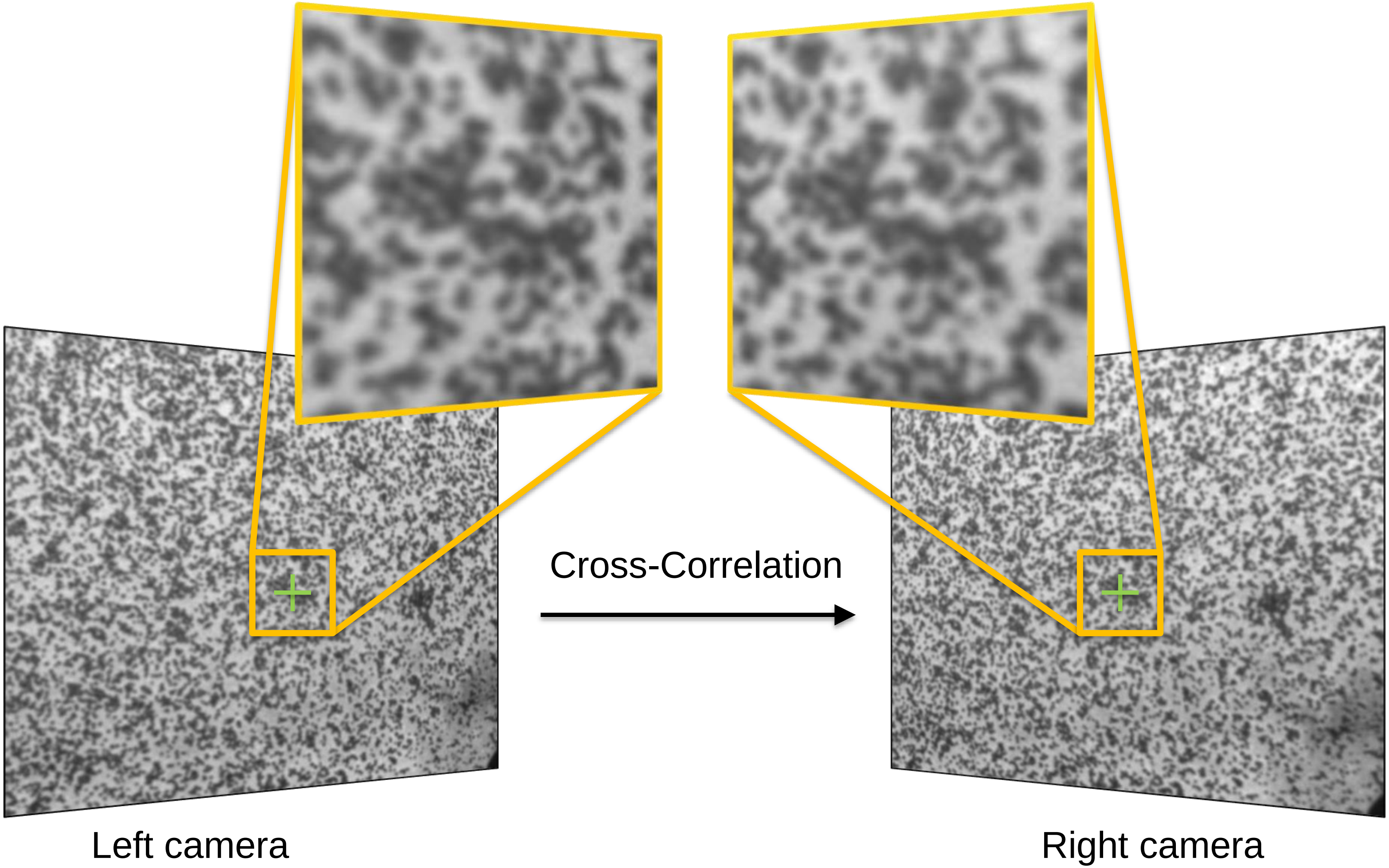

Stereo DIC provides locations and displacements in three dimensions.

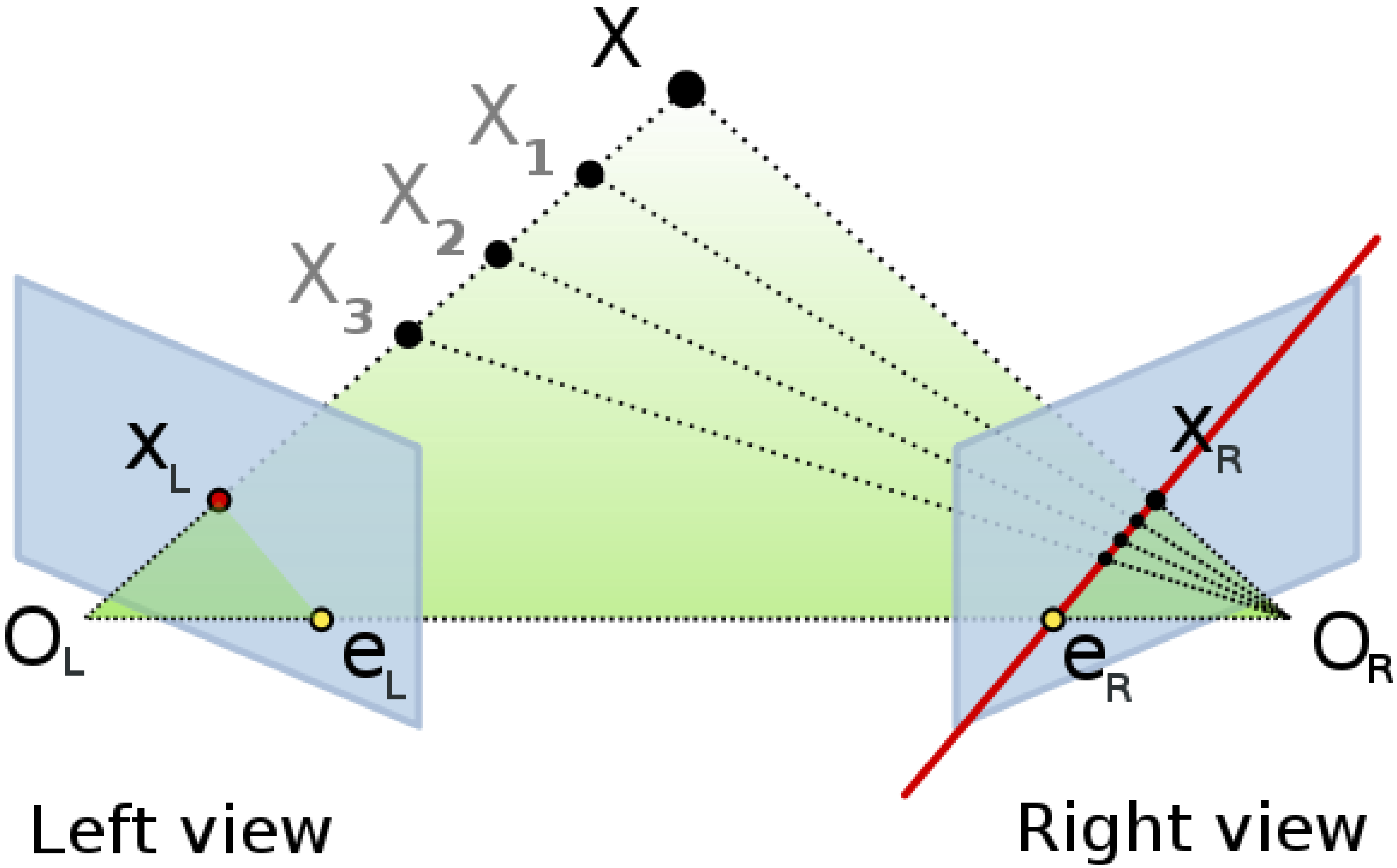

https://en.wikipedia.org/wiki/Epipolar_geometry

International Digital Image Correlation Society

- Founded in 2015
- Composed of members of academia, government, and industry
- Developing world-recognized DIC training, certification, and standardization
- www.idics.org

Digital Image Correlation at Sandia

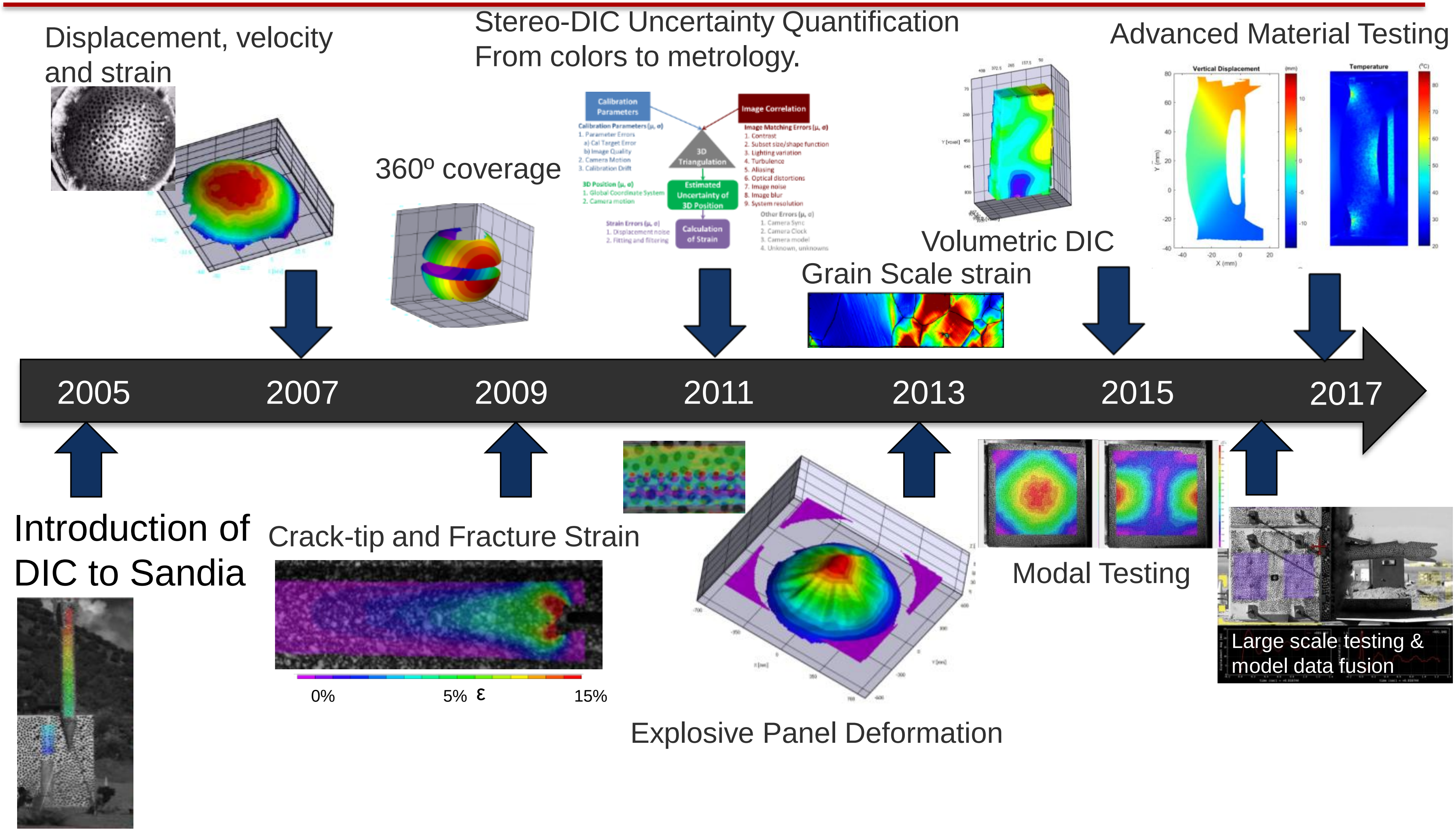

Credit: Phillip Reu

Outline

- Digital Image Correlation
  - Fundamentals
  - International DIC Society (iDICs)
  - Applications at Sandia
- Material Characterization
  - Background
  - Viscoplastic Material Model
  - Traditional Calibration Technique
  - Advanced, Full-Field Calibration Technique
- Finite-Element Model Validation
  - Global Data
  - Full-Field Data
  - Boundary Conditions
- Conclusions and Future Work

Special thanks goes to…

Phillip L. Reu, Ph.D.

Sharlotte L. B. Kramer, Ph.D.

Danial Z. Turner, Ph.D.

Daniel T. Seidl, Ph.D.

Richard B. Lehoucq, Ph.D.

Kyle N. Karlson, Ph.D.

Jay Carroll, Ph.D.

William M. Scherzinger, Ph.D.

Paul A. Farias

Darren L. Pendley

Modeling material and component behavior is critical for modern engineering.

Sandia National Laboratories

- Material model:

$$\sigma = \mathrm{f}(\underbrace{\zeta(\varepsilon, p, \dot{p}, T)}_{\text{loading conditions}}, \underbrace{\xi(E, \upsilon, \sigma_o, H)}_{\text{model parameters}})$$

- Model parameters ≠ material properties

- Finding model parameters:
  - Model calibration
  - Material identification
  - Material characterization

Material models are traditionally calibrated from global, homogeneous data.

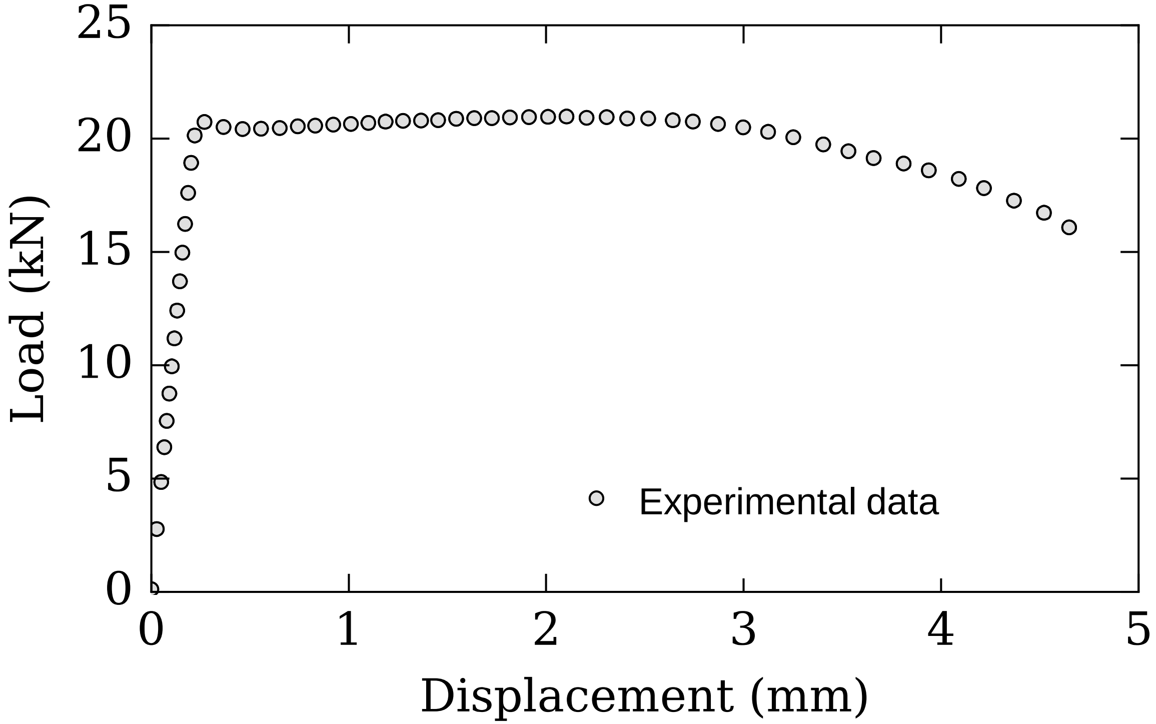

Material models are traditionally calibrated from global, homogeneous data.

Low strain regime:

- Uniaxial tension
- Identification of model parameters accomplished analytically

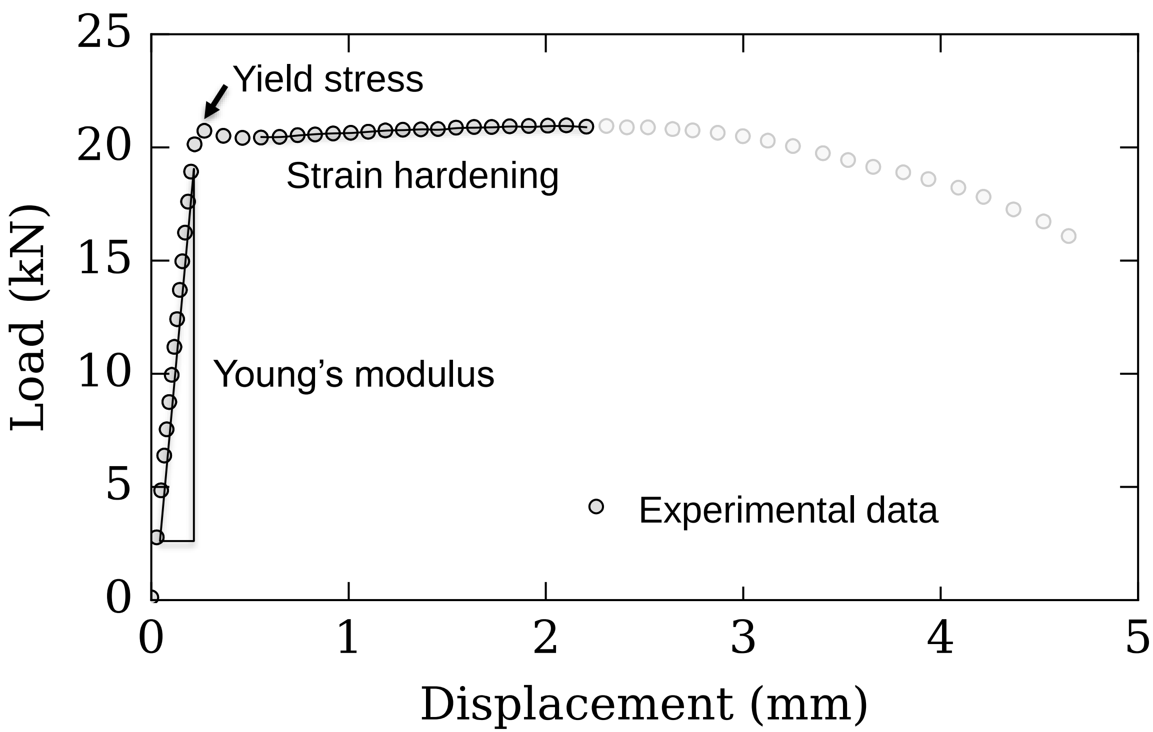

Material models are traditionally calibrated from global, homogeneous data.

High strain regime:

- Multiaxial stress state
- Identification of model parameters requires inverse problem

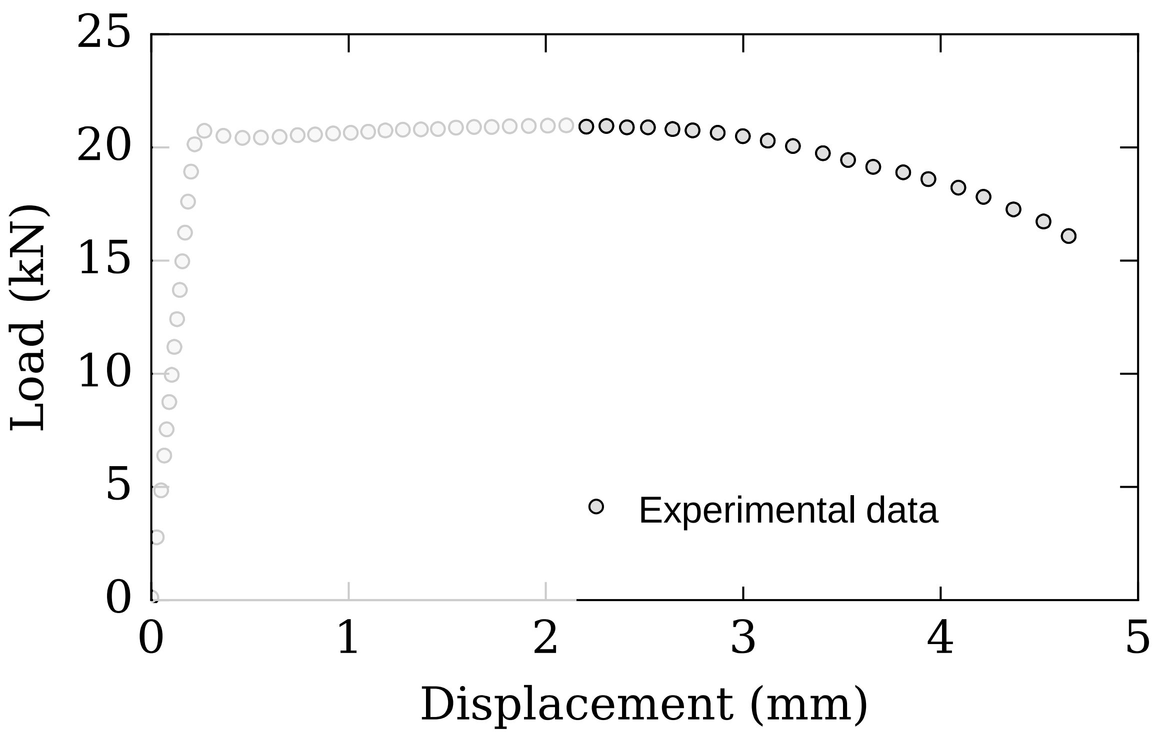

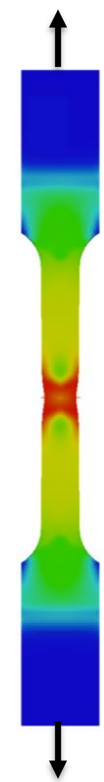

High strain regime:

- Multiaxial stress state
- Identification of model parameters requires inverse problem

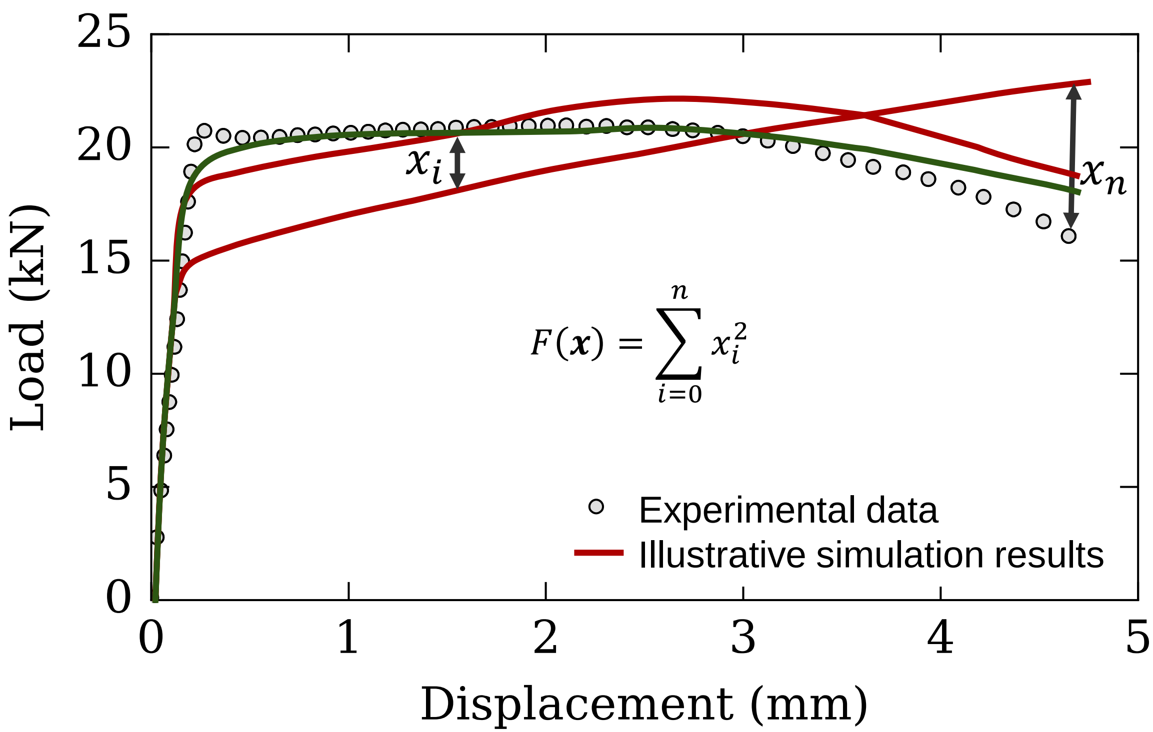

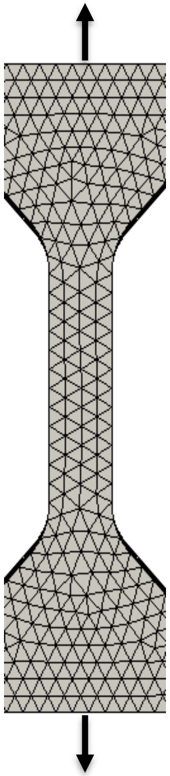

Traditional material identification has limitations.

- Global information misses local deformation
- Many tests required to calibrate complex models
- Simple stress state does not reflect complex, real-world loading conditions

≠

http://money.cnn.com/2014/01/22/autos/small-car-crash-test/
Accessed 29 Aug 2016

High-throughput, high-quality material identification addresses limitations of traditional material ID.

Contour Plot of σ_{22}

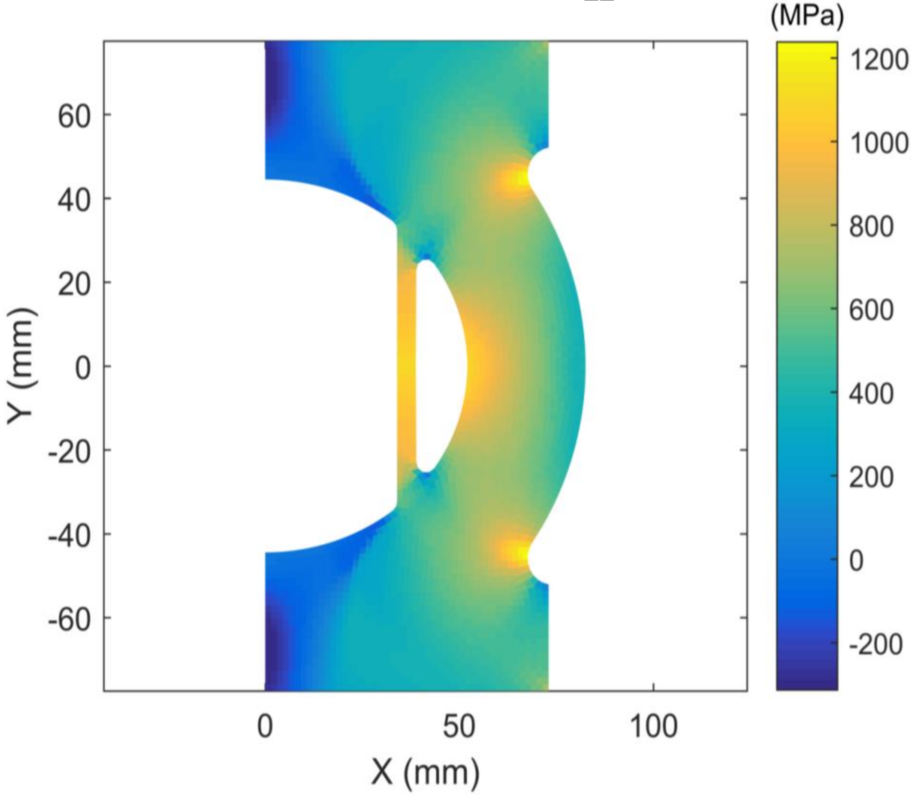

Capitalize on:

- Full-field deformation measurements: Digital Image Correlation (DIC)
- Inverse techniques: Virtual Fields Method (VFM)

Outline

- Digital Image Correlation
  - Fundamentals
  - International DIC Society (iDICs)
  - Applications at Sandia
- Material Characterization
  - Background
  - Viscoplastic Material Model
  - Traditional Calibration Technique
  - Advanced, Full-Field Calibration Technique
- Finite-Element Model Validation
  - Global Data
  - Full-Field Data
  - Boundary Conditions
- Conclusions and Future Work

Strain-rate dependence is modeled with the Bammann-Chiesa-Johnson (BCJ) material model.

Sandia National Laboratories

$$\sigma_f(p, \dot{p}, \xi) = \cdots$$

$$\sigma_Y \left\{ 1 + \operatorname{asinh}\left[\left(\frac{\dot{p}}{b} \right)^{1/m} \right] \right\} + \cdots$$

← Strain-rate dependence of initial yield stress

$$\frac{H}{R_d}\left[1 - \exp(-R_d p)\right]$$

← Voce-type hardening

σ_f flow stress
p equivalent plastic strain
$\dot{p}$ equivalent plastic strain rate

σ_Y quasi-static yield stress
b rate-dependent coefficient
m rate-dependent exponent

H hardening variable
R_d dynamic recovery

Strain-rate dependence is modeled with the Bammann-Chiesa-Johnson (BCJ) material model.

$$\sigma_f(p, \dot{p}, \xi) = \cdots$$

$$\sigma_Y \left\{ 1 + \operatorname{asinh}\left[\left(\frac{\dot{p}}{b} \right)^{1/m} \right] \right\} + \cdots$$

$$\frac{H}{R_d}\left[1 - \exp(-R_d p)\right]$$

σ_f flow stress
p equivalent plastic strain
$\dot{p}$ equivalent plastic strain rate

σ_Y quasi-static yield stress
b rate-dependent coefficient
m rate-dependent exponent

H hardening variable
R_d dynamic recovery

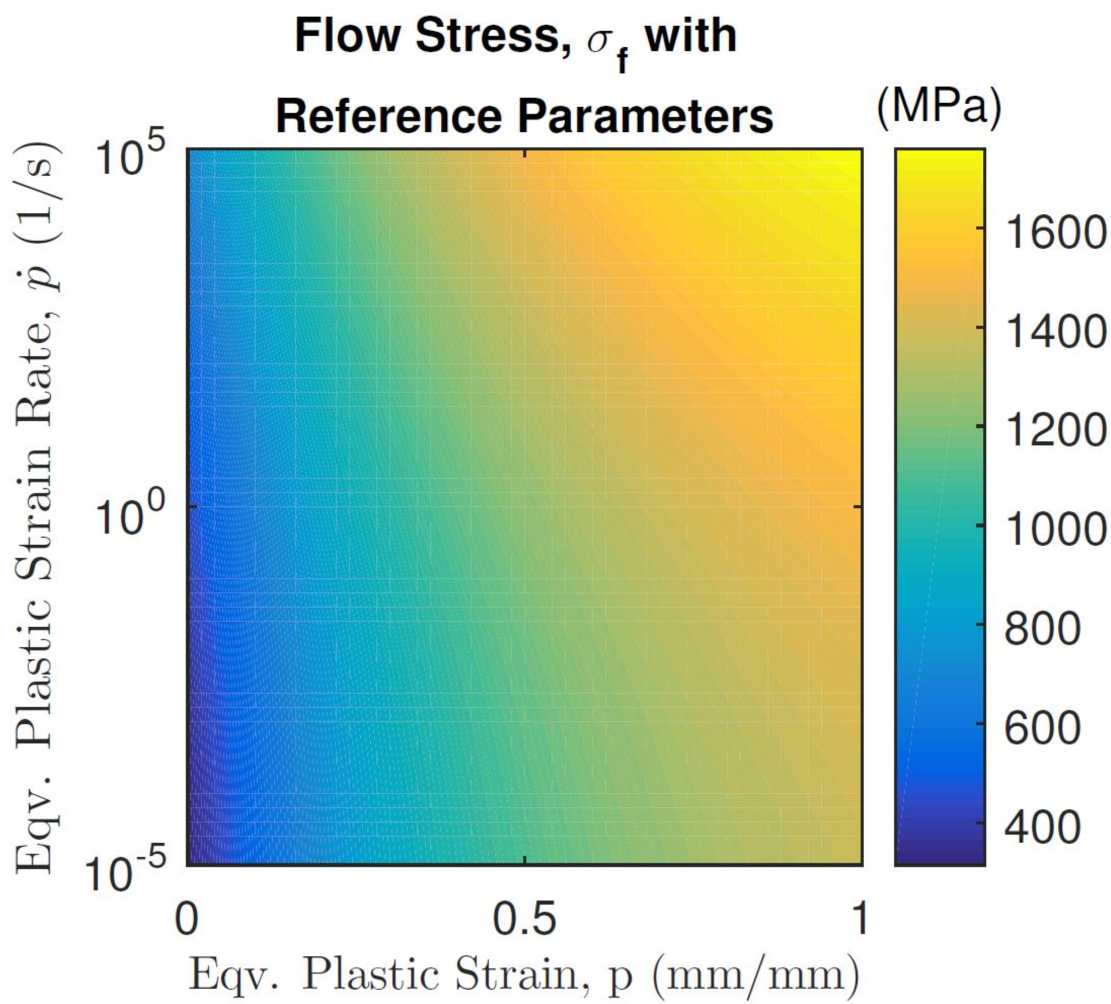

The influence of model parameters is complex and multidimensional.

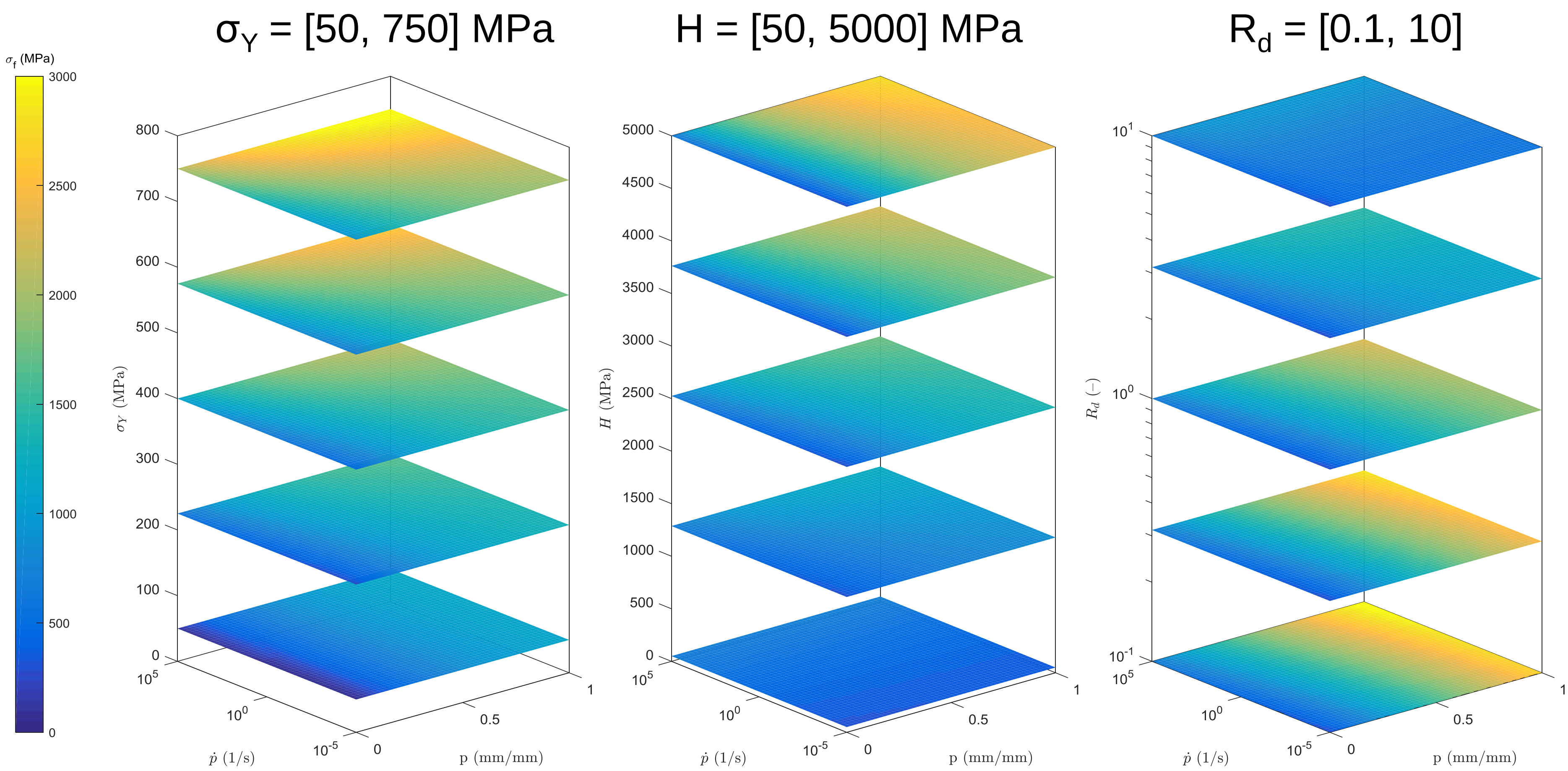

The influence of model parameters is complex and multidimensional.

b = [10^{-5}, 10^{5}]

m = [1, 20]

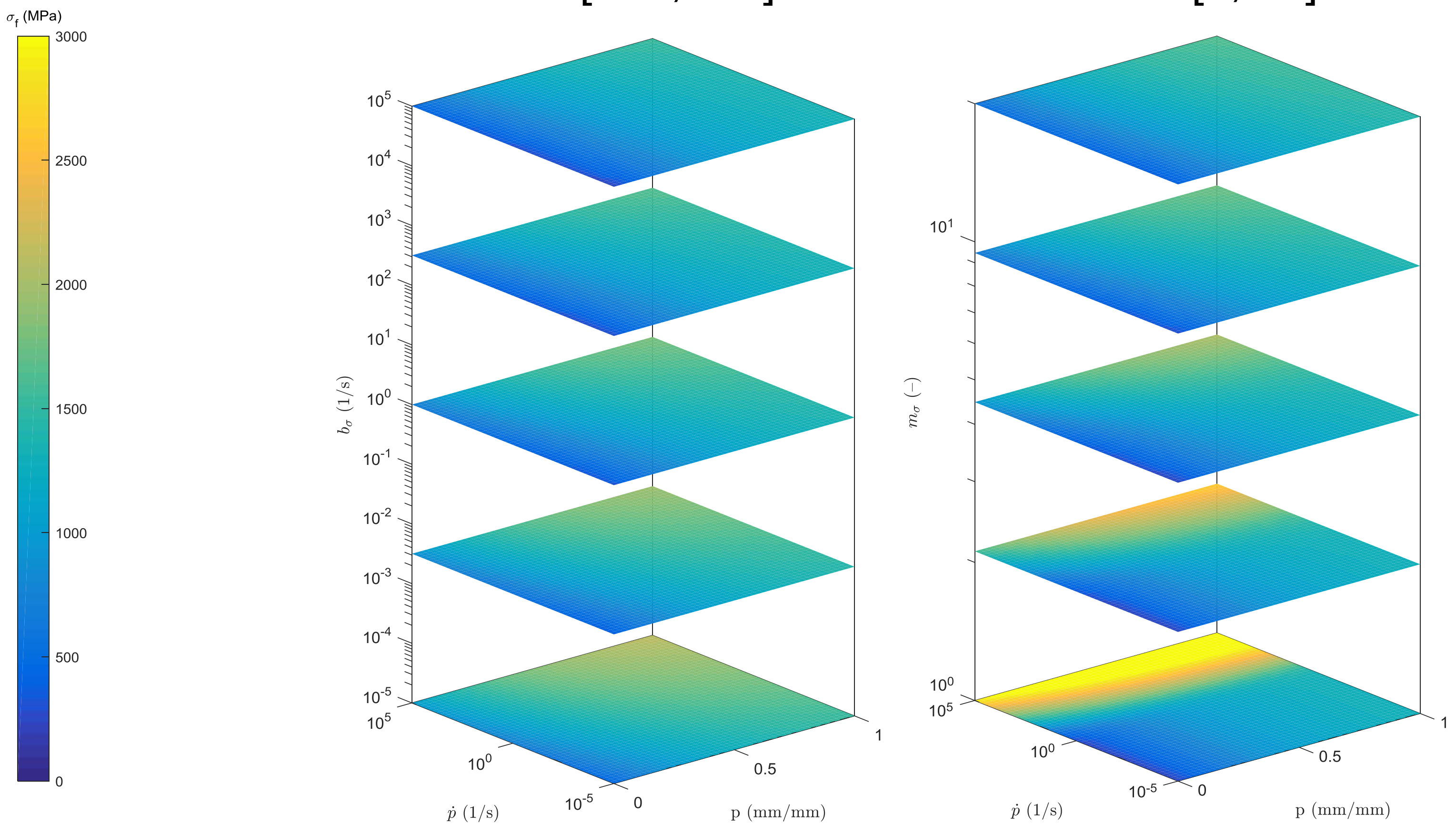

Outline

- Digital Image Correlation
  - Fundamentals
  - International DIC Society (iDICs)
  - Applications at Sandia
- Material Characterization
  - Background
  - Viscoplastic Material Model
  - Traditional Calibration Technique
  - Advanced, Full-Field Calibration Technique
- Finite-Element Model Validation
  - Global Data
  - Full-Field Data
  - Boundary Conditions
- Conclusions and Future Work

Tensile dog bones were tested experimentally.

- Material:
  - 304L stainless steel rolled sheet, 1.5 mm thick
- Dog bone gauge section:
  - 50.8 mm x 12.7 mm
- Three nominal strain rates (s^{-1}):
  - $1.0 \cdot 10^{-4}$
  - $3.2 \cdot 10^{-3}$
  - $1.0 \cdot 10^{-1}$
- Virtual extensometer from DIC
  - 22 mm gauge section

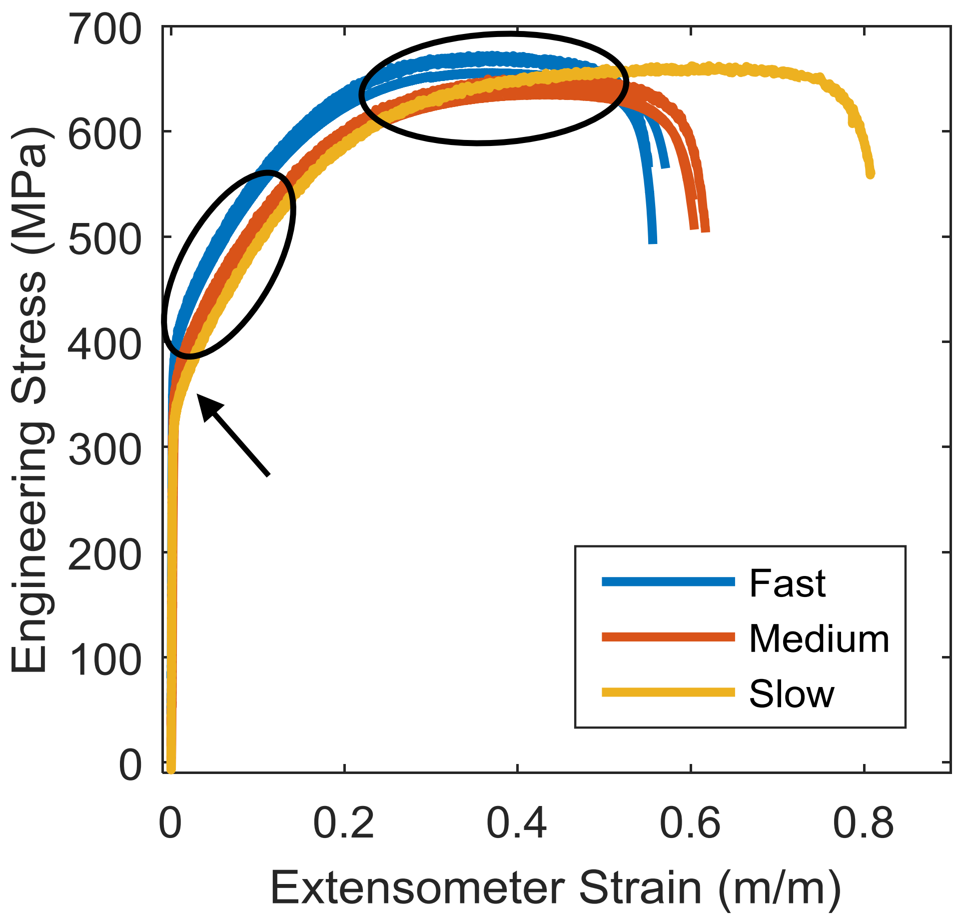

Because of material model complexity, data is fit in successive steps.

Step 1:

- Each tensile test is fit individually to a rate-independent model:
  - $\sigma_f(p, \dot{p}, \xi) = \sigma_Y + \cdots \frac{H}{R_d}[1 - \exp(-R_d p)]$

- Actual strain rate is calculated from DIC extensometer data

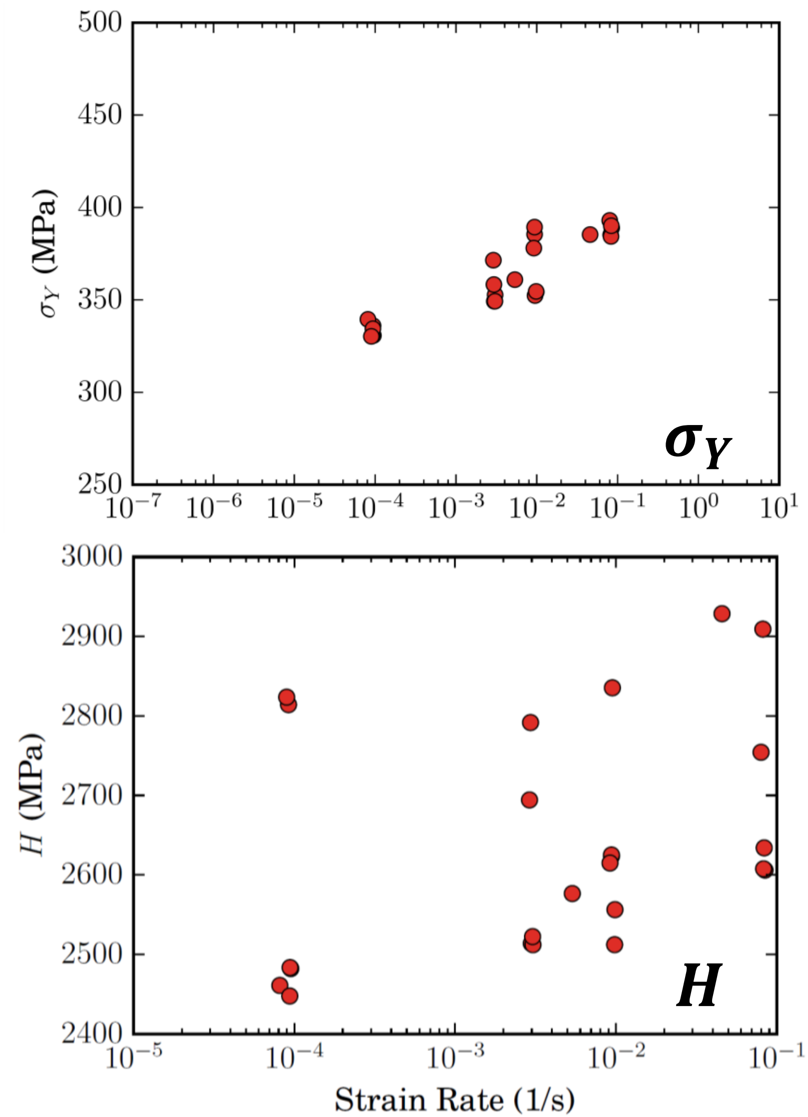

Initial guesses are found for all five parameters.

Step 2:

- σ_Y, b, m:
  - $\sigma_f = \sigma_Y \left\{1 + \operatorname{asinh}\left[\left(\frac{\dot{p}}{b}\right)^{1/m}\right]\right\}$
- H, R_D:
  - No significant rate-dependence
  - Averaged from step 1

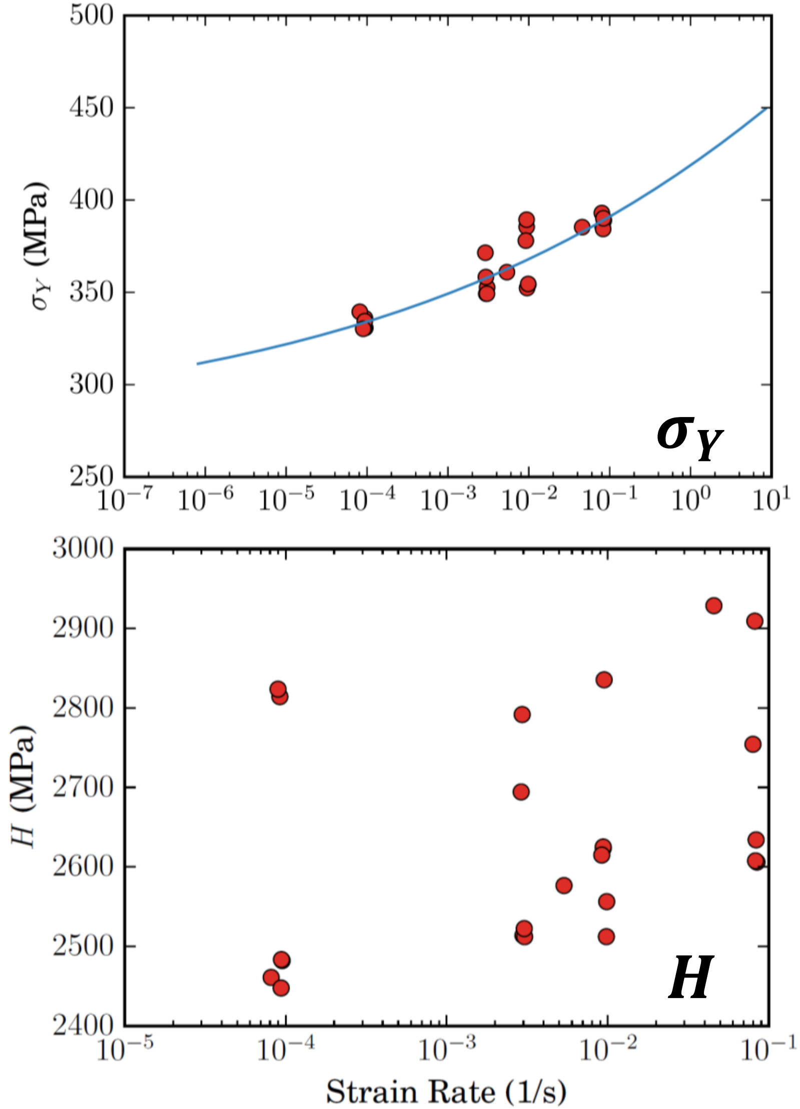

Finite-element method updating (FEMU) is used for final traditional calibration.

Step 3:

- FEA model is created for each tensile specimens
- Cost function is built as the error between experimental and FE uniaxial stress-strain curves

$$\sigma_f(p, \dot{p}, \xi) = \sigma_Y \left\{1 + \operatorname{asinh}\left[\left(\frac{\dot{p}}{b}\right)^{1/m}\right]\right\} + \frac{H}{R_d}[1 - \exp(-R_d p)]$$

Parameter	Symbol	Value	Units
Quasi-static Yield Stress	σ_y	253.8	MPa
Hardening Variable	H	2538	MPa
Dynamic Recovery	R_d	2.110	--
Rate-Dependent Coefficient	b	4.728	s^{-1}
Rate-Dependent Exponent	m	9.229	--

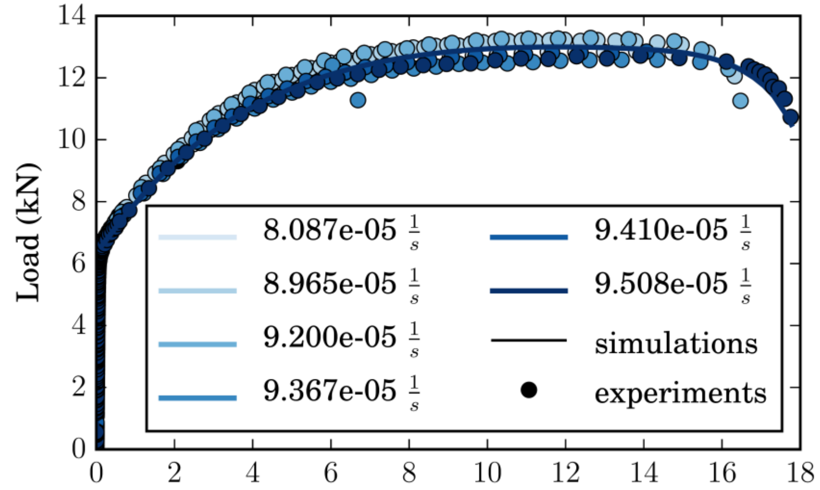

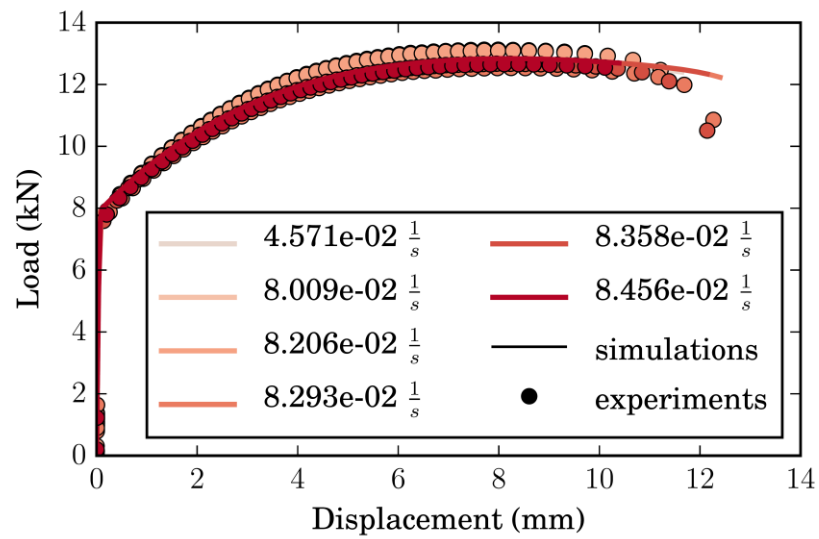

Outline

- Digital Image Correlation
  - Fundamentals
  - International DIC Society (iDICs)
  - Applications at Sandia
- Material Characterization
  - Background
  - Viscoplastic Material Model
  - Traditional Calibration Technique
  - Advanced, Full-Field Calibration Technique
- Finite-Element Model Validation
  - Global Data
  - Full-Field Data
  - Boundary Conditions
- Conclusions and Future Work

Virtual Fields Method is a powerful inverse technique.

Sandia National Laboratories

Principle of Virtual Power

$$\underbrace{\int_{V_o} \left((\det \boldsymbol{F})\boldsymbol{\sigma}\boldsymbol{F}^{-T}\right):\dot{\boldsymbol{F}}^* \, dV}_{\text{Internal Power, } P_{int}} = \underbrace{\boldsymbol{f} \cdot \overline{\boldsymbol{v}^*}}_{\text{External Power, } P_{ext}}$$

σ	Cauchy Stress
F	Deformation Gradient
f	Resultant Load
V_o	Sample Volume (Reference)
v^*	Virtual Velocity
$\dot{F}^*$	Virtual Velocity Gradient

Material Identification Procedure

1. Select material model and specimen geometry
2. Measure specimen deformation during loading
3. Calculate stress with initial guess of model parameters
4. Select one or more kinematically-admissible virtual velocity fields
5. Compute internal and external power
6. Compute cost function: $\Phi = \sum_{\text{time}}[P_{int} - P_{ext}]^2$
7. Iterate on model parameters until cost function is minimized

Pierron and Grédiac (2012) *The Virtual Fields Method*. Springer.
Rossie, Pierron, Štamborská (2016) *Int. J. Solids Struct.*
Kramer and Scherzinger (2014) SAND2014-17871

Virtual Fields Method is a powerful inverse technique.

Principle of Virtual Power

$$\int_{V_0} \left((\det \boldsymbol{F})\boldsymbol{\sigma}\boldsymbol{F}^{-T}\right) : \dot{\boldsymbol{F}}^* \, dV = \boldsymbol{f} \cdot \overline{\boldsymbol{v}^*}$$

- σ Cauchy Stress
- F Deformation Gradient
- f Resultant Load

VFM utilizes **heterogeneous calibration data** and requires **fewer tests** than traditional calibration techniques.

5. Compute cost function
   - $\Psi = \sum_{\text{time}} [P_{int} - P_{ext}]^2$
6. Iterate on model parameters until cost function is minimized

Pierron and Grédiac (2012) *The Virtual Fields Method*. Springer.
Rossie, Pierron, Štamborská (2016) *Int. J. Solids Struct.*
Kramer and Scherzinger (2014) SAND2014-17871

Complex specimen geometry is available when using full-field diagnostics.

Design Criteria

- Objective:
  - Maximize strain/stress heterogeneity
  - Maximize range of strain rates
- Constraints:
  - Minimize large gradients near sample edges
  - Uniaxial loading
  - Planar sample

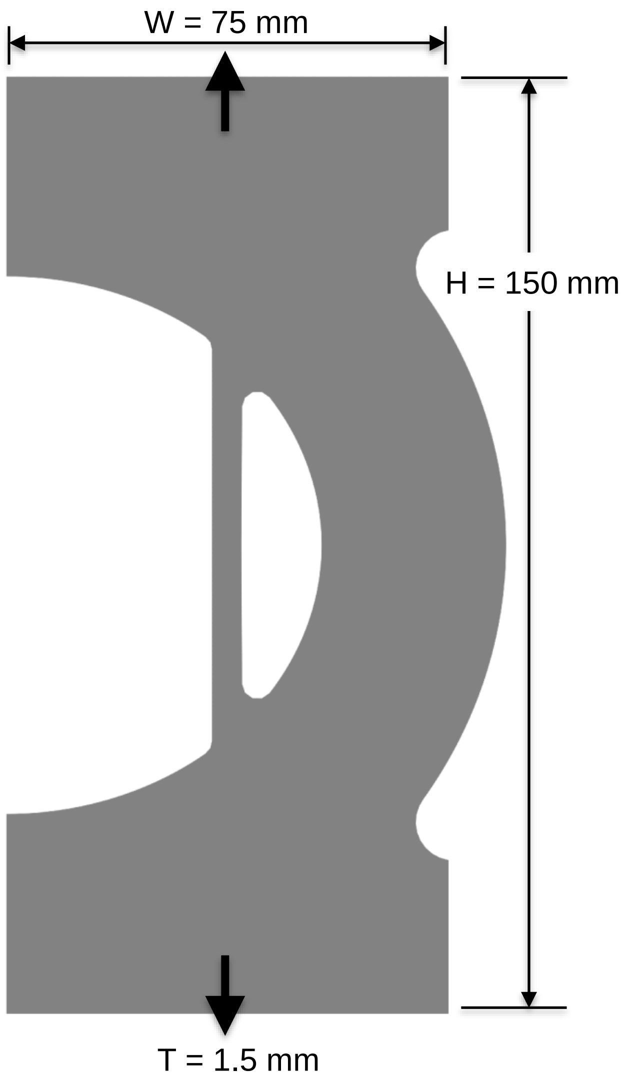

Complex specimen geometry induces stress and strain rate heterogeneity in sample.

Predicted Results from FEM Simulation

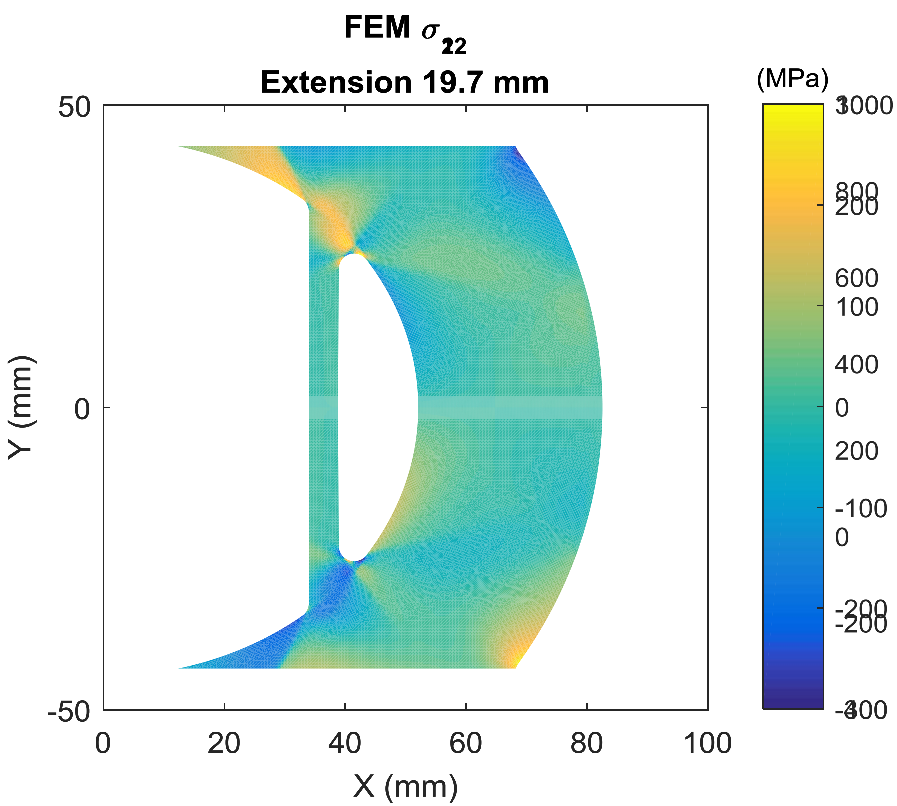

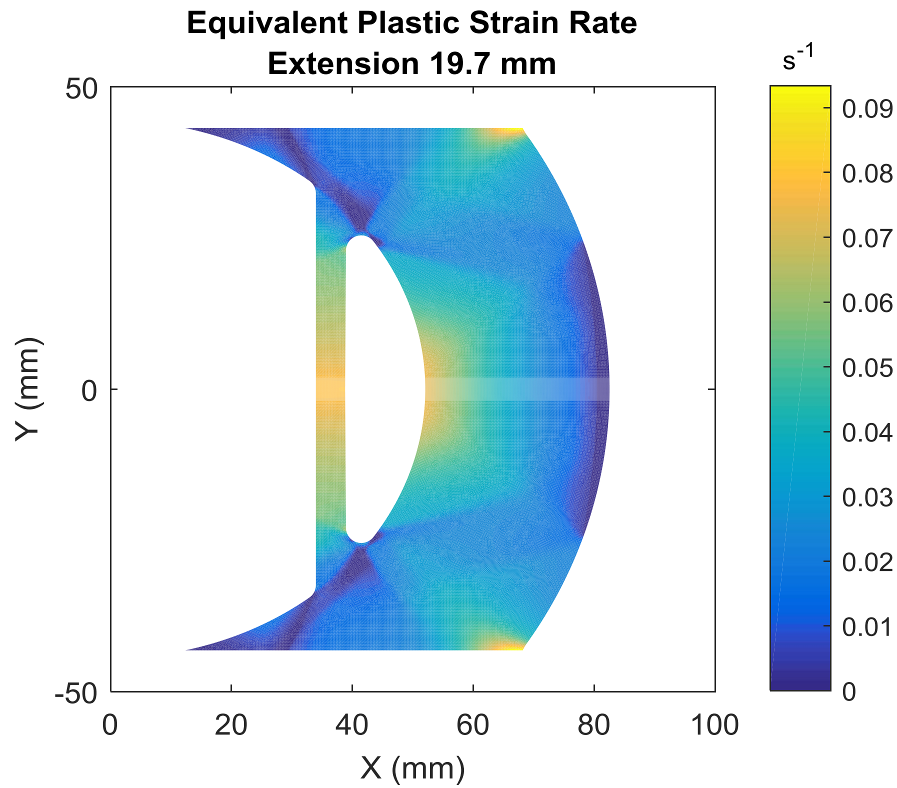

Complex specimen geometry induces stress and strain rate heterogeneity in sample.

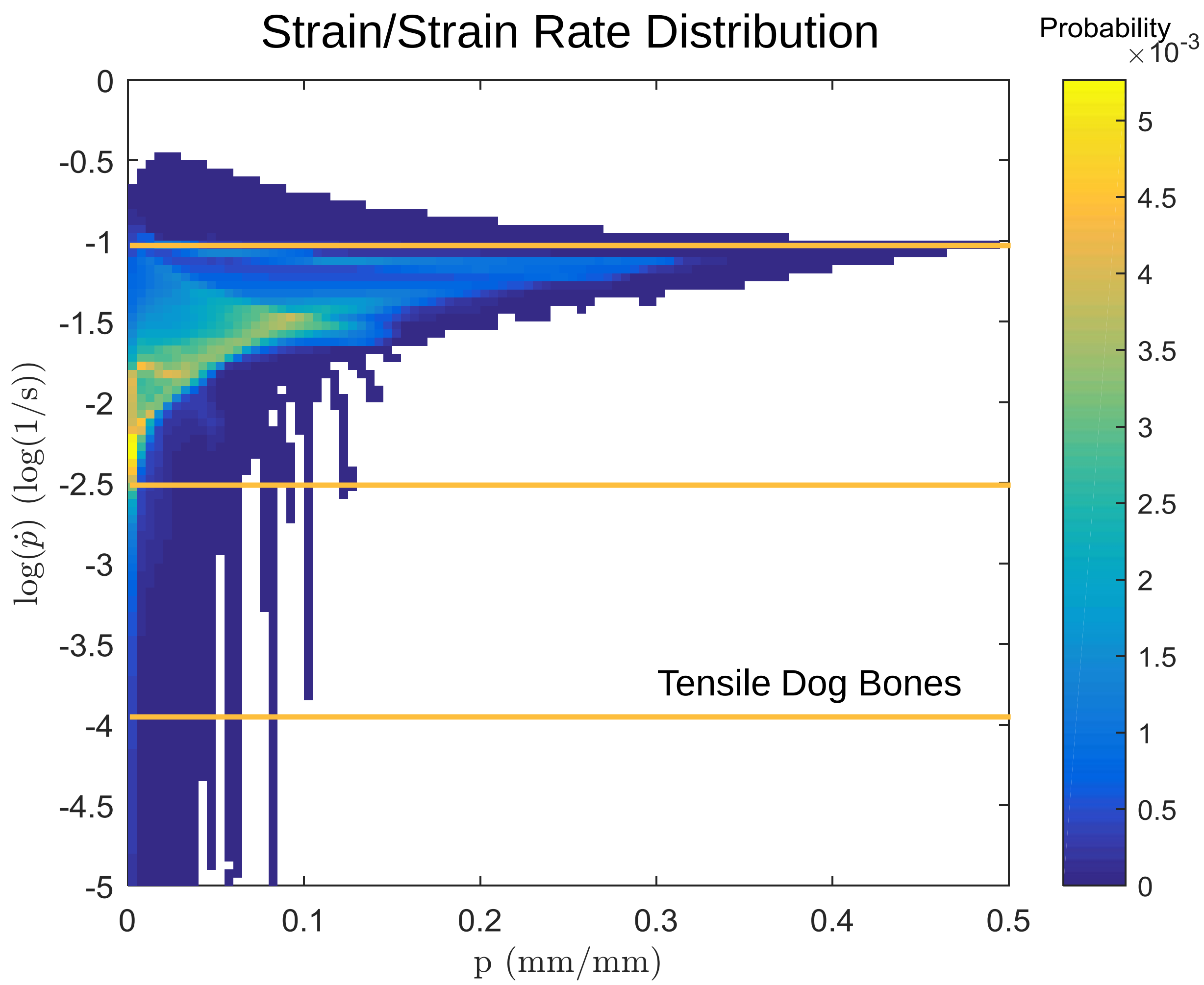

Specimen deformation, temperature and applied load are measured experimentally.

Top View

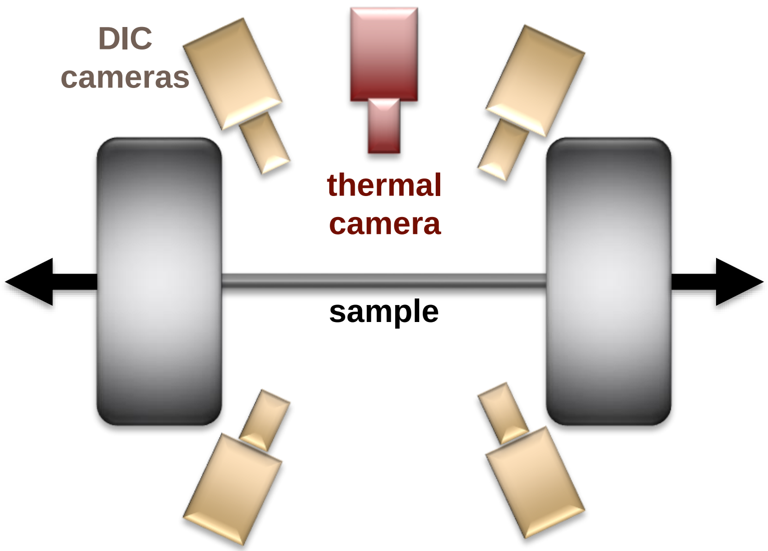

Key Features

- Dual actuator load frame
- Stereo DIC on both sides of specimen
- Rigid camera mounts
- Thermal camera on one side of specimen
- Cross-polarized light

Front View

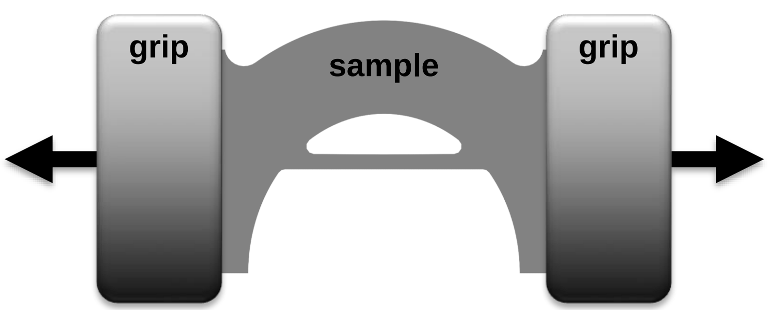

Side View

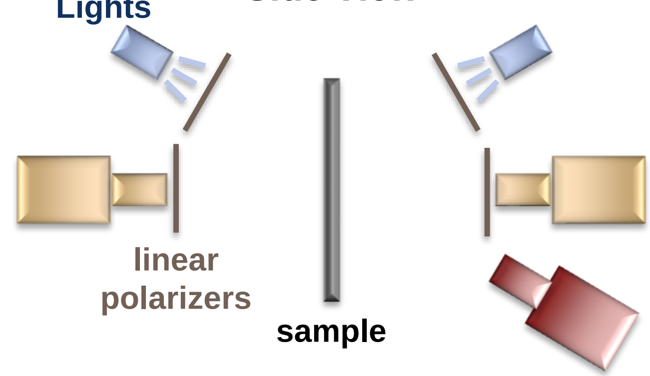

Specimen deformation, temperature and applied load are measured experimentally.

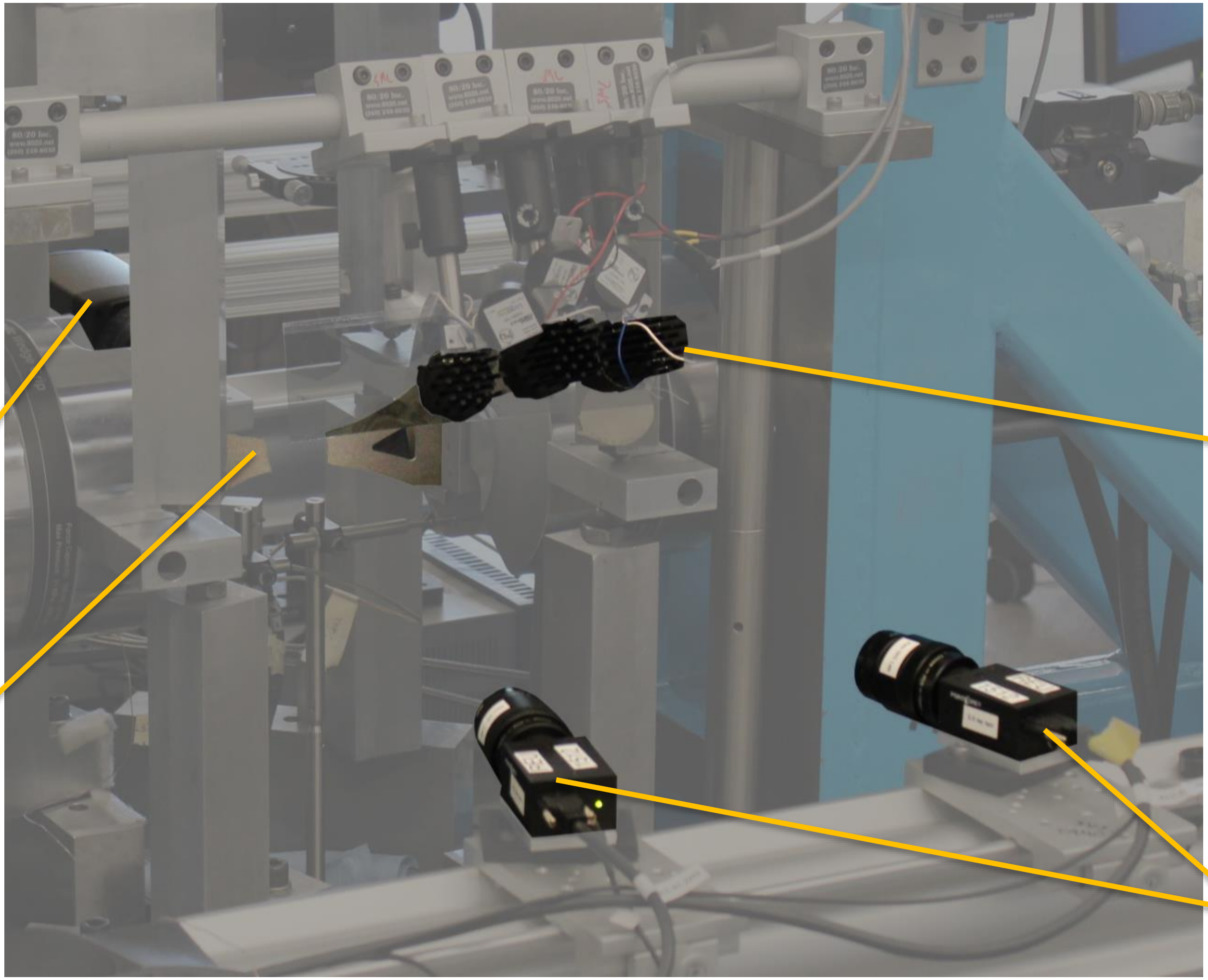

Standard speckling techniques fail at high strain.

Speckle Pattern 1: White base paint with black speckles

Undeformed Specimen

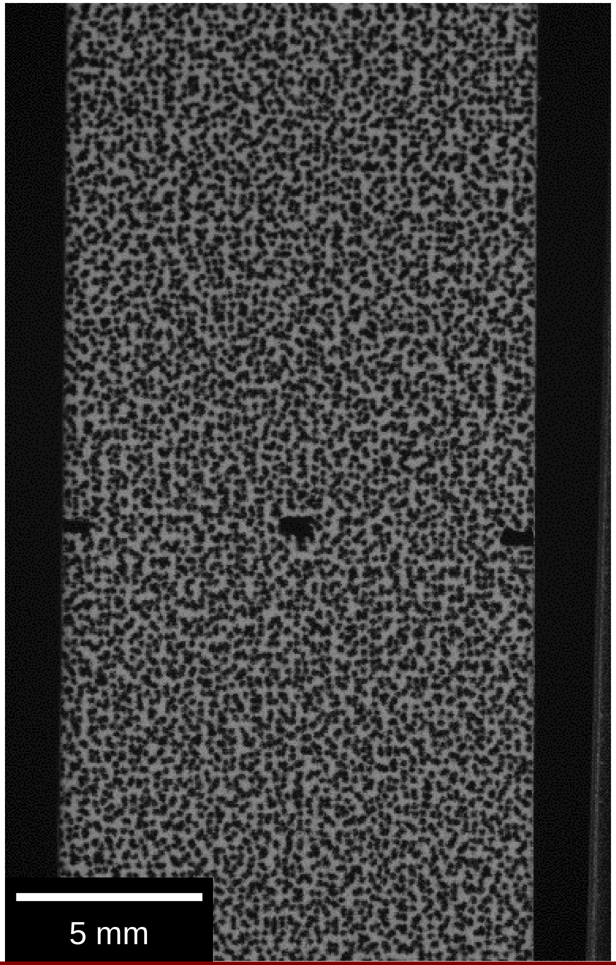

Deformed Specimen

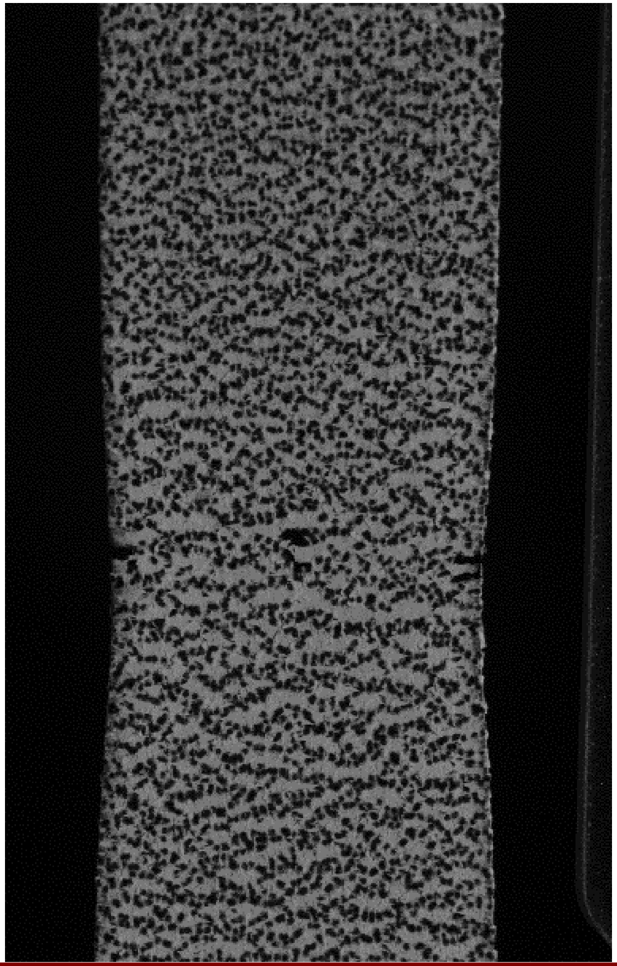

Cross-polarized light creates a robust speckle pattern.

Speckle Pattern 2: White speckles on bare metal

Unpolarized Light

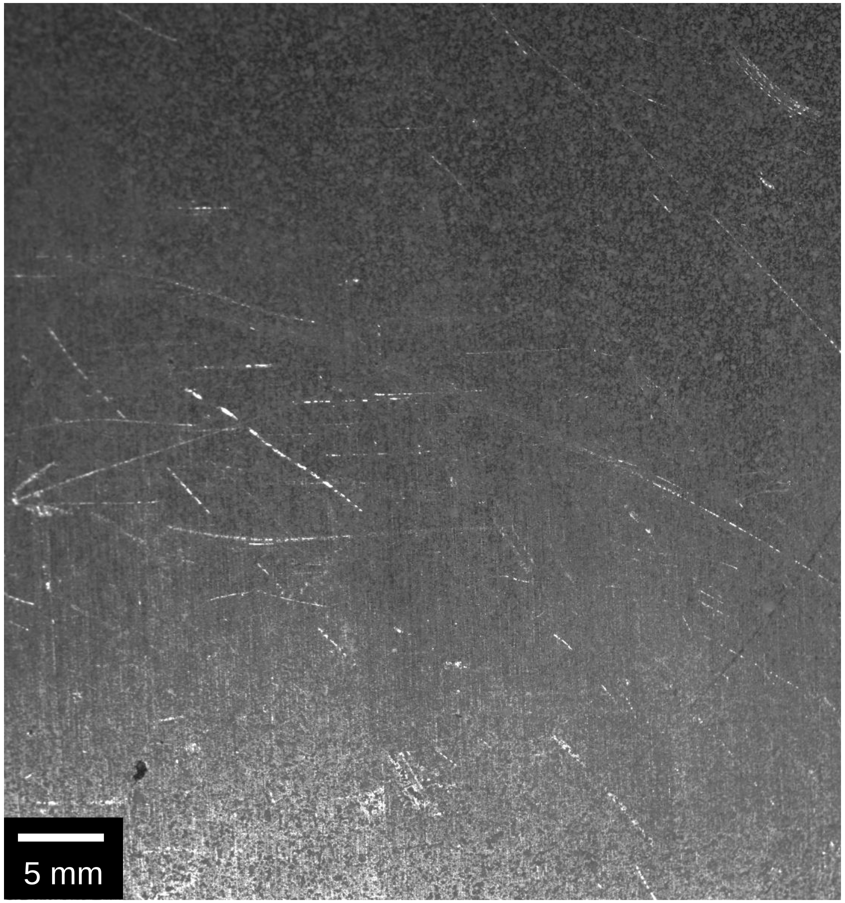

Cross-Polarized Light

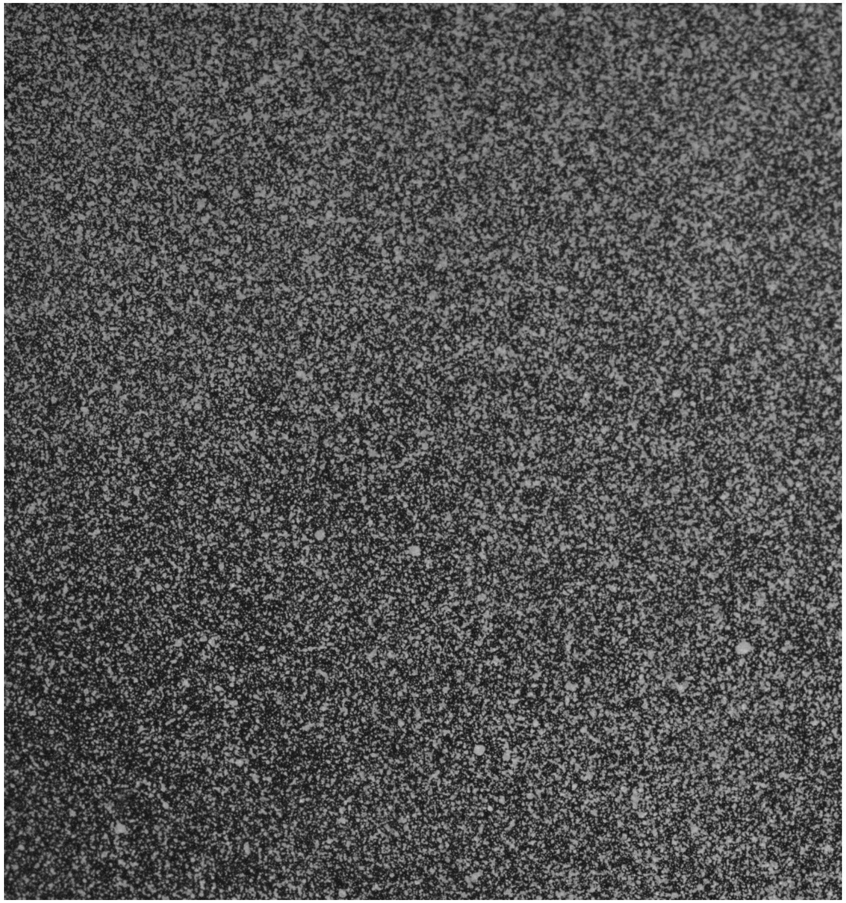

W. LePage, S. Daly, J. Shaw (2016) *Exp. Mech.*

Full-field displacements are measured using DIC.

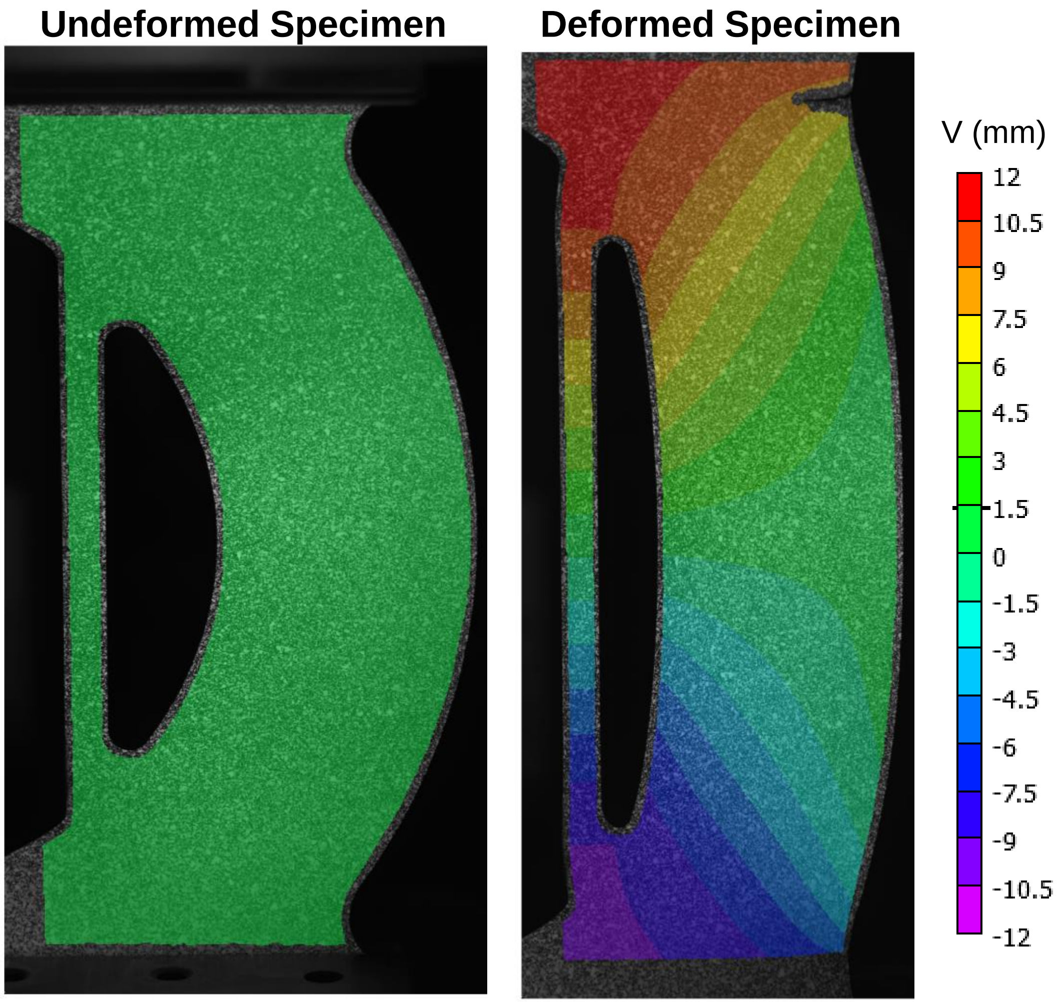

Parameter	Value
Camera	2.3 MP Grasshopper
Lens	35 mm Edmund Optics
Stereo Angle	~ 20^o
Field of View	~ 100 mm
Image Scale	~ 17 px/mm
Frame Rate	85 Hz
Software	Vic3D
Subset Size	23 x 23 px
Step Size	5 px
Subset Shape Function	Affine
Displacement Noise Floor	~ 0.01 mm

Kinematics calculated from a least-squares polynomial fit to displacement data.

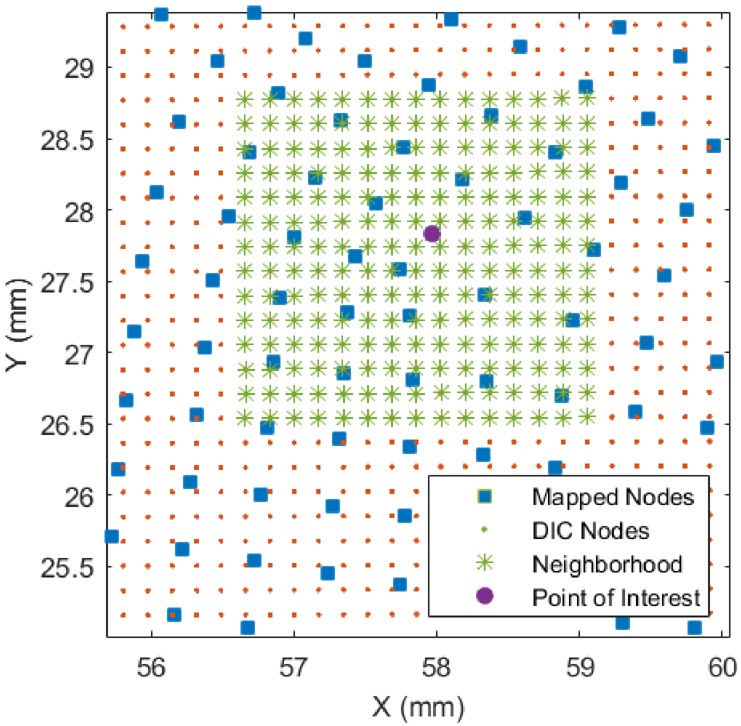

$$u_i = C_1 + C_2x + C_3y + C_4x^2 + C_5y^2 + C_6xy + \\ +C_7x^3 + C_8y^3 + C_9x^2y + C_{10}xy^2$$

$$\frac{\partial u_i}{\partial x} = C_2 + 2C_4x + C_6y + 3C_7x^2 + 2C_9xy + C_{10}y^2$$

$$\frac{\partial u_i}{\partial y} = C_3 + 2C_5y + C_6\,x + 3C_8y^2 + C_9x^2 + 2C_{10}xy$$

- 2D polynomial surface fitted to neighborhood of displacement nodes.
- Deformation gradient obtained directly from coefficients of polynomial fit.

Kinematics calculated from a least-squares polynomial fit to displacement data.

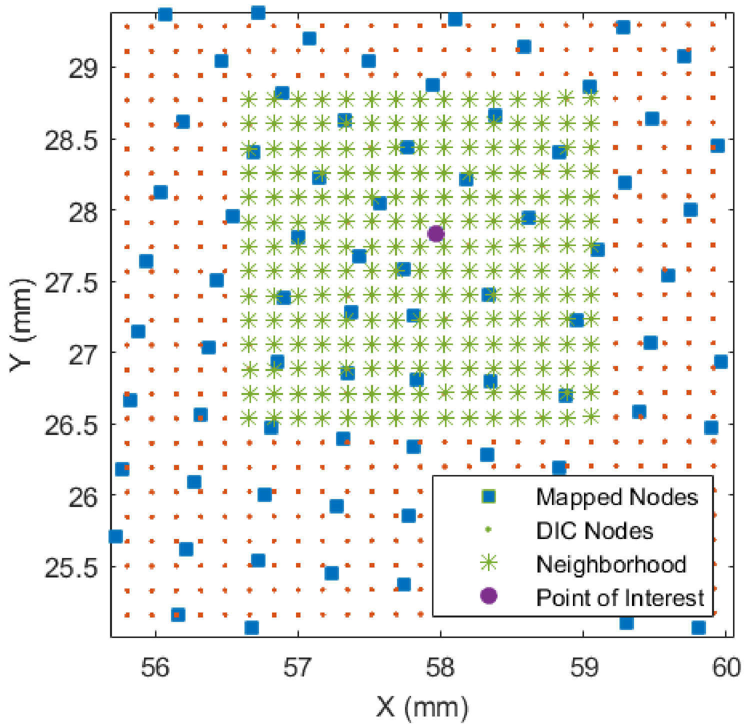

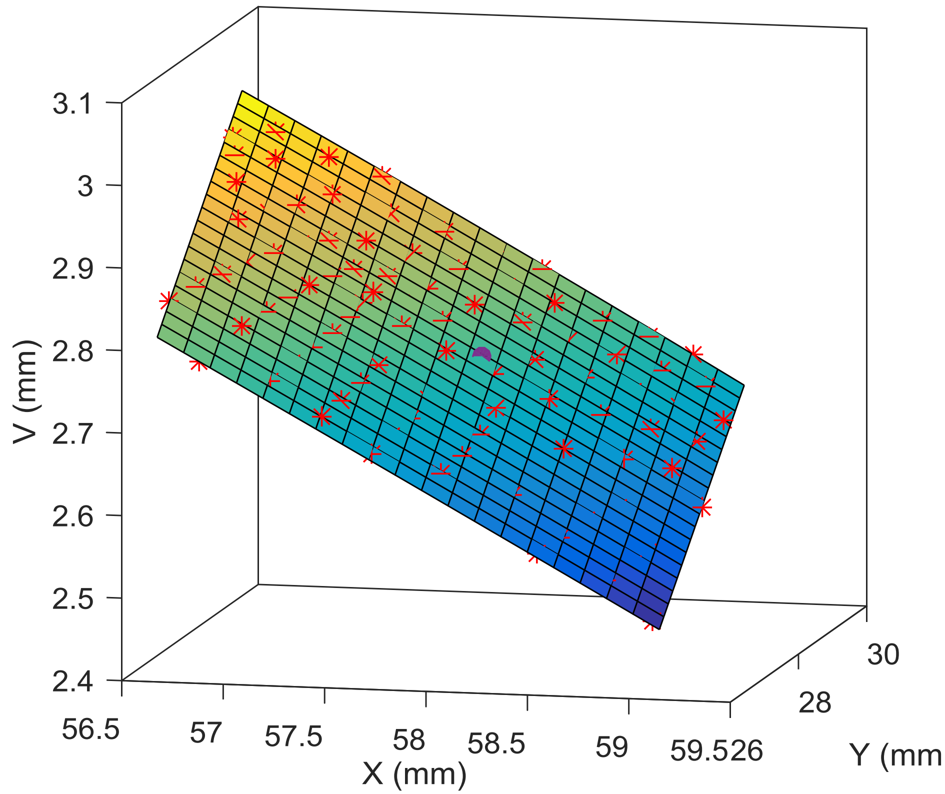

- 2D polynomial surface fitted to neighborhood of displacement nodes.
- Deformation gradient obtained directly from coefficients of polynomial fit.
- Spatially filters noise in DIC displacements.

Kinematics calculated from a least-squares polynomial fit to displacement data.

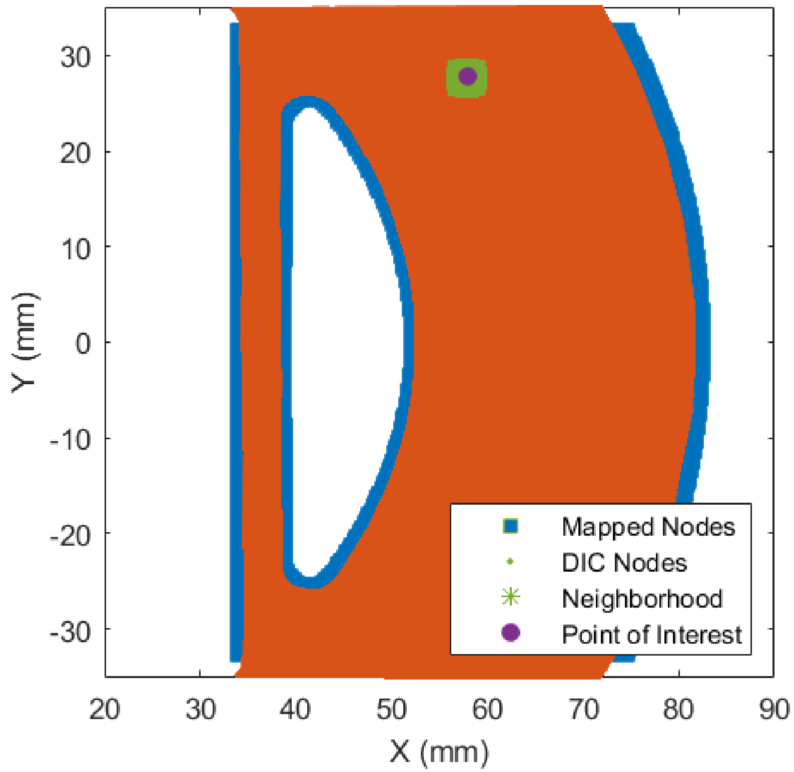

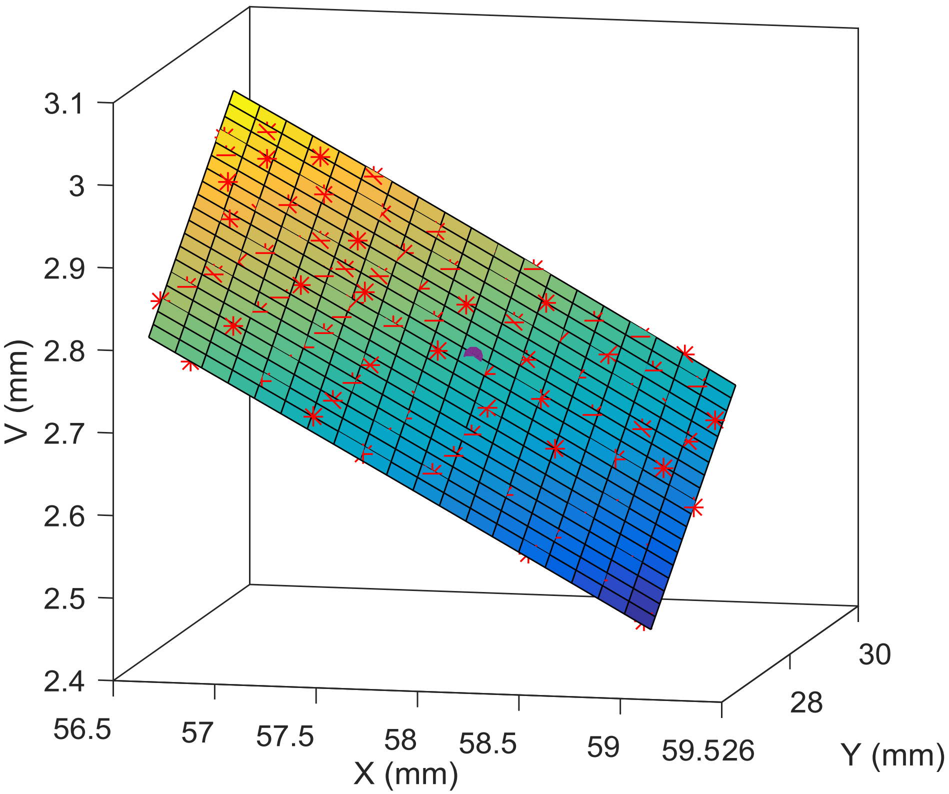

- 2D polynomial surface fitted to neighborhood of displacement nodes.
- Deformation gradient obtained directly from coefficients of polynomial fit.
- Spatially filters noise in DIC displacements.
- Extrapolate data to sample edges.

Rate of deformation is approximated using finite differences.

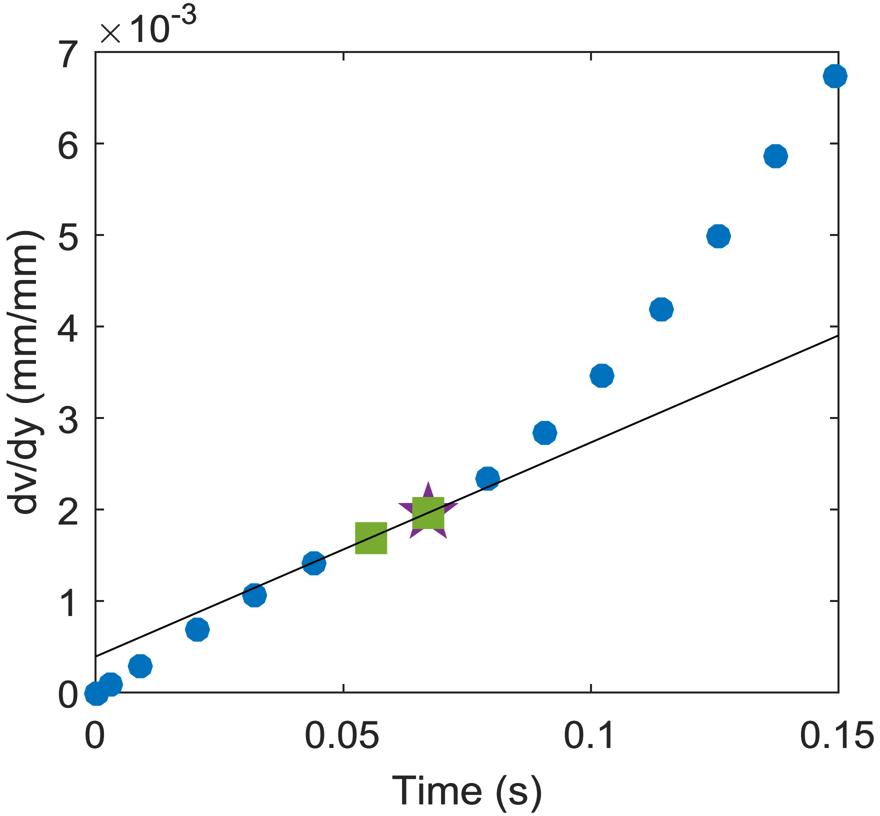

- Rate of deformation can be calculated via:
  - Backward difference

Rate of deformation is approximated using finite differences.

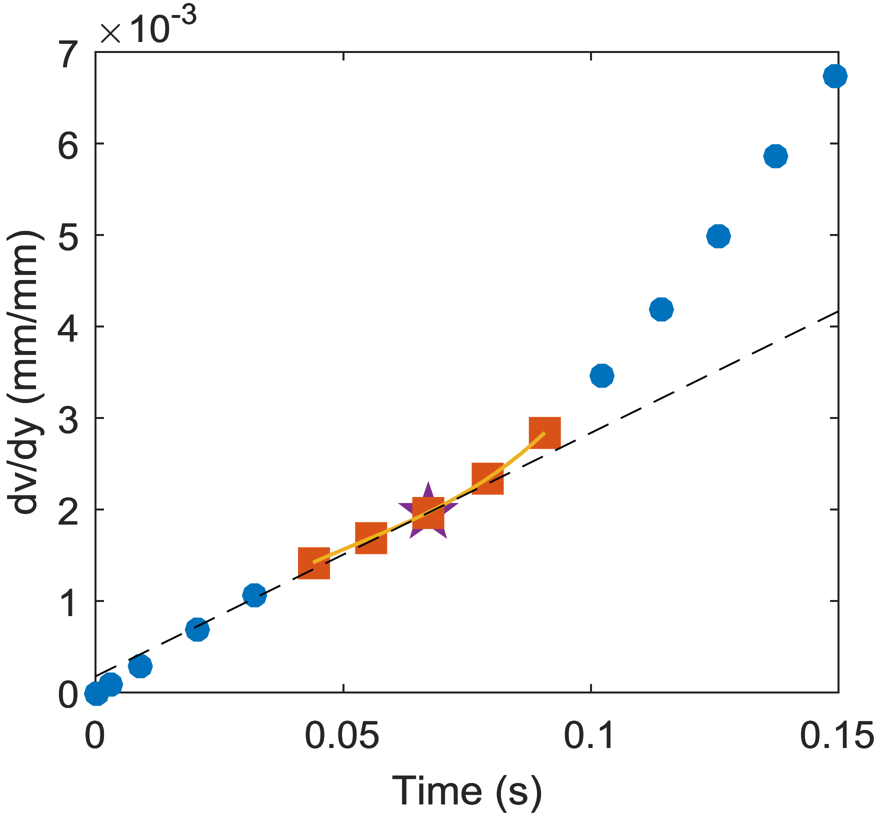

- Rate of deformation can be calculated via:
  - Backward difference
  - Central difference

Rate of deformation is approximated using finite differences.

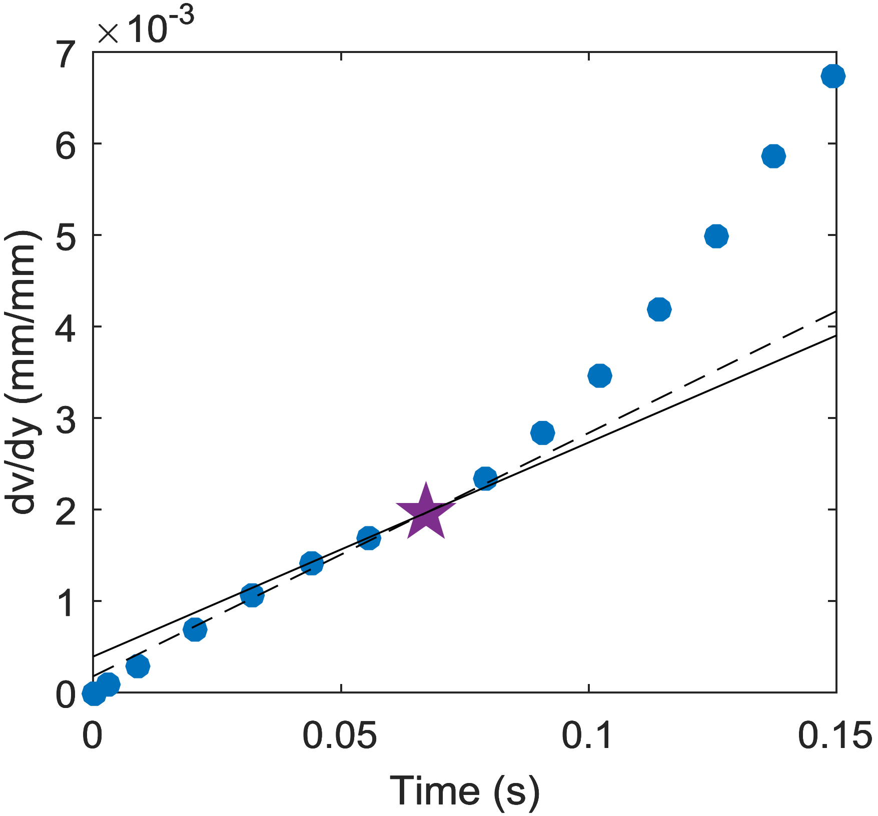

- Rate of deformation can be calculated via:
  - Backward difference
  - Central difference

Rate of deformation is approximated using finite differences.

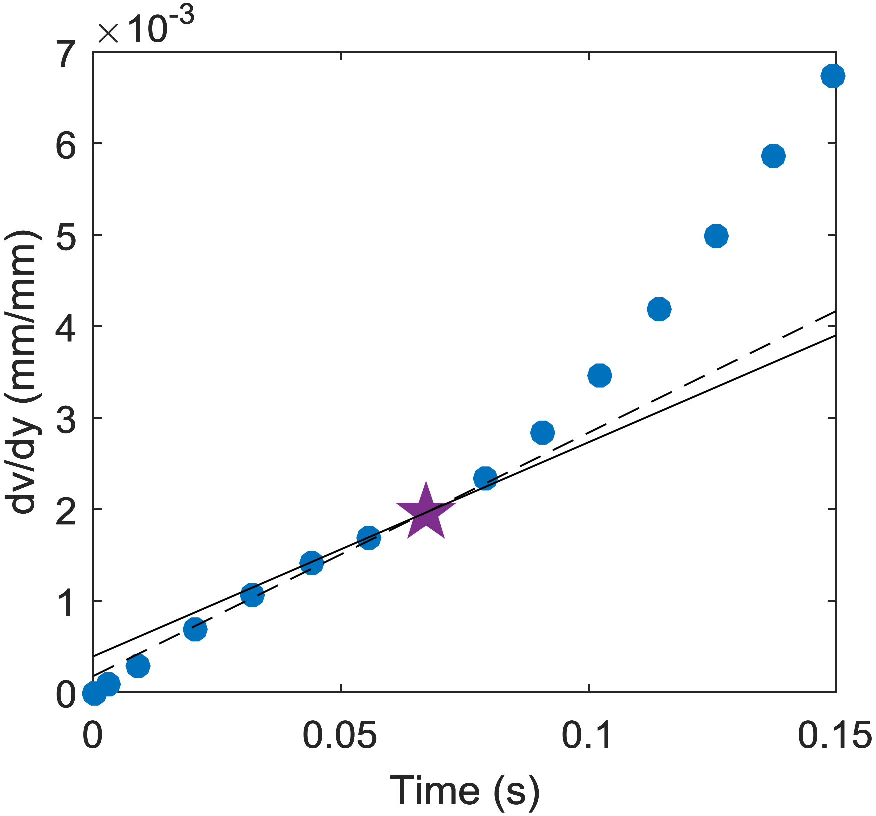

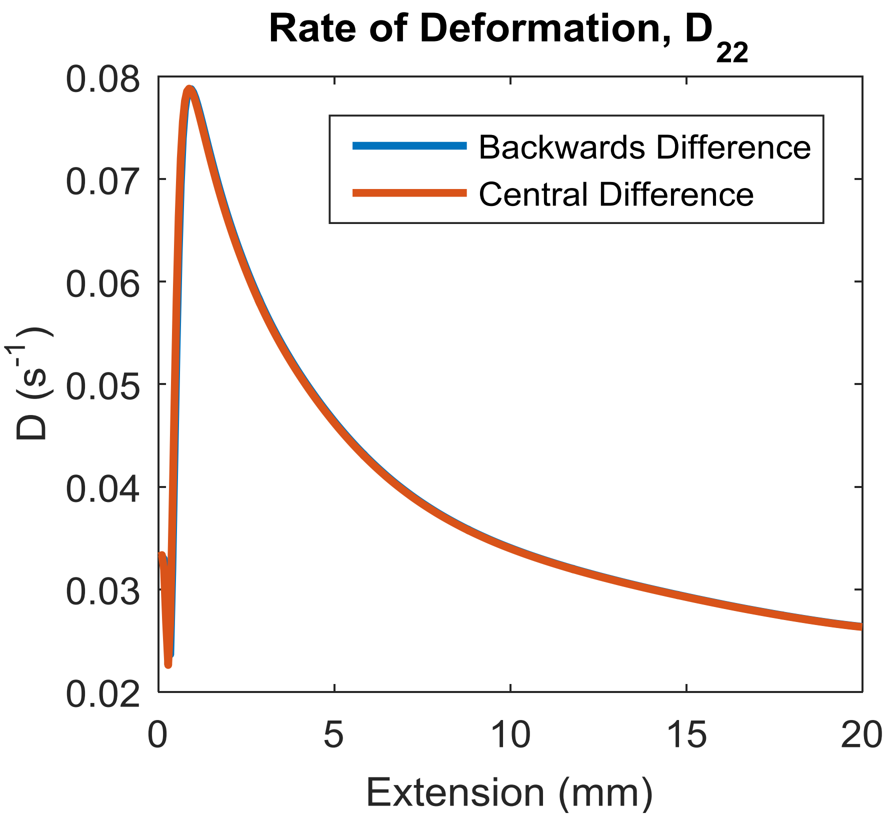

- Rate of deformation can be calculated via:
  - Backward difference
  - Central difference

Rate of deformation is approximated using finite differences.

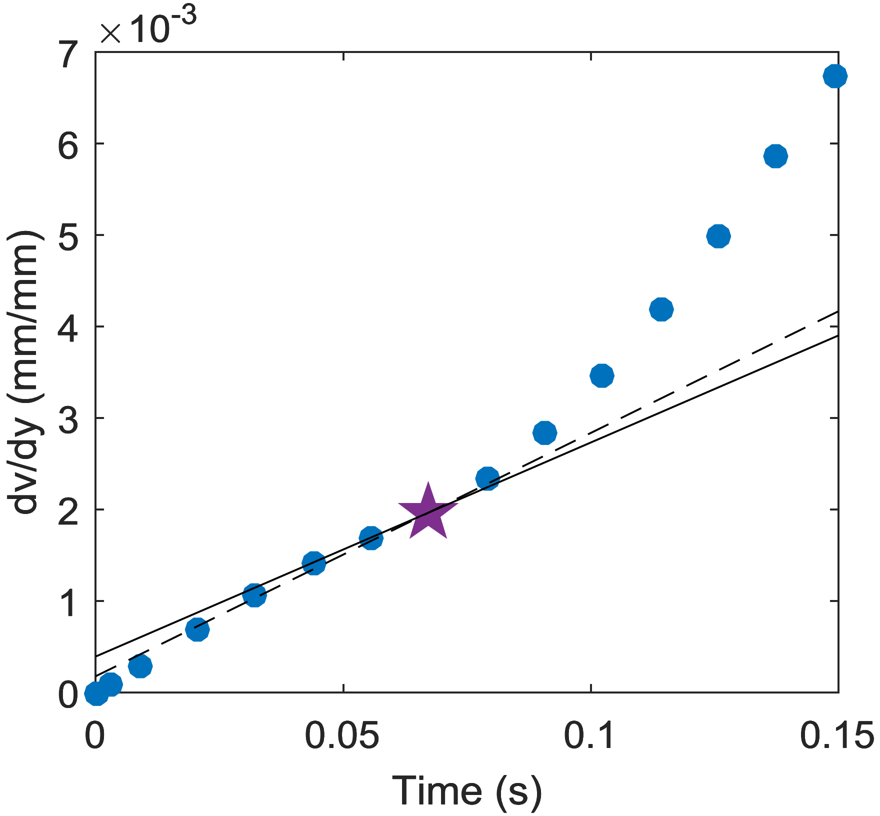

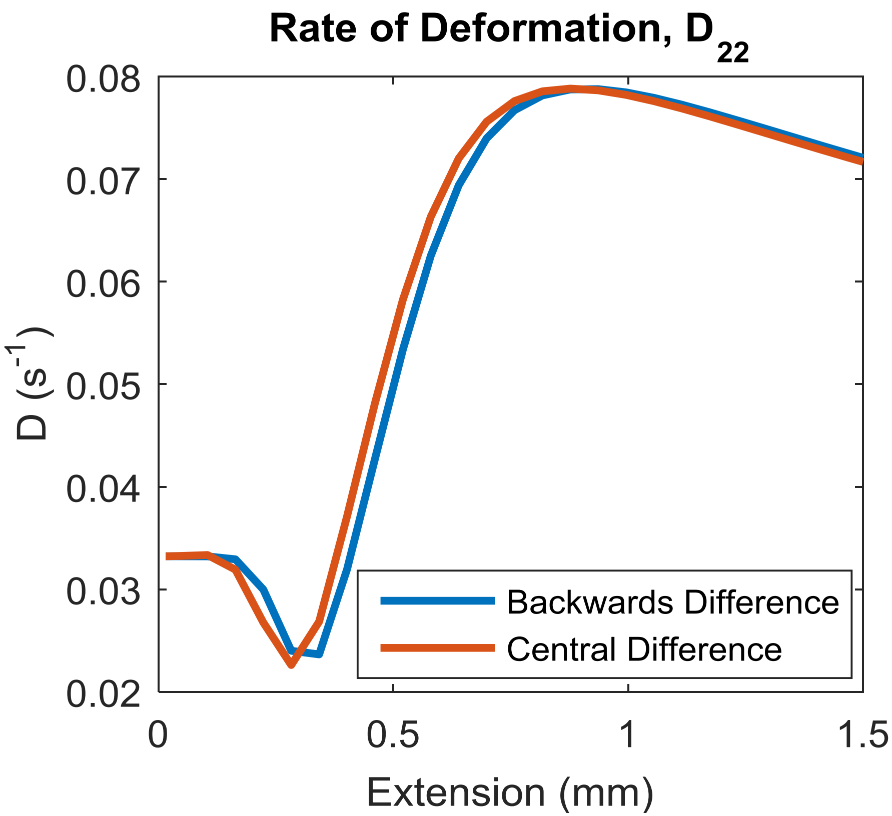

- Rate of deformation can be calculated via:
  - Backward difference
  - Central difference
- Significant difference near yield

Stresses are reconstructed using the radial return method.

- Non-trivial, but direct, computation
- Material Model
  - Flow stress: $\sigma_f = g_0(\xi)$
- Von Mises Flow Criterion
  - Equivalent Stress: $\bar{\sigma} = \sqrt{\frac{3}{2} s : s} \quad \left(s = \sigma - \frac{1}{3}\mathrm{tr}(\sigma) I\right)$
  - Equivalent Plastic Strain Rate: $\dot{p} = \sqrt{\frac{2}{3} \dot{\varepsilon}^p : \dot{\varepsilon}^p}$
  - Flow Criterion: $f_c = \bar{\sigma} - \sigma_f = 0$
- Cauchy Stress: $\boldsymbol{\sigma} = g_1\left(\sigma_f(\xi), \dot{p}\right)$

Cost function is the balance between internal and external virtual work.

- Kinematically-admissible virtual fields
  - Virtual Velocity: $v_x^* = \cos\left(\frac{\pi y}{H}\right);\ v_y^* = \frac{2y+H}{2H}$
    - Kim et al (2014) *Exp Mech*
  - Virtual Velocity Gradient: $\dot{\boldsymbol{F}}^* = \begin{bmatrix} \frac{\partial v_x^*}{\partial x} & \frac{\partial v_x^*}{\partial y} \\ \frac{\partial v_y^*}{\partial x} & \frac{\partial v_y^*}{\partial y} \end{bmatrix}$
- Internal and external virtual work
  - $W_{int} = \int \int_{V_o} \left((\det \boldsymbol{F})\boldsymbol{\sigma}(\xi)\boldsymbol{F}^{-T}\right) : \dot{\boldsymbol{F}}^*\, dV\, dt$
  - $W_{ext} = \int \boldsymbol{f} \cdot \overline{\boldsymbol{v}^*}\, dt$
- Cost function
  - $\Phi = (W_{int}(\xi) - W_{ext})^2$

Parameters must be scaled for a more tractable optimization.

Bounds: Chosen such that $\sim 50 < \sigma_f < \sim 3000$ MPa over $p = [0,1]$ and $\dot{p} = [10^{-5}, 10^{5}]$

	Lower Bound, ξ_L	Upper Bound, ξ_H	Scaling
σ_Y	50	750	Linear
H	50	5000	Linear
R_d	0.1	10	Log
b	10^{-5}	10^{5}	Log
m	1	20	Log

Parameter scaling →

Linear (σ_Y, H):

$$\hat{\xi} = \frac{\xi - \xi_L}{\xi_H - \xi_L}$$

Log (R_d, b, m):

$$\hat{\xi} = \frac{\log(\xi) - \log(\xi_L)}{\log(\xi_H) - \log(\xi_L)}$$

	Lower Bound, ξ_L	Upper Bound, ξ_H	Scaling
$\hat{\sigma}_y$	0	1	Linear
$\hat{H}$	0	1	Linear
$\hat{R}_d$	0	1	Linear
$\hat{b}$	0	1	Linear
$\hat{m}$	0	1	Linear

Initial guess: Latin Hyper Cube sampling

	Run 1	Run 2	Run 3	Run 4	Run 5	Run 6
$\hat{\sigma}_y$	0.2911	0.6644	0.5895	0.0398	0.2643	0.8108
$\hat{H}$	0.5025	0.1817	0.4183	0.2980	0.6770	0.9368
$\hat{R}_d$	0.6621	0.3845	0.0299	0.9711	0.7259	0.4755
$\hat{b}$	0.5675	0.0005	0.8965	0.2019	0.7547	0.5204
$\hat{m}$	0.7418	0.2607	0.7871	0.4505	0.9159	0.0377

Parameters must be scaled for a more tractable optimization.

Sandia National Laboratories

Bounds: Chosen such that $\sim 50 < \sigma_f < \sim 3000$ MPa over $p = [0,1]$ and $\dot{p} = [10^{-5}, 10^{5}]$

	Lower Bound, ξ_L	Upper Bound, ξ_H	Scaling
σ_Y	50	750	Linear
H	50	5000	Linear
R_d	0.1	10	Log
b	10^{-5}	10^{5}	Log
m	1	20	Log

Parameter scaling →

$$\hat{\xi} = \frac{\xi - \xi_L}{\xi_H - \xi_L}$$

$$\hat{\xi} = \frac{\log(\xi) - \log(\xi_L)}{\log(\xi_H) - \log(\xi_L)}$$

	Lower Bound, ξ_L	Upper Bound, ξ_H	Scaling
$\hat{\sigma}_y$	0	1	Linear
$\hat{H}$	0	1	Linear
$\hat{R}_d$	0	1	Linear
$\hat{b}$	0	1	Linear
$\hat{m}$	0	1	Linear

Initial guess: Latin Hyper Cube sampling

	Run 1	Run 2	Run 3	Run 4	Run 5	Run 6
σ_Y	253.8	515.1	462.7	77.86	235.0	617.6
H	2538	949.4	2121	1525	3401	4687
R_d	2.110	0.5875	0.1148	8.754	2.830	0.8933
b	9.229	1.01e-5	9.23e3	1.04e3	352.4	1.600
m	4.728	2.184	10.57	3.856	15.55	1.120

Cost function is sensitive to all parameters.

- Sensitivity of flow stress, σ_f
  - $\sigma_f = g_0(\xi)$
  - Function of mathematical form of material model only
  - Parameter scaling required
- Sensitivity of cost function, Φ
  - $\Phi = g_2\big(W_{int}(\dot{p}, \boldsymbol{v}^*), W_{ext}(\boldsymbol{v}^*)\big)$
  - Function of data richness
  - Function of virtual fields

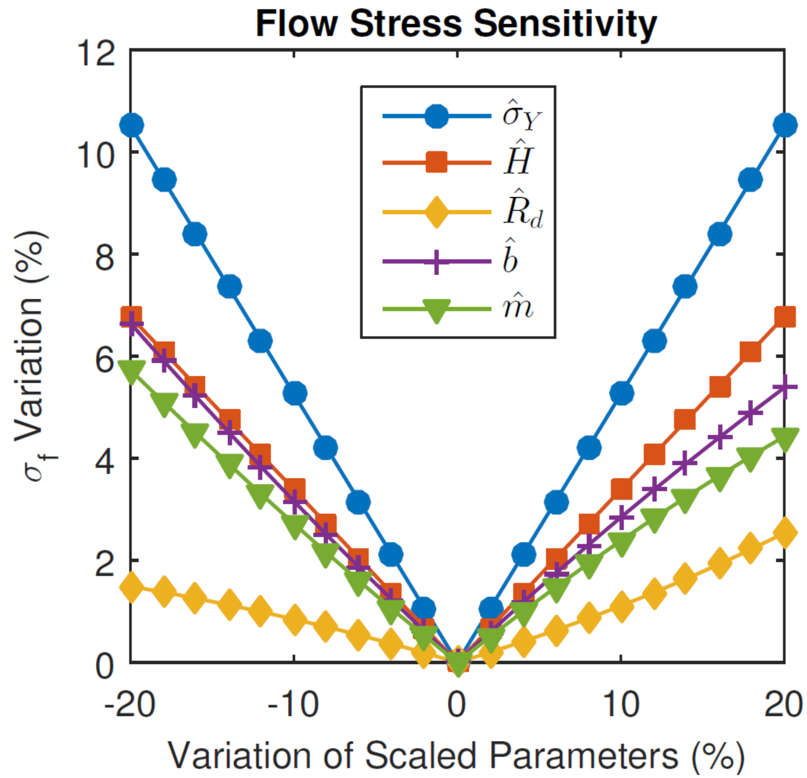

Cost function is sensitive to all parameters.

- Sensitivity of flow stress, σ_f
  - $\sigma_f = g_0(\xi)$
  - Function of mathematical form of material model only
  - Parameter scaling required
- Sensitivity of cost function, Φ
  - $\Phi = g_2\big(W_{int}(\dot{p}, \boldsymbol{v}^*), W_{ext}(\boldsymbol{v}^*)\big)$
  - Function of data richness
  - Function of virtual fields

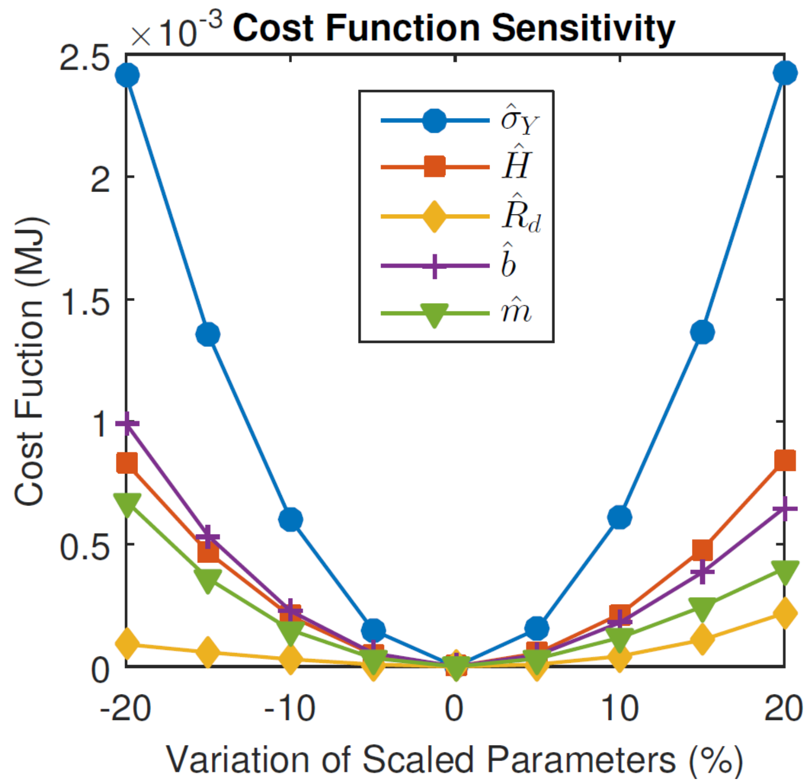

Parameters are identified using a non-linear, gradient-based optimizer in Matlab.

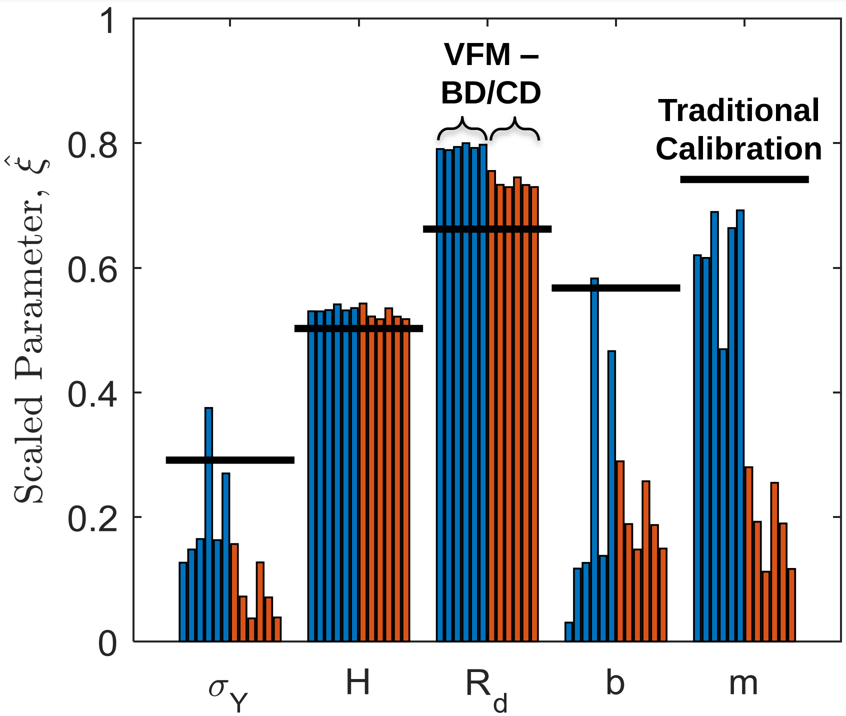

Parameter	Symbol	Value	Units
Quasi-static Yield Stress	σ_y	253.8	MPa
Hardening Variable	H	2538	MPa
Dynamic Recovery	R_d	2.110	--
Rate-Dependent Coefficient	b	4.728	s^{-1}
Rate-Dependent Exponent	m	9.229	--

$$\sigma_f(p, \dot{p}, \xi) = \sigma_Y \left\{1 + \operatorname{asinh}\left[\left(\frac{\dot{p}}{b}\right)^{1/m}\right]\right\} + \frac{H}{R_d}[1 - \exp(-R_d p)]$$

- 12 different parameter sets identified from VFM
  - 2 different approximations for the strain rate
    1. Backwards difference
    2. Central difference
  - 6 different initial guesses
    1. Reference parameters
    2. Latin hypercube sampling (5 sets)
- Hardening parameters (H, R_d) are relatively constant
- Strain-rate dependent parameters (σ_Y, b, m) have significant variation.
  - Parameter co-variance!

The flow stress is invariant with respect to the different parameter sets.

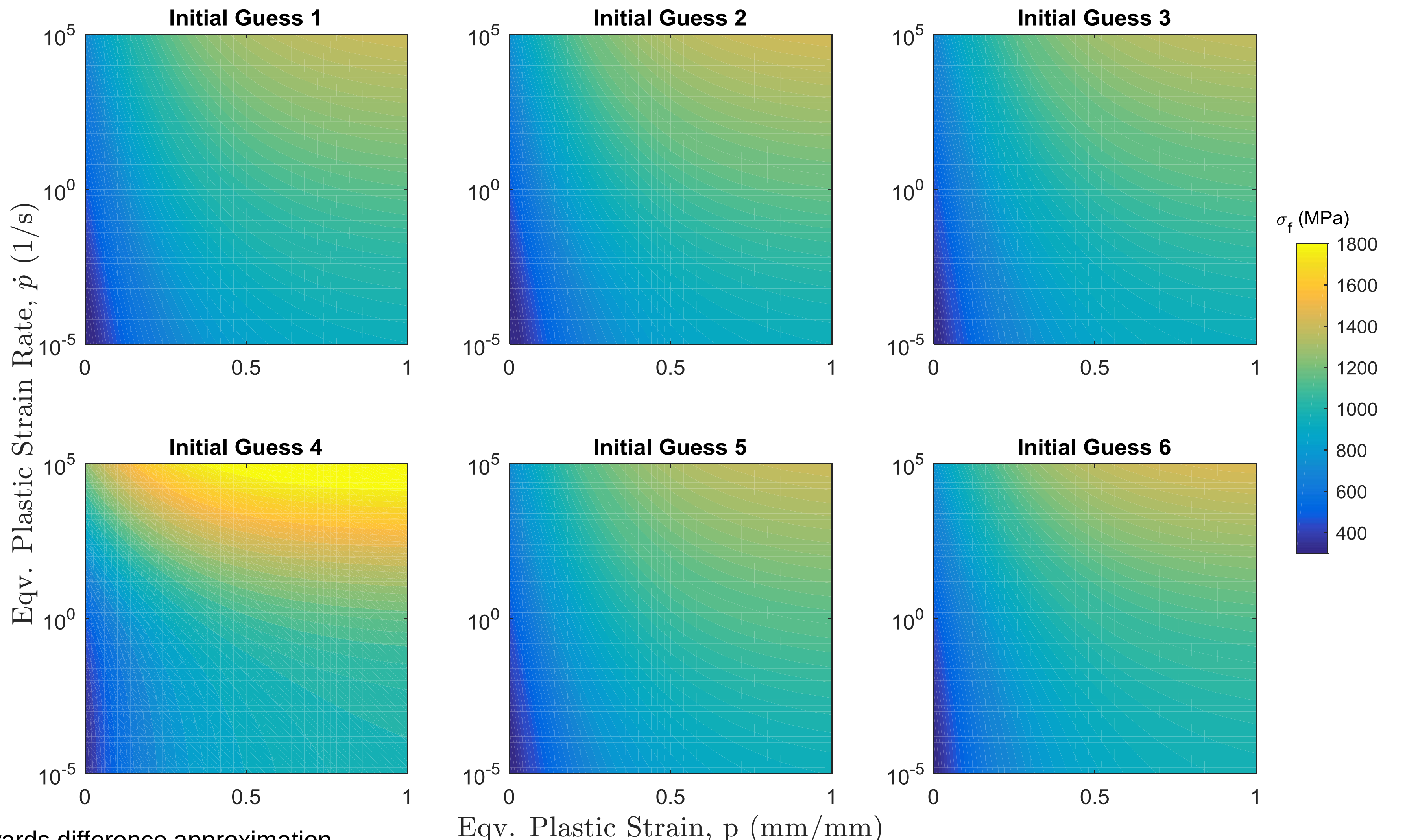

Backwards difference approximation

The flow stress is invariant with respect to the different parameter sets.

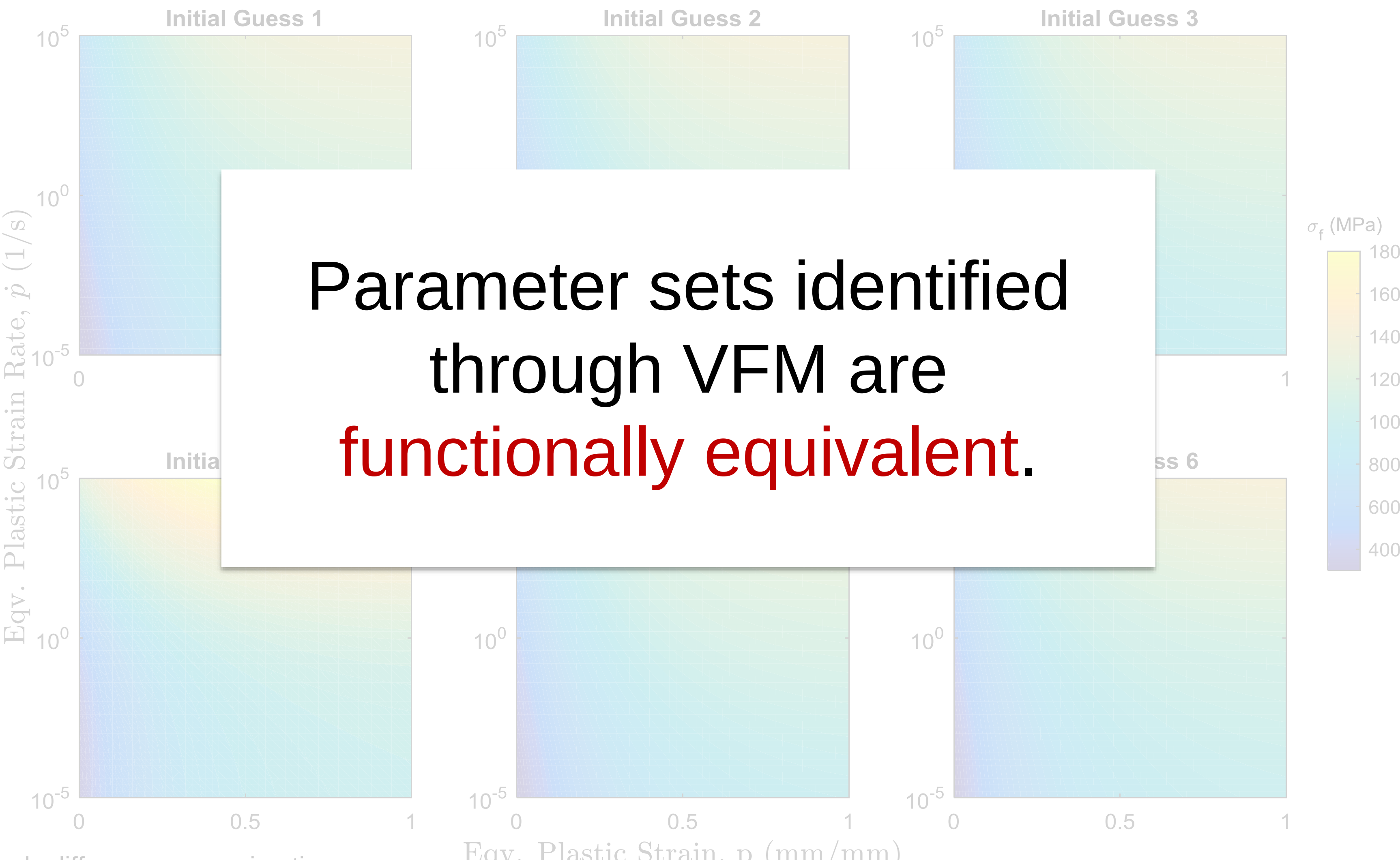

Parameter sets identified through VFM are functionally equivalent.

Backwards difference approximation

Outline

- Digital Image Correlation
  - Fundamentals
  - International DIC Society (iDICs)
  - Applications at Sandia
- Material Characterization
  - Background
  - Viscoplastic Material Model
  - Traditional Calibration Technique
  - Advanced, Full-Field Calibration Technique
- Finite-Element Model Validation
  - Global Data
  - Full-Field Data
  - Boundary Conditions
- Conclusions and Future Work

Validation experiments conducted with an X-specimen.

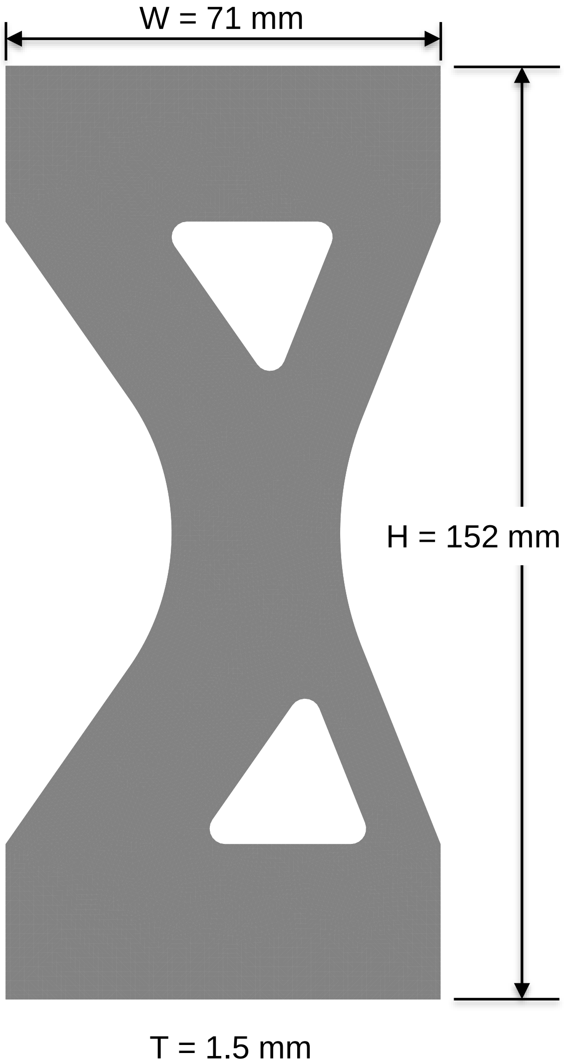

- Experimental DIC data of X-specimen with 6 repeats
- FEA of X-specimen using each of the different parameter sets
- Map FEA and Experimental displacement results to a common grid
- Green-Lagrangian finite strains computed from local polynomial fit
- Strains interpolated onto a common time vector

Global data is similar for all model parameter sets.

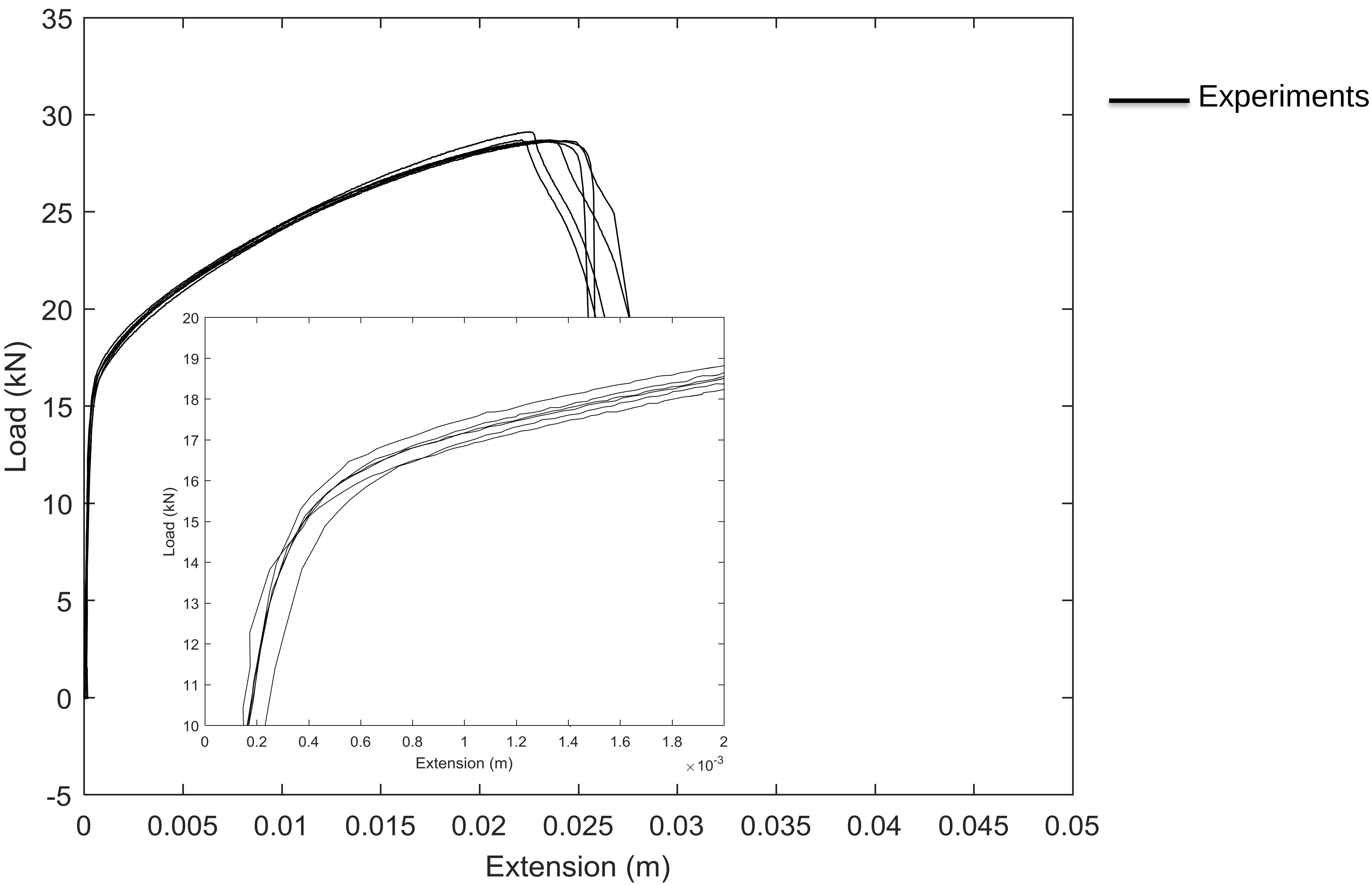

Global data is similar for all model parameter sets.

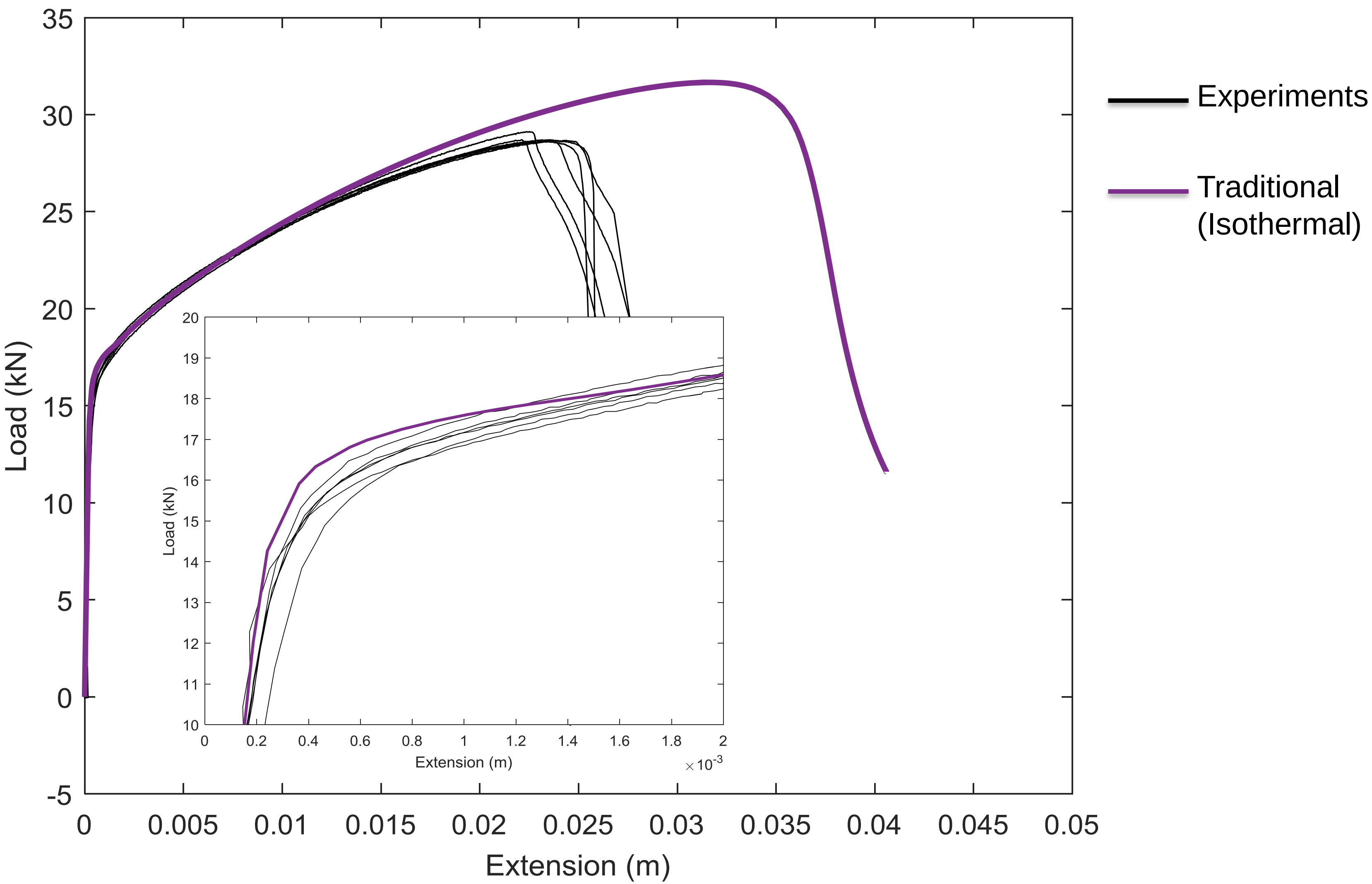

Global data is similar for all model parameter sets.

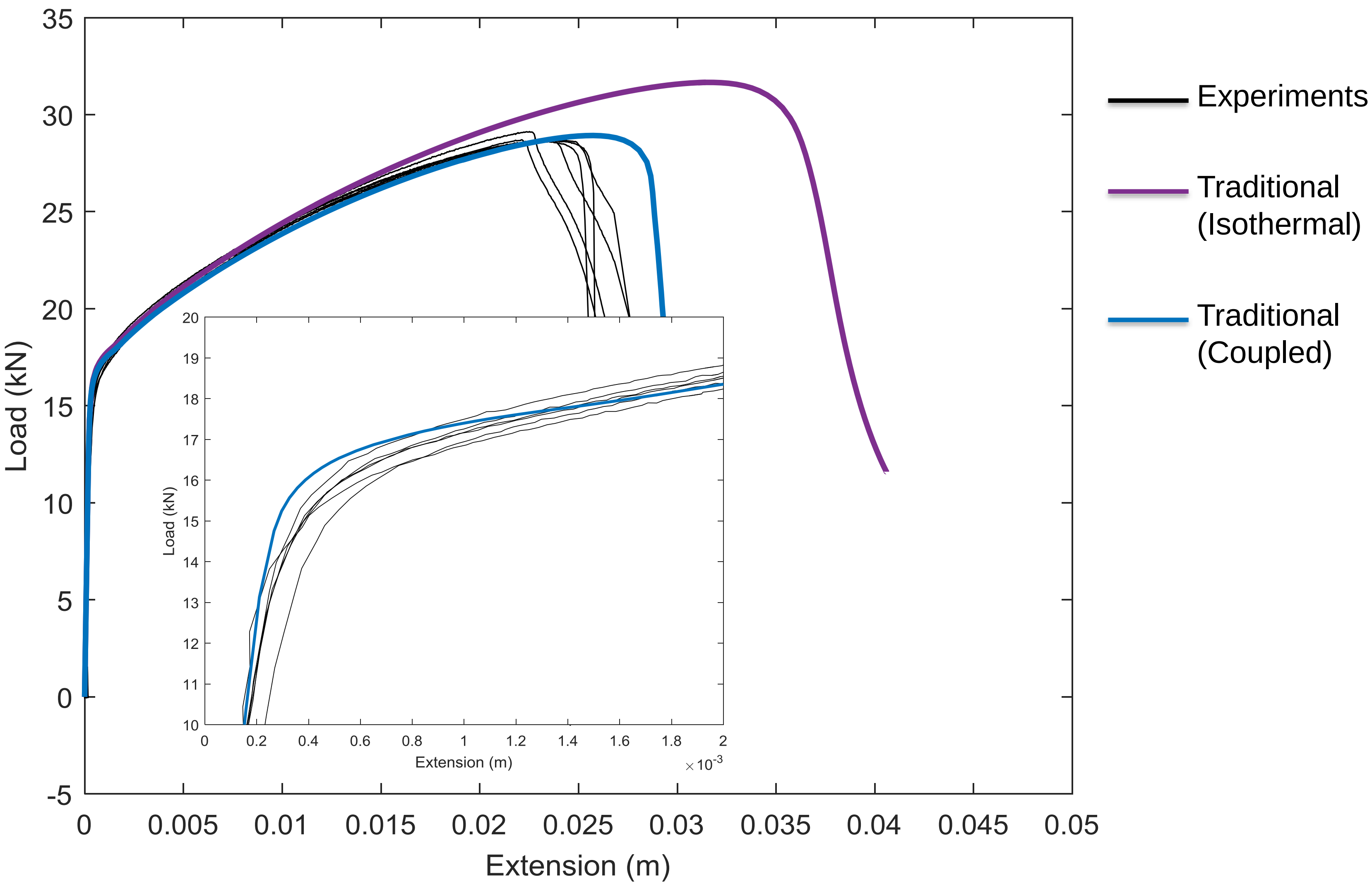

Global data is similar for all model parameter sets.

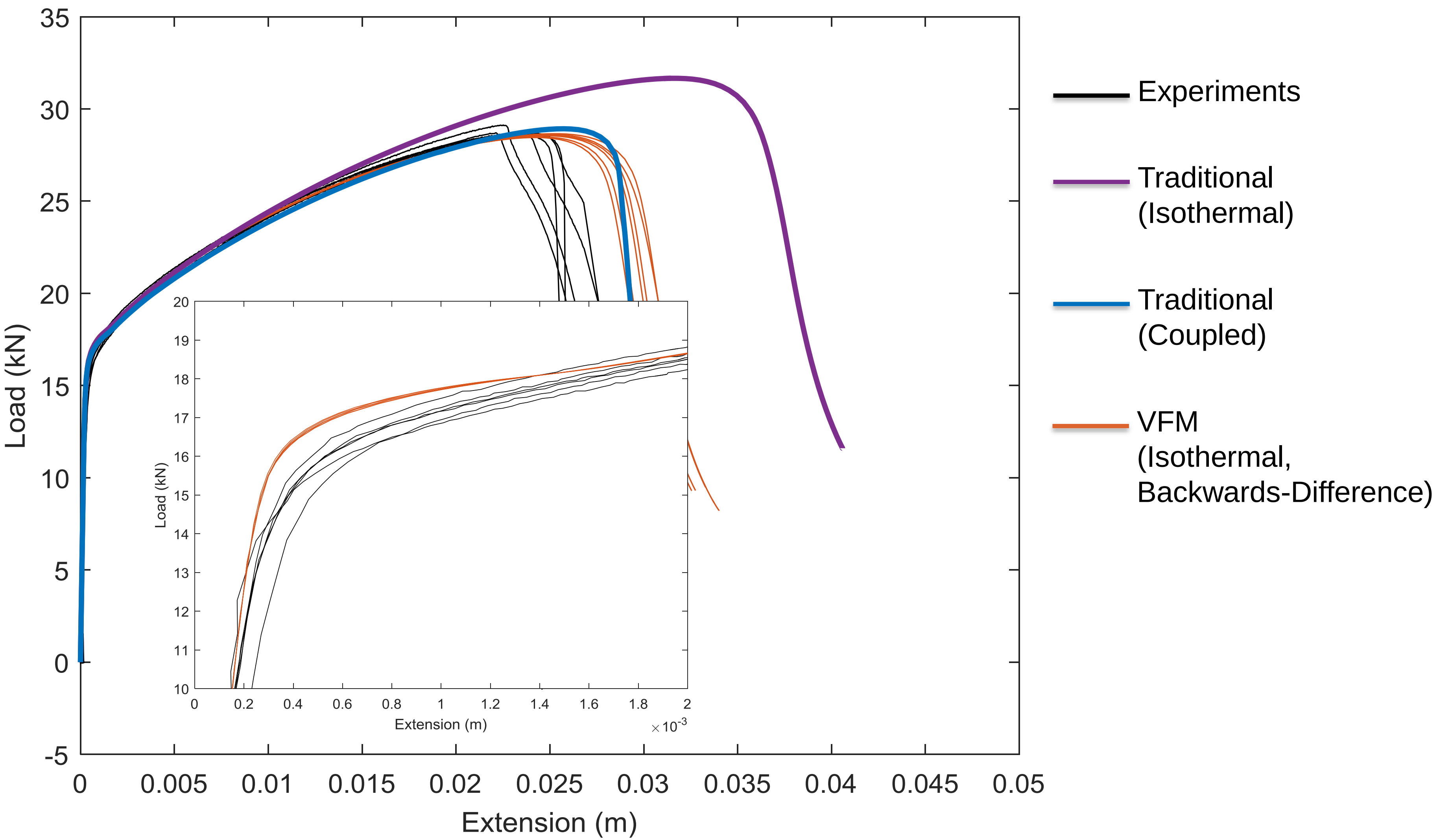

Global data is similar for all model parameter sets.

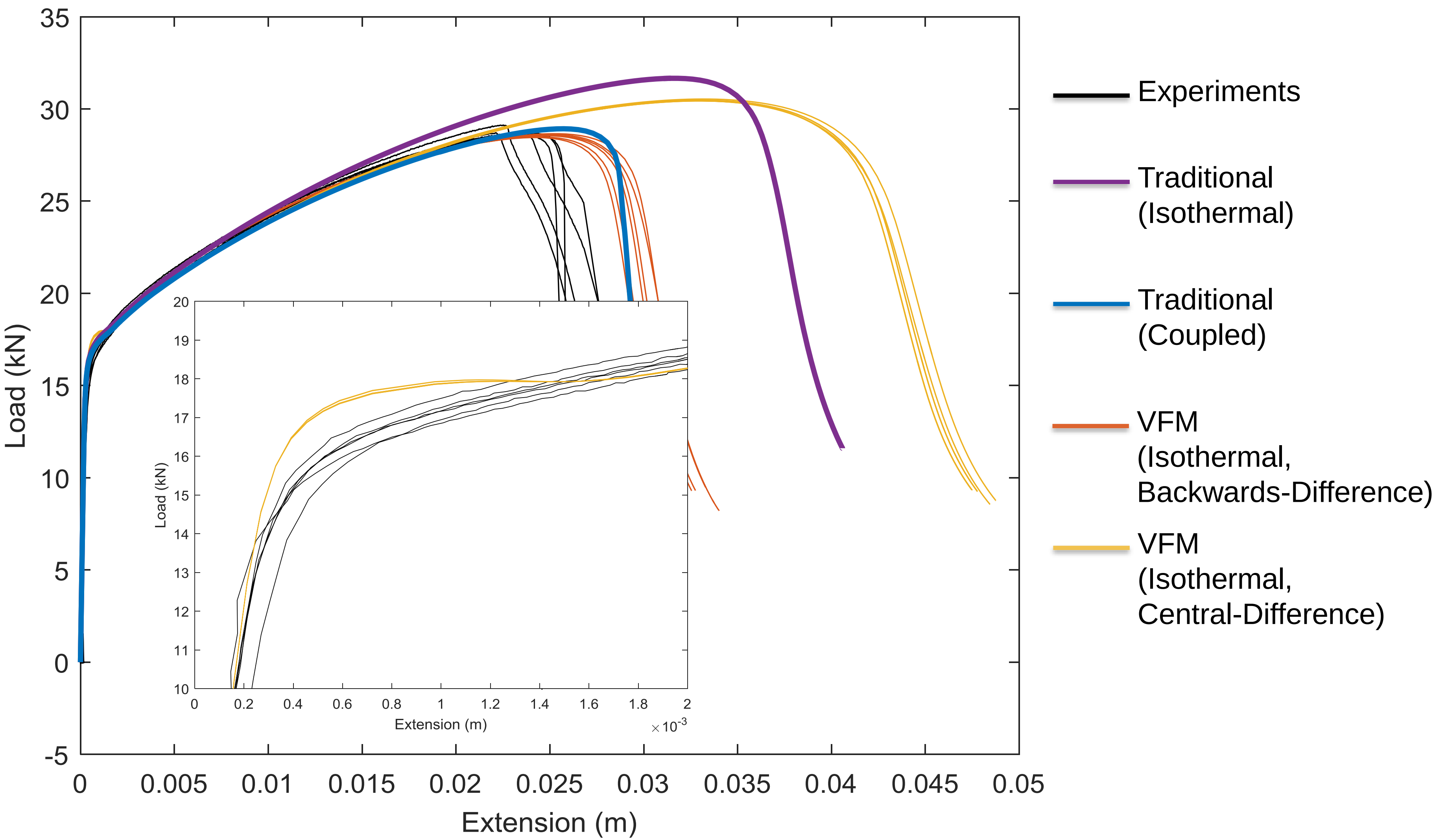

Global data is similar for all model parameter sets.

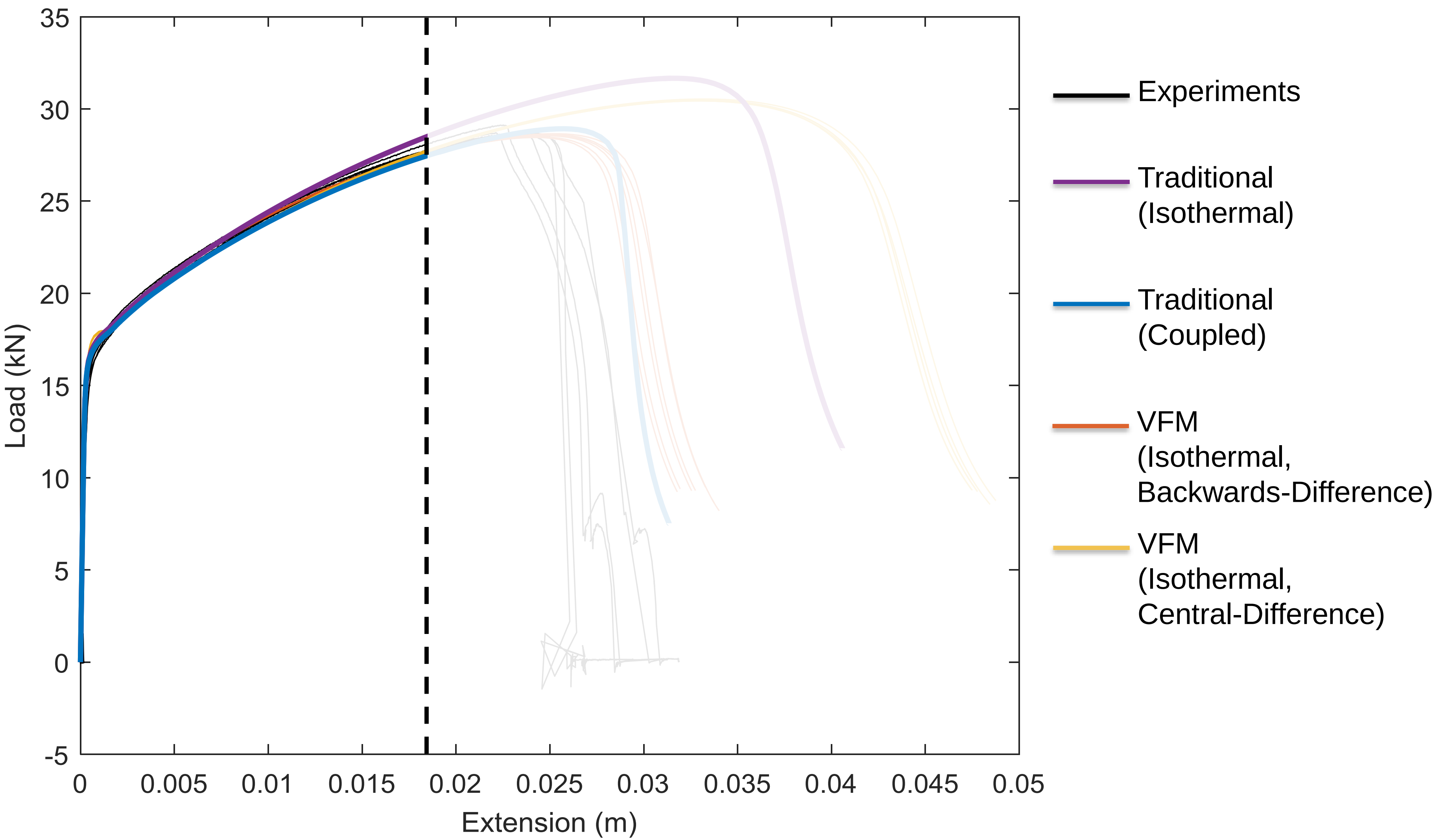

Global data is similar for all model parameter sets.

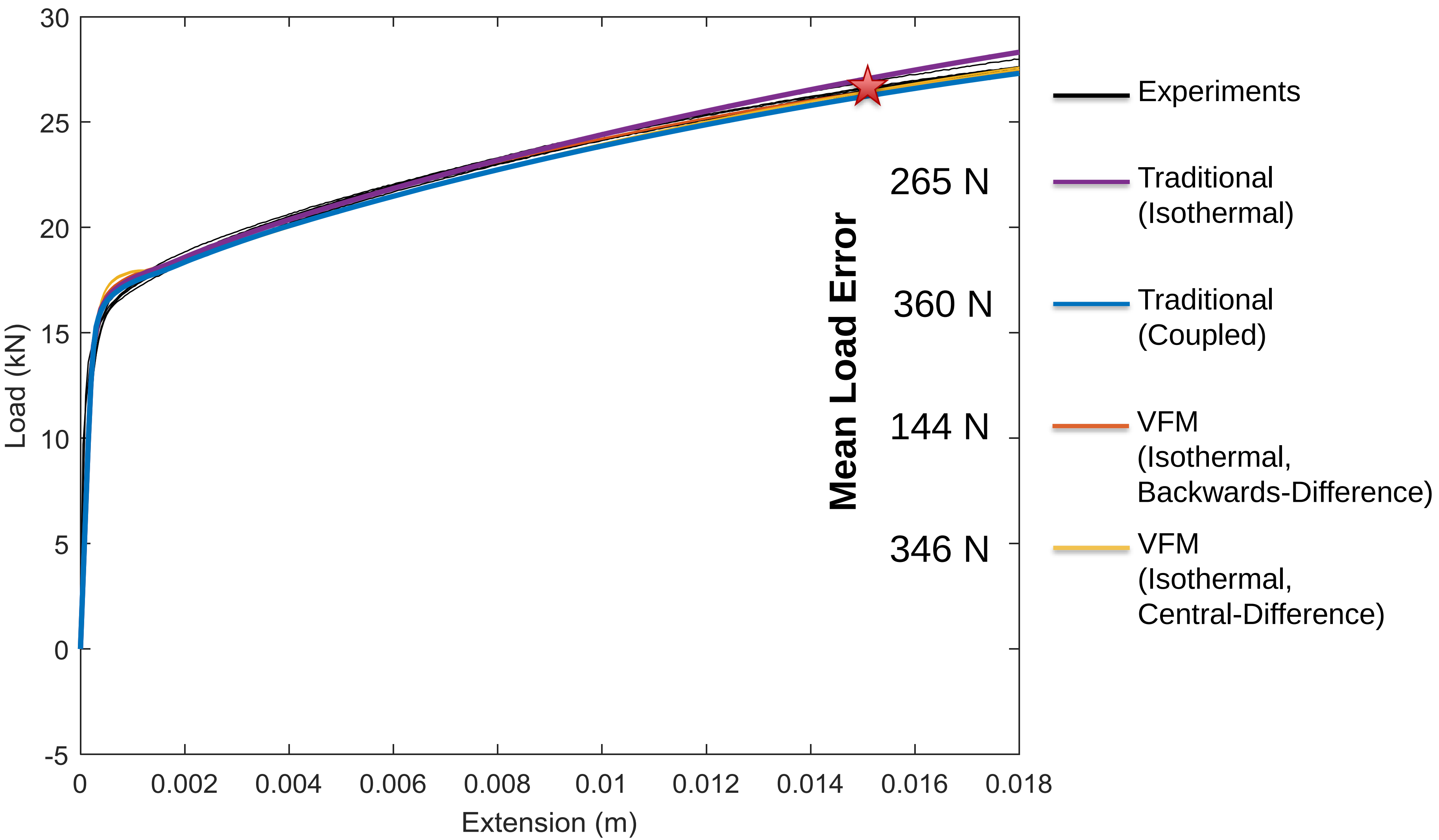

Experimental results are repeatable: Vertical normal strain at 15 mm total extension.

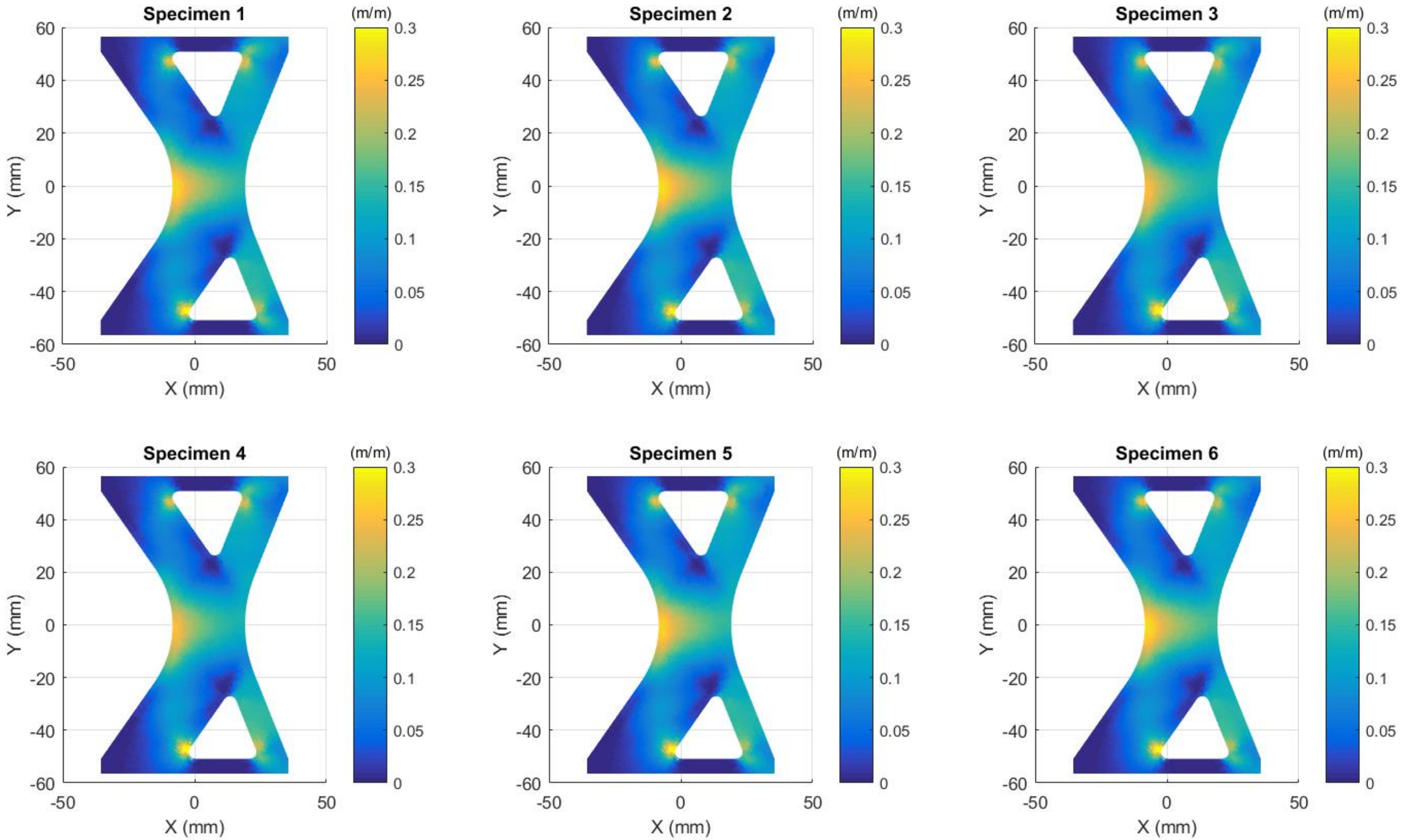

Experimental results are repeatable: Vertical normal strain at 15 mm total extension.

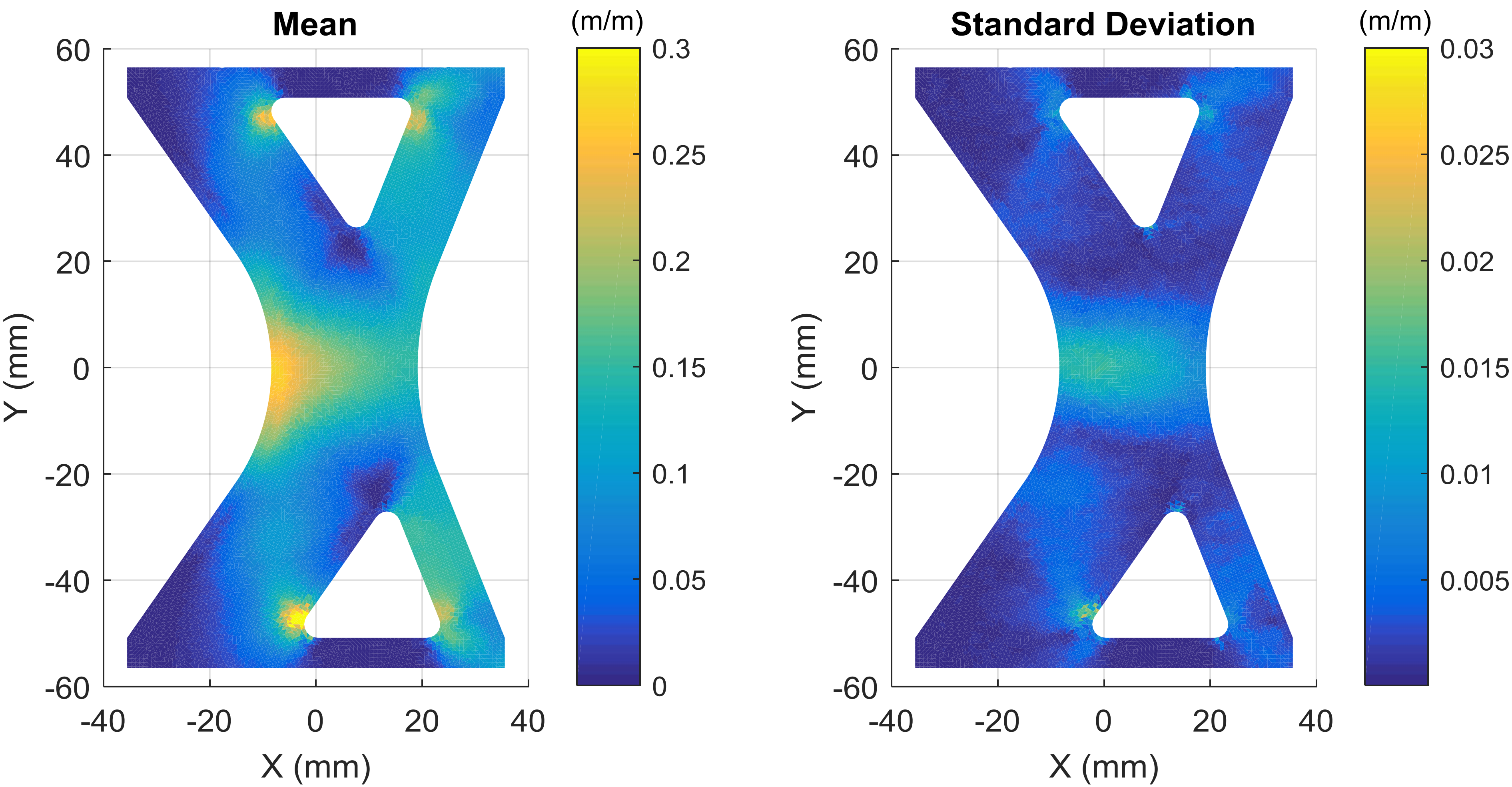

Finite-Element Models using different parameter sets are also very similar.

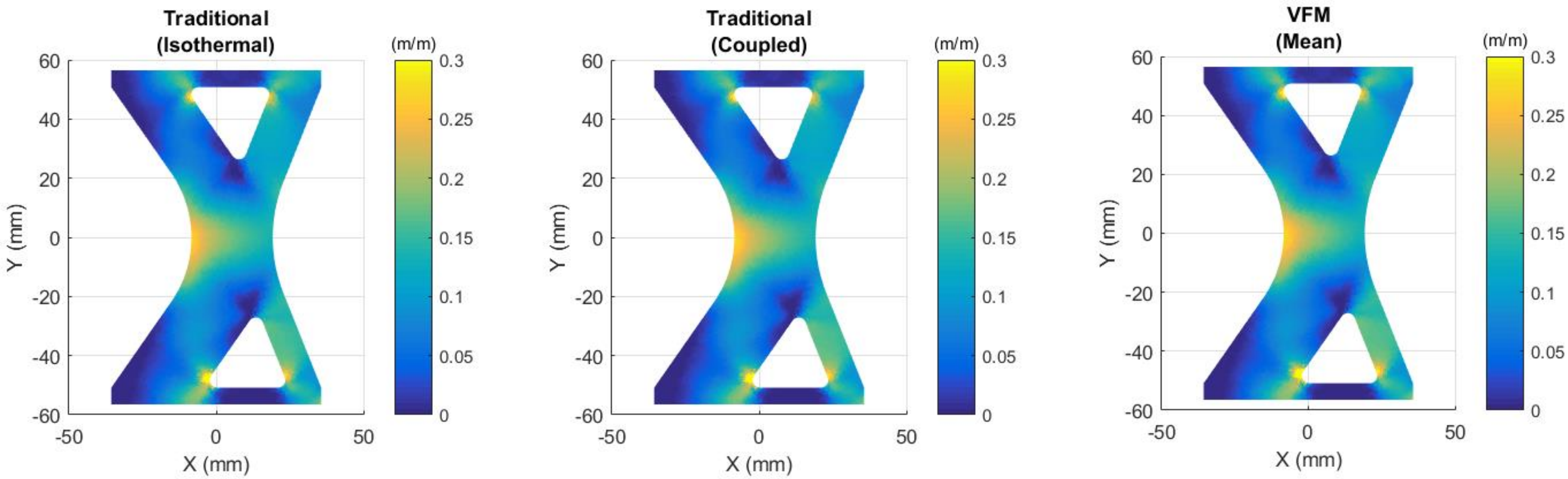

All material models have similar errors compared to experimental data.

Strain Error = FEM Strain – Experimental Strain

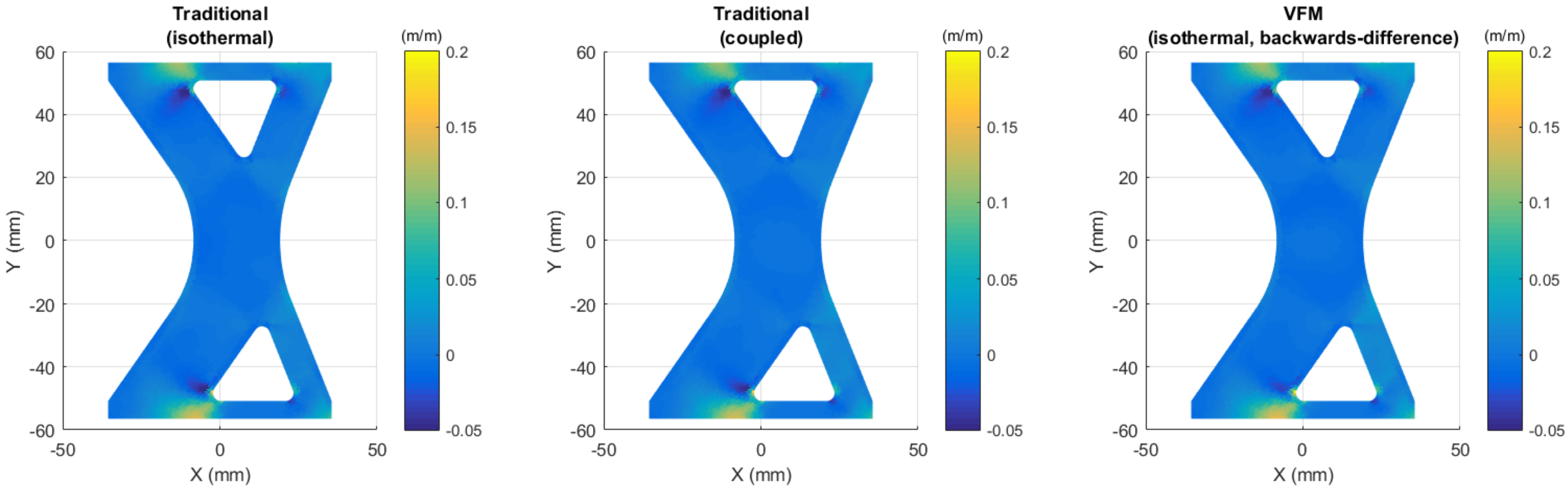

Average Strain Errors (με)			
	Traditional (isothermal)	**Traditional (coupled)**	**VFM (backwards difference)**
E_{11}	5450	5460	5480
E_{22}	8090	8030	8480
E_{12}	3020	3040	3050

- All material models have approximately the same error.
- Full-field data provides much more information for validation.

All material models have similar errors compared to experimental data.

Strain Error = FEM Strain – Experimental Strain

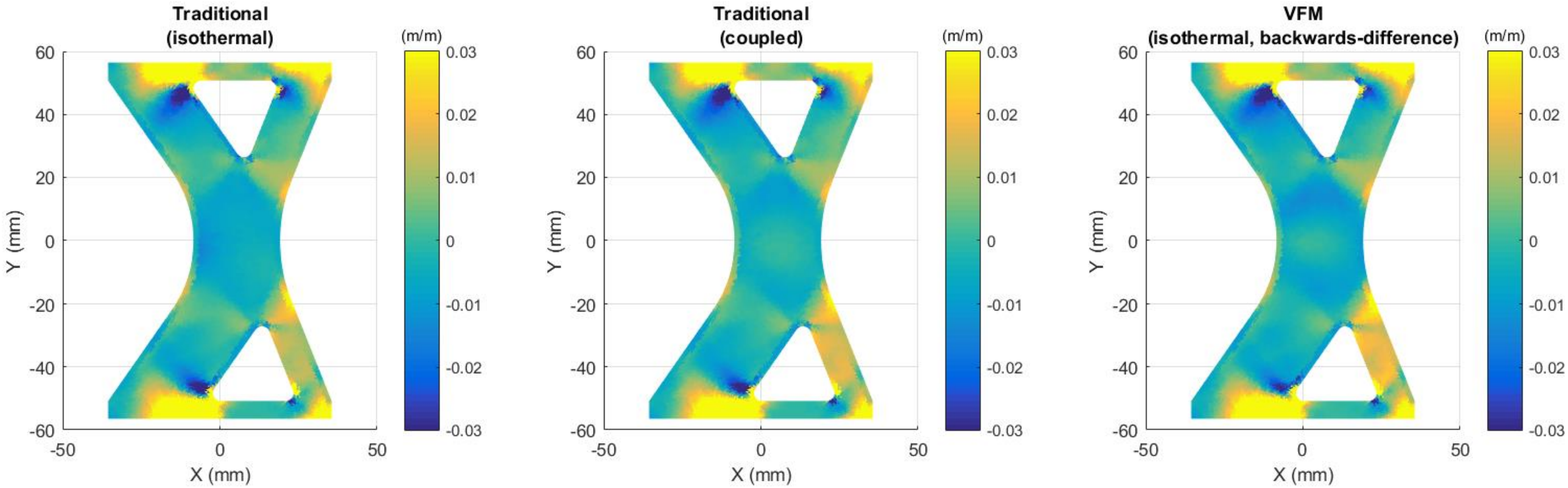

Average Strain Errors (με)			
	Traditional (isothermal)	**Traditional (coupled)**	**VFM (backwards difference)**
E_{11}	5450	5460	5480
E_{22}	8090	8030	8480
E_{12}	3020	3040	3050

- All material models have approximately the same error.
- Full-field data provides much more information for validation.

Outline

- Digital Image Correlation
  - Fundamentals
  - International DIC Society (iDICs)
  - Applications at Sandia
- Material Characterization
  - Background
  - Viscoplastic Material Model
  - Traditional Calibration Technique
  - Advanced, Full-Field Calibration Technique
- Finite-Element Model Validation
  - Global Data
  - Full-Field Data
  - Boundary Conditions
- Conclusions and Future Work

Experimental boundary conditions are not perfect.

FE Model BCs (Ideal)

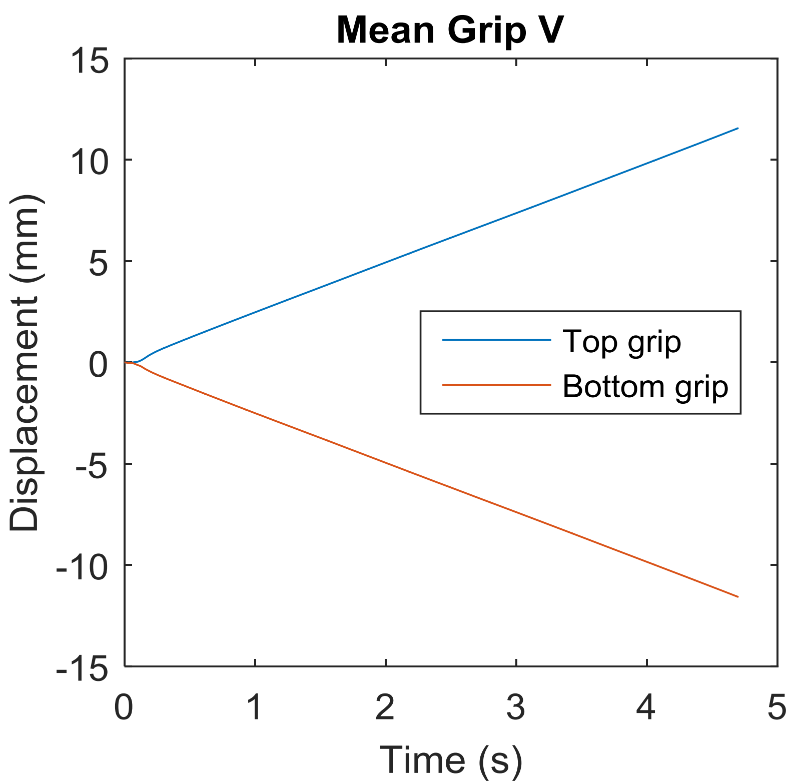

No displacement in U or W.

Experimental BCs

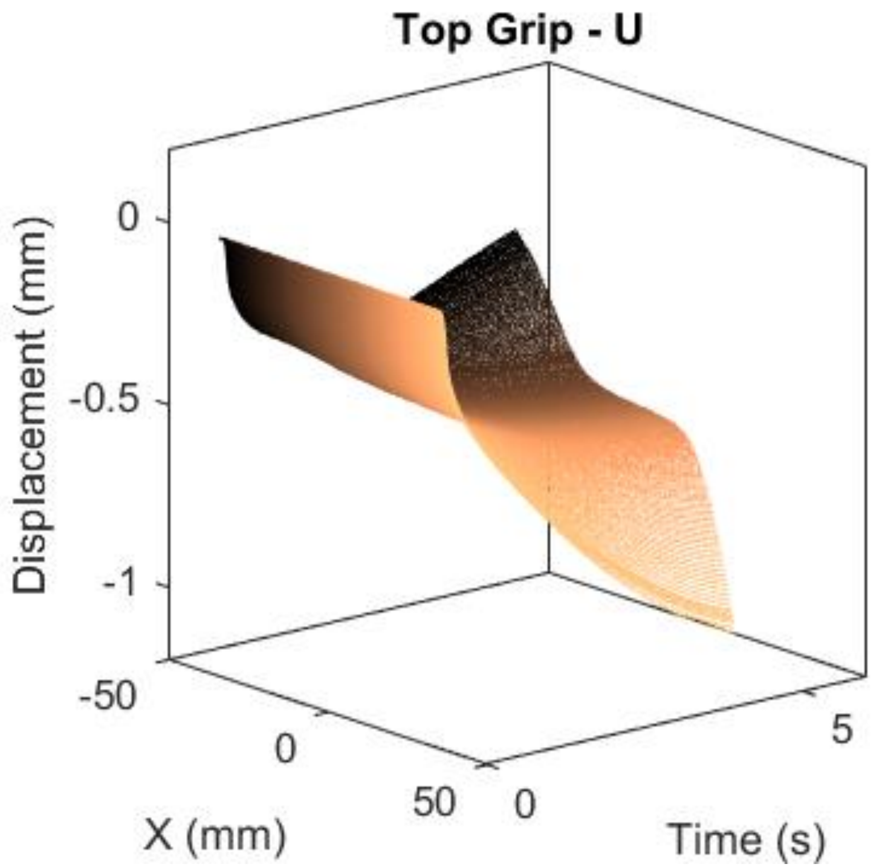

Experimental boundary conditions are not perfect.

FE Model BCs (Ideal)

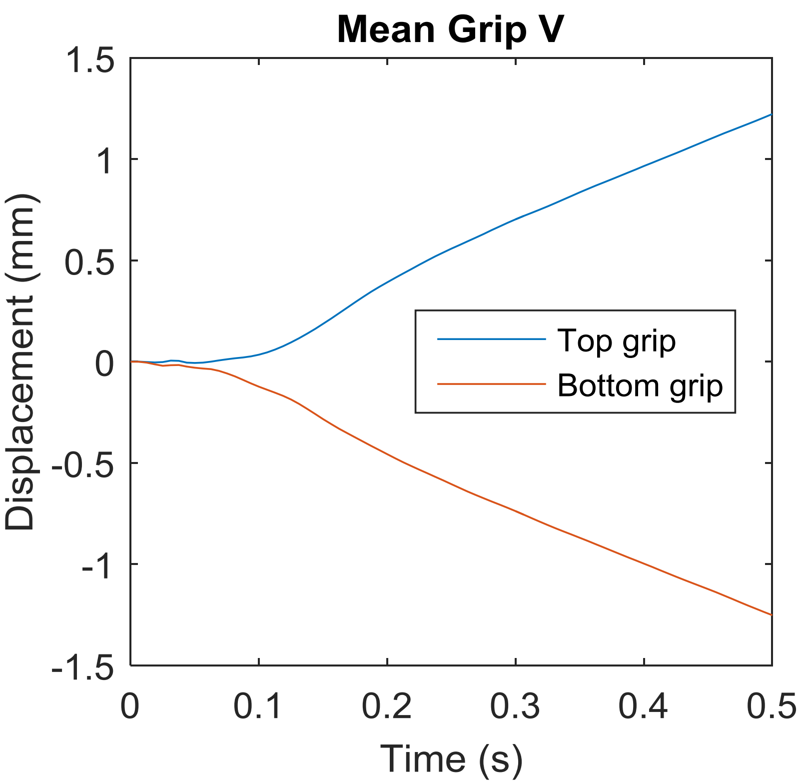

No displacement in U or W.

Experimental BCs

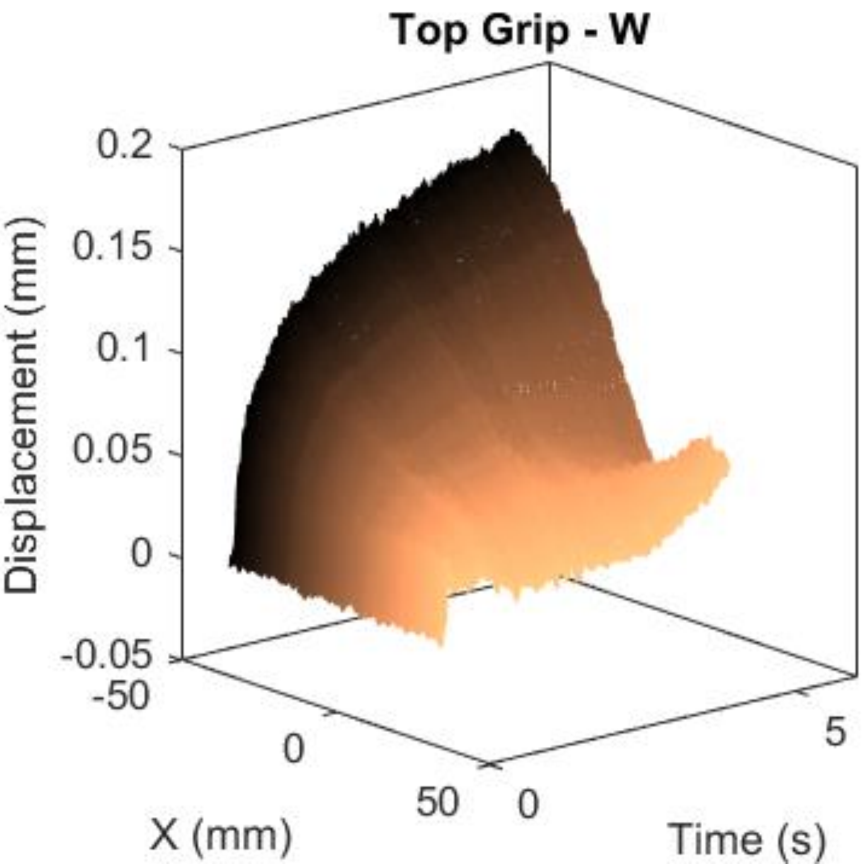

Modeling actual boundary conditions is critical for FE model validation.

Strain Error = FEM Strain – Experimental Strain

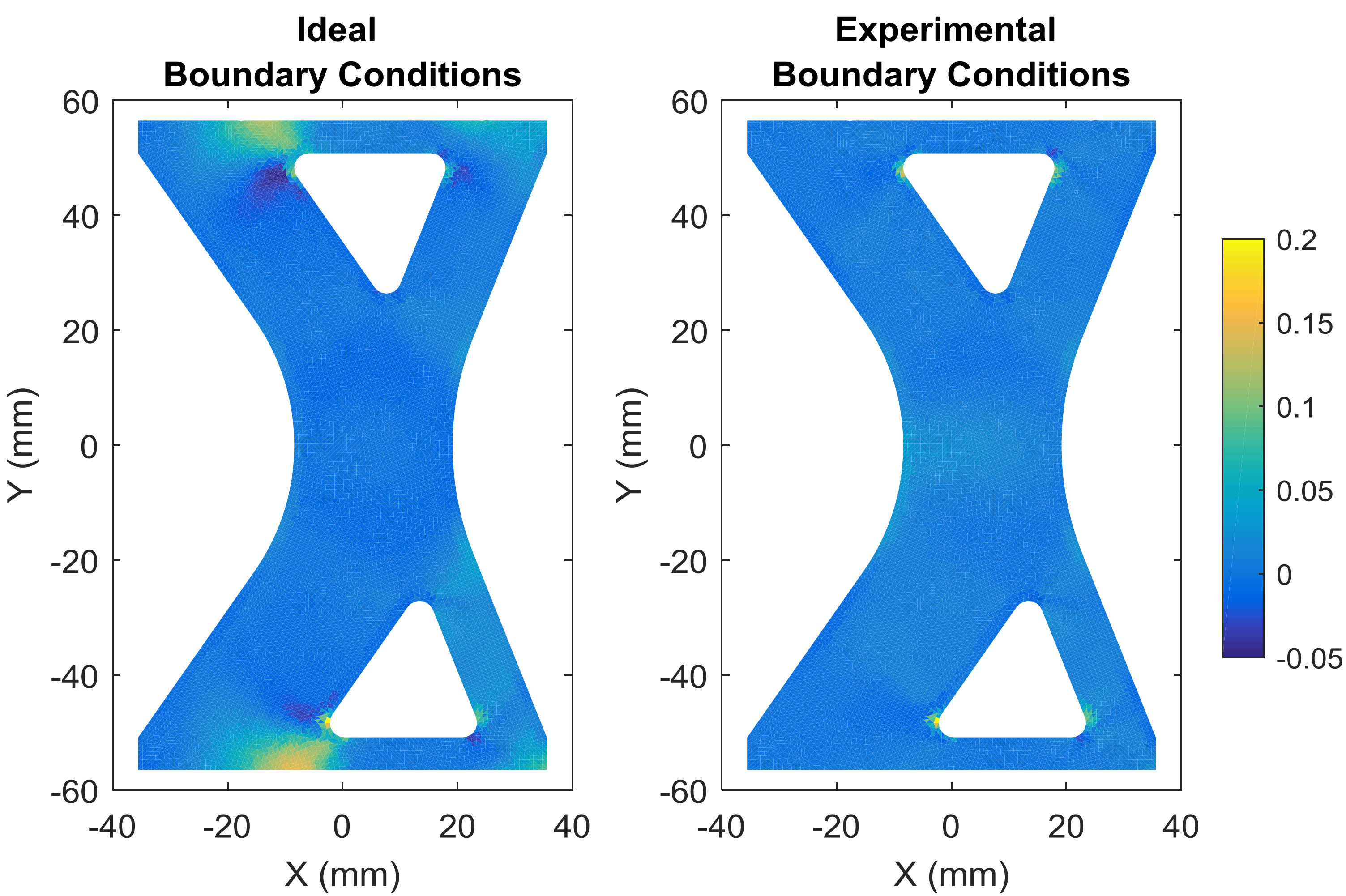

Outline

- Digital Image Correlation
  - Fundamentals
  - International DIC Society (iDICs)
  - Applications at Sandia
- Material Characterization
  - Background
  - Viscoplastic Material Model
  - Traditional Calibration Technique
  - Advanced, Full-Field Calibration Technique
- Finite-Element Model Validation
  - Global Data
  - Full-Field Data
  - Boundary Conditions
- Conclusions and Future Work

Goal: Perform better material characterization by utilizing full-field data instead of only global measurements

Sandia National Laboratories

Calibrated a viscoplastic material model using traditional tensile tests.

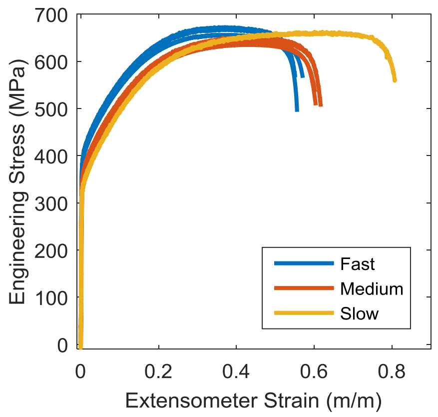

Calibrated a viscoplastic material model using a single specimen and VFM.

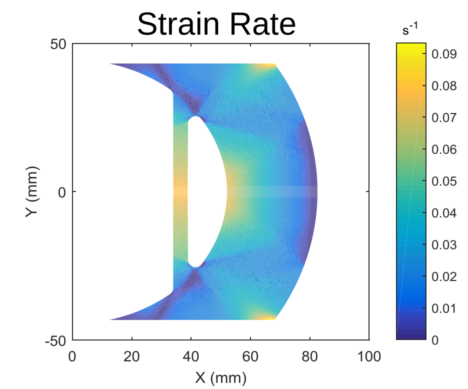

Validated FE models against experimental data – both global and full-field.

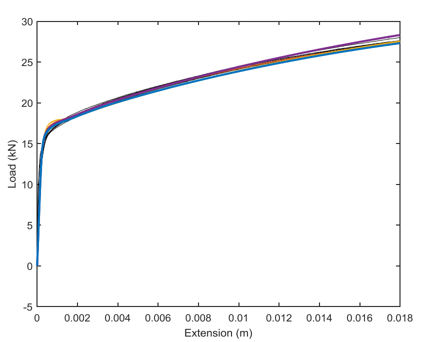

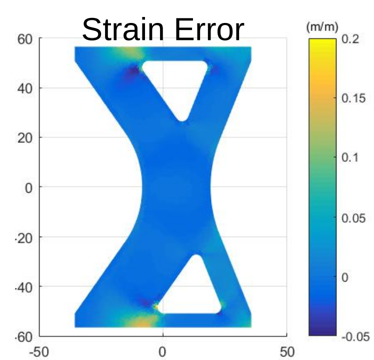

Determined that boundary conditions play a critical role in FE model validation.

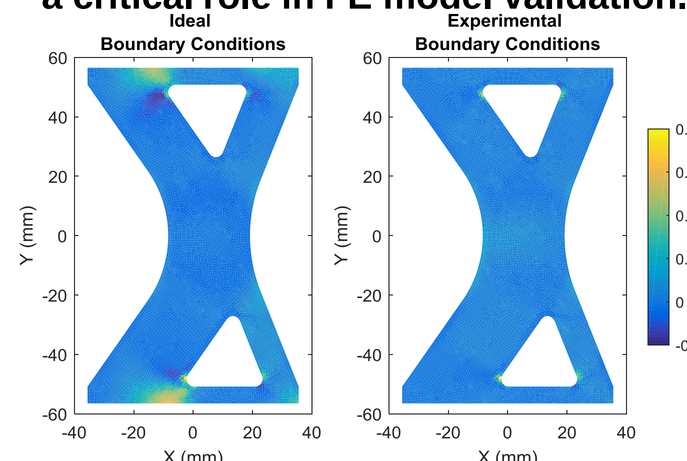

Much left to do

Near term:

- Investigate effect of sample-to-sample variation on VFM model calibration
- Explore other material models (Johnson-Cook)
- Include temperature dependence and anisotropy in material model

Long term:

- Optimize specimen geometry
- Understand implications of non-unique parameters
- Determine advantages/disadvantages of VFM compared to traditional techniques

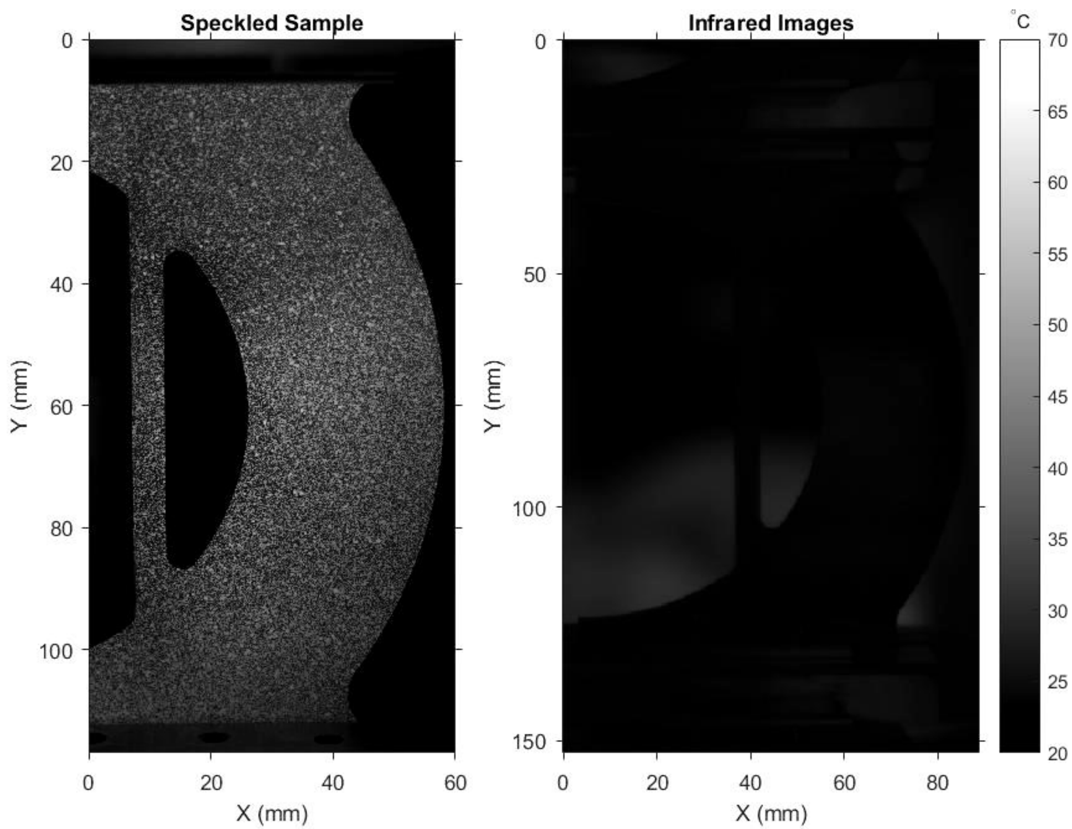

304L stainless steel sheet exhibits mild plastic anisotropy.

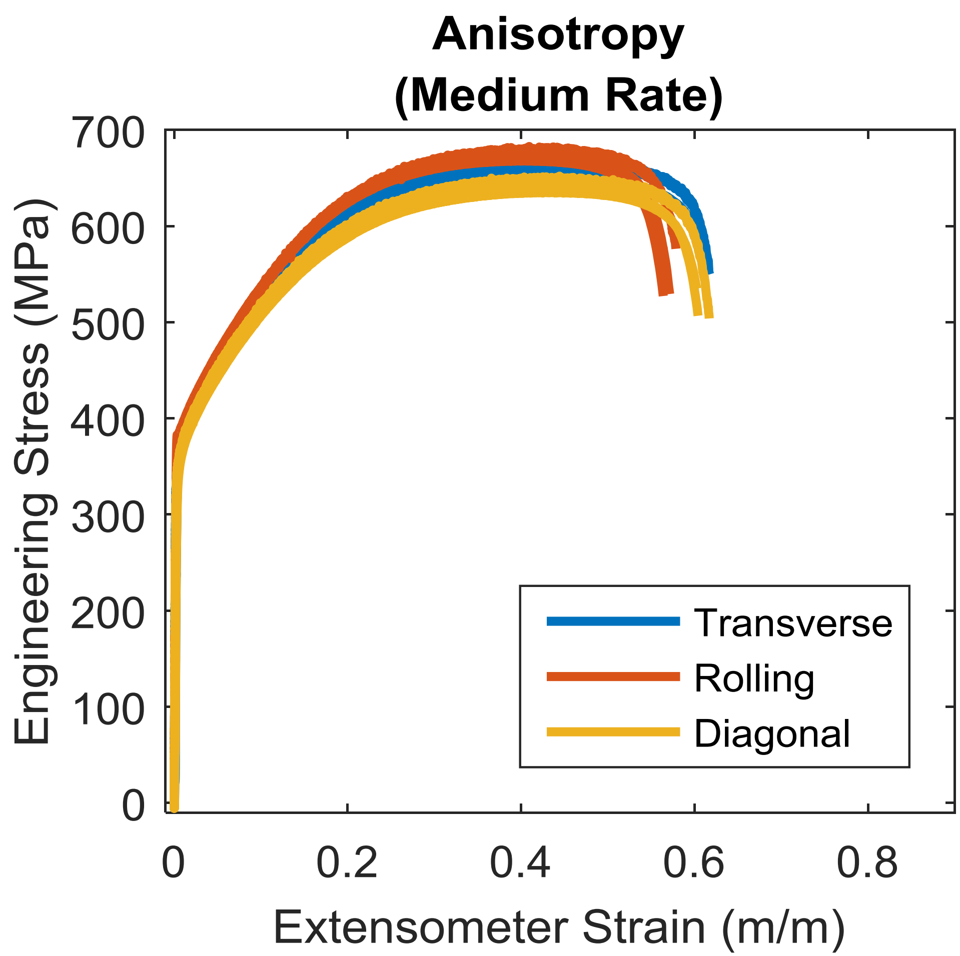

Thickness change must be measured or estimated.

- Internal power requires volume integral
- Plane stress assumption → area integral times sample thickness
- Thickness can be computed by:
  - Measuring with DIC on both sides of the sample
  - Assuming incompressible plasticity and calculating from in-plane strains

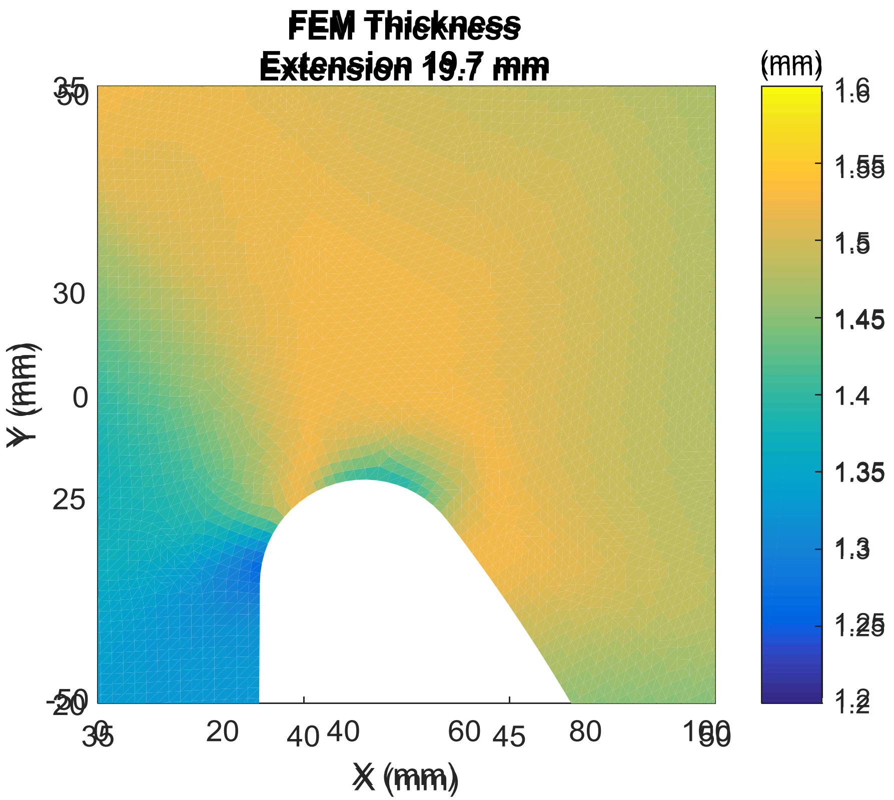

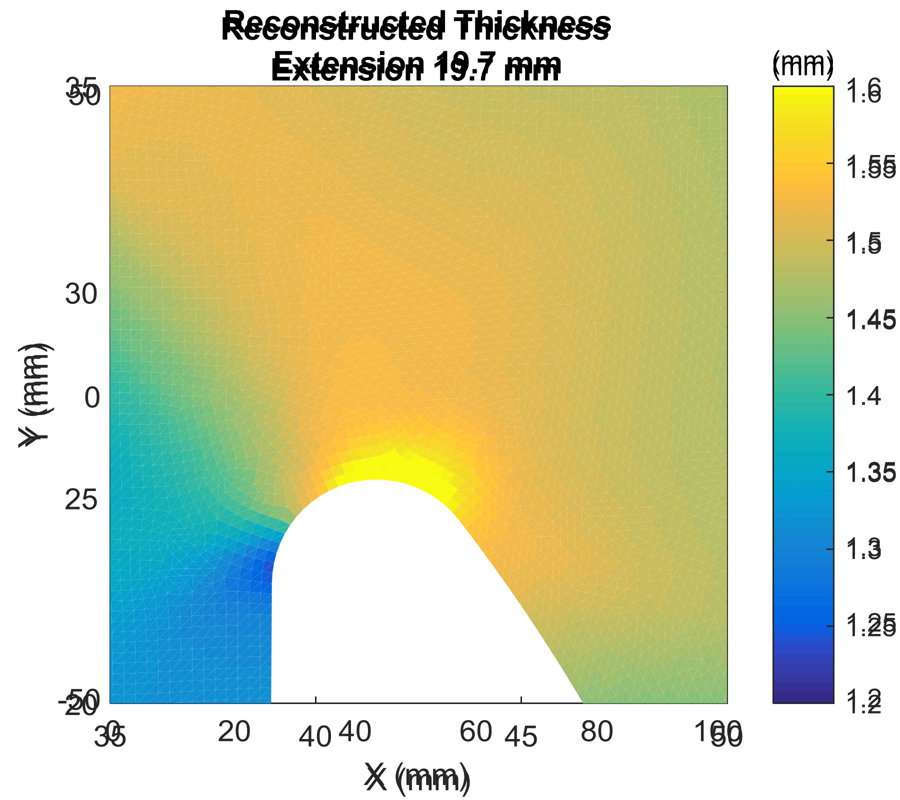

Accuracy of VFM algorithm quantified by error in internal vs. external power.

6 Cases

Increasing Realism for DIC
Decreasing Fidelity to FEA

1. FEA algorithms
2. Plane stress assumption; discrete volume integral approximation
3. Incompressible plasticity
4. Kinematics calculated from polynomial fit, with backward difference temporal derivative
5. Central difference temporal derivative

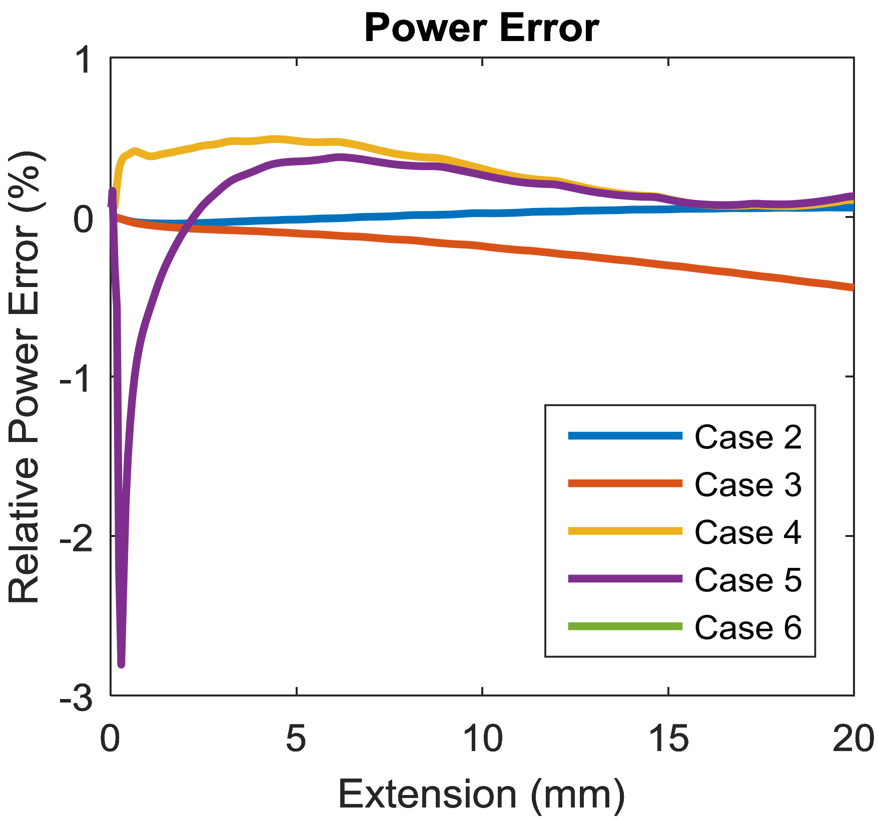

Stereo DIC simulator brings the simulated experiment one step closer to reality.

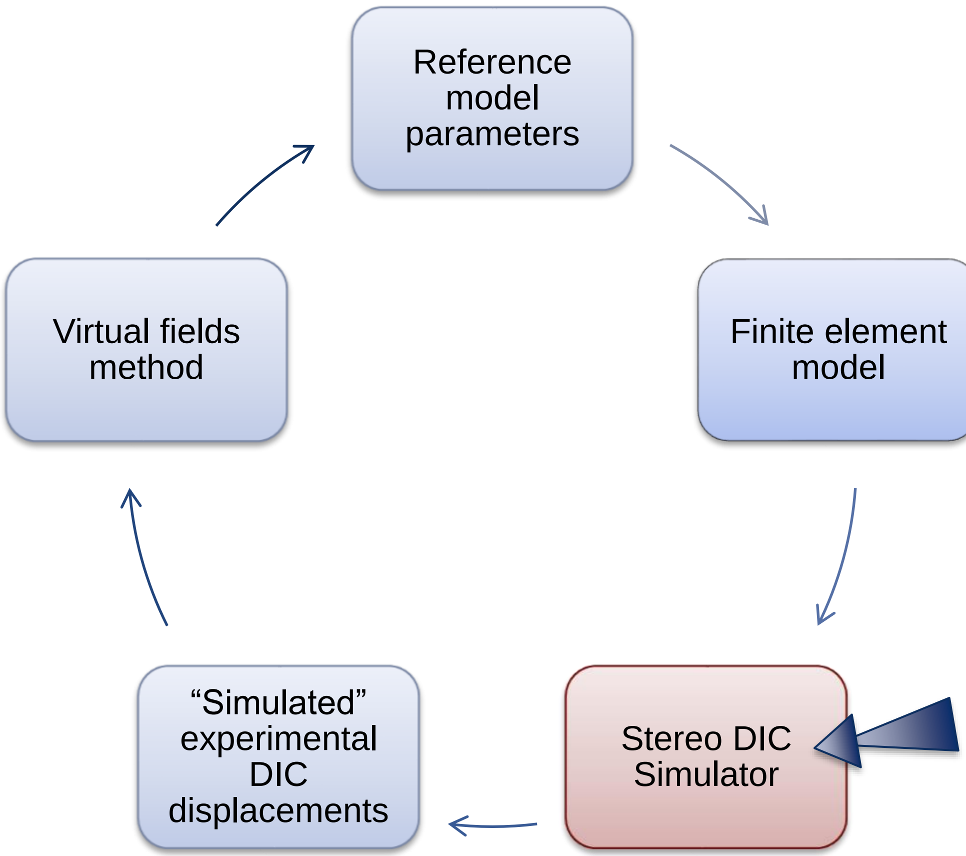

- Camera noise
- Matching error
- Spatial filtering
- Shape function
- Interpolation error

Collaboration with Ruben Balcaen at KU Leuven

Stereo DIC simulator brings the simulated experiment one step closer to reality.

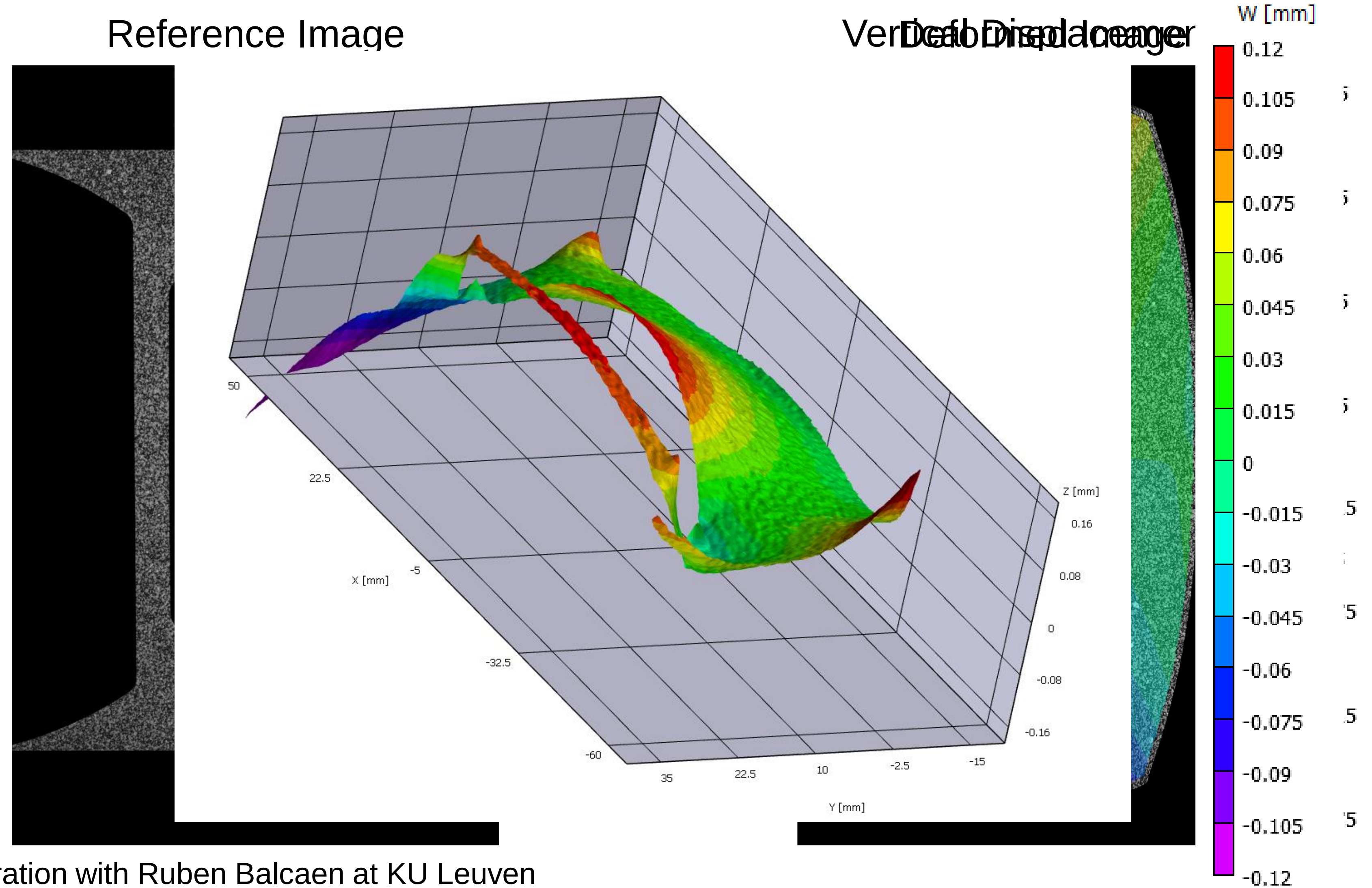

Collaboration with Ruben Balcaen at KU Leuven

Accuracy of VFM algorithm quantified by error in internal vs. external power.

Sandia National Laboratories

6 Cases

Increasing Realism for DIC
Decreasing Fidelity to FEA

1. FEA algorithms
2. Plane stress assumption; discrete volume integral approximation
3. Incompressible plasticity
4. Kinematics calculated from polynomial fit, with backward difference temporal derivative
5. Central difference temporal derivative
6. Simulated DIC images

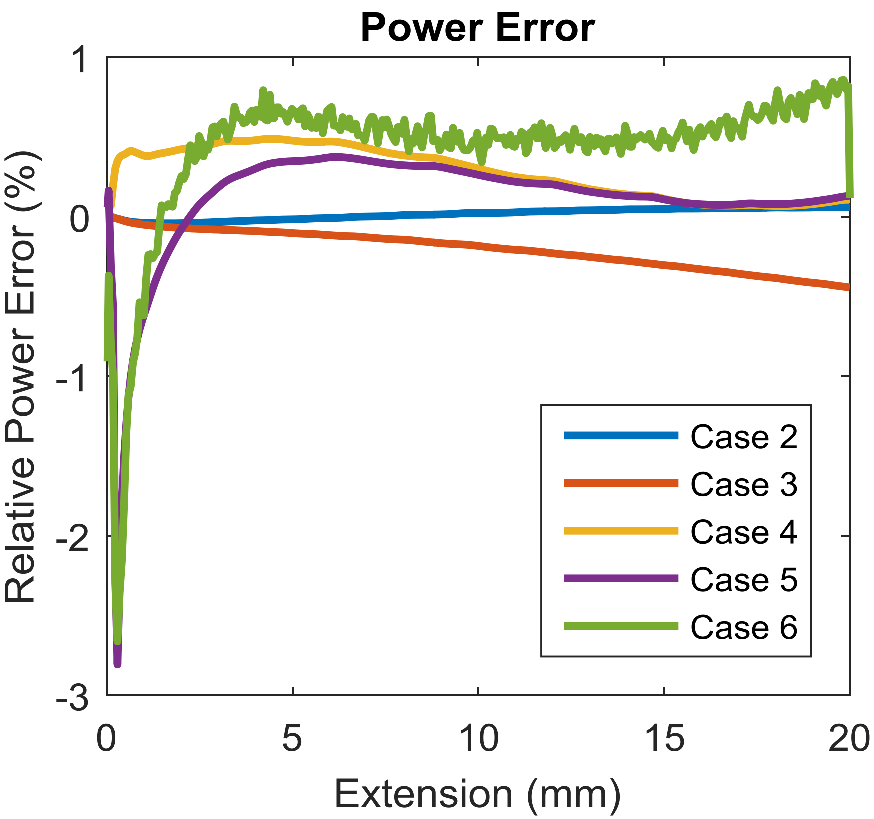

Simplified, 1D visualization of parameter effects

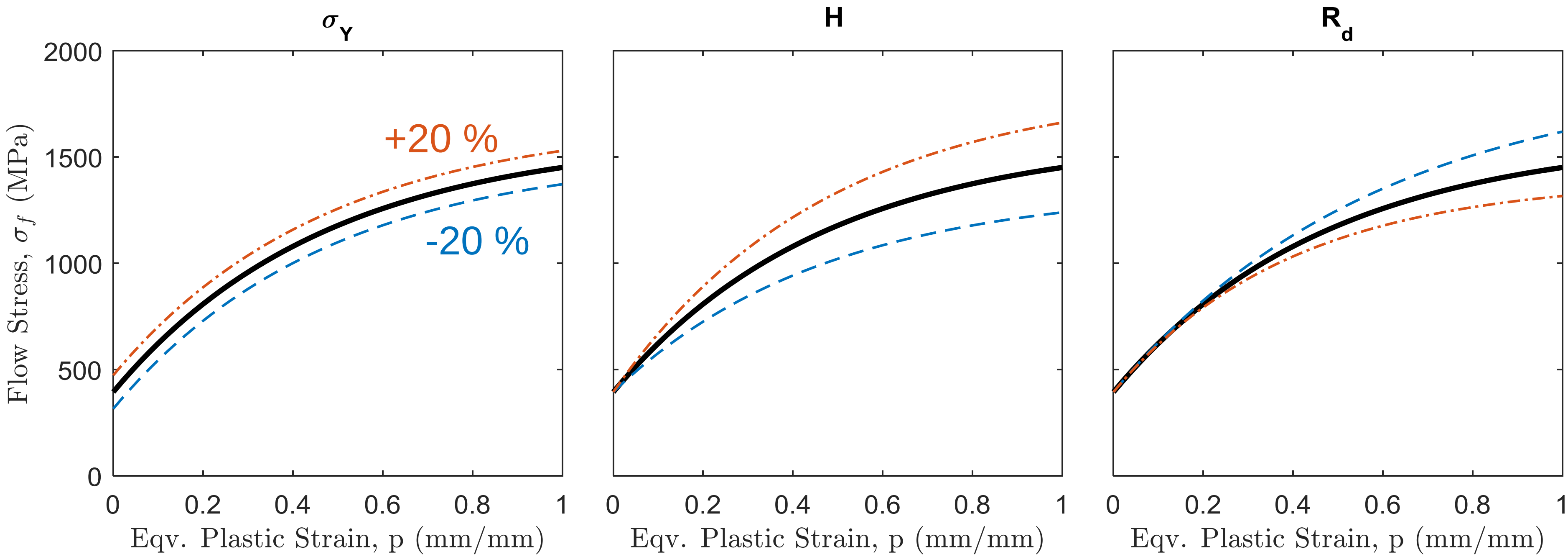

Constant strain rate, $\dot{p} = 10^{-1.5}$

Simplified, 1D visualization of parameter effects

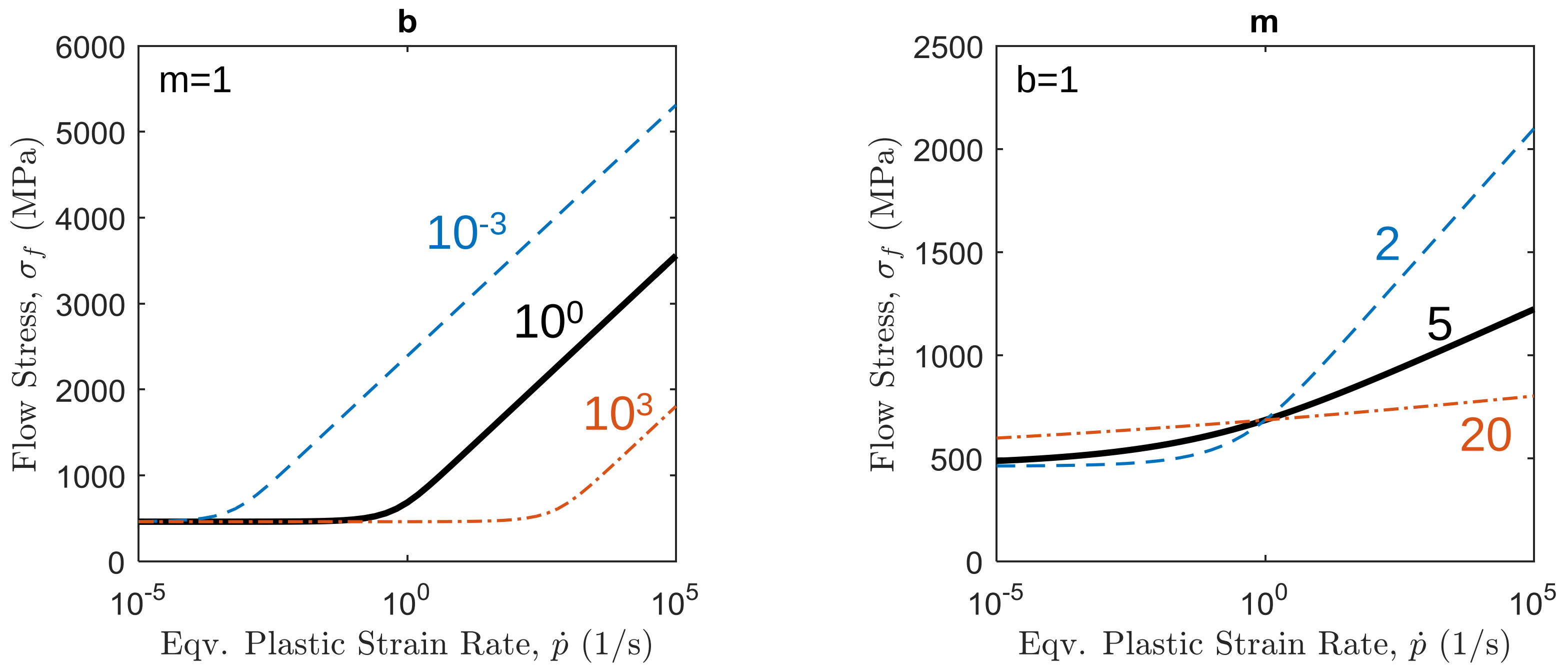

Constant strain, $\mathrm{p} = 0.09$

BCJ-MEM Material Model

- Von Mises Flow Criterion
  - Equivalent Stress: $\bar{\sigma} = \sqrt{\frac{3}{2} s : s} \quad \left(s = \sigma - \frac{1}{3}\mathrm{tr}(\sigma) I \right)$
  - Equivalent Plastic Strain Rate: $\dot{p} = \sqrt{\frac{2}{3} \dot{\varepsilon}^p : \dot{\varepsilon}^p}$
  - Flow Criterion: $f = \bar{\sigma} - \sigma_f = 0$

- Hardening Law
  - $\sigma_f(p, \dot{p}, \xi) = \sigma_o \left\{ 1 + \mathrm{asinh}\left[\left(\frac{\dot{p}}{b_\sigma} \right)^{1/m_\sigma} \right] \right\} + \kappa \left\{ 1 + \mathrm{asinh}\left[\left(\frac{\dot{p}}{b_\kappa} \right)^{1/m_\kappa} \right] \right\}$
  - $\dot{\kappa} = (H - R_d \kappa)\dot{p}$
    - Constant strain rate: $\kappa = \frac{H}{R_d}[1 - \exp(-R_d p)]$

VFM utilizes multi-axial calibration data and requires fewer tests than traditional calibrations.

$$\sigma = \mathrm{f}(\underbrace{\zeta(\varepsilon, p, \dot{p}, T)}_{\text{loading conditions}}, \xi\underbrace{(E, \upsilon, \sigma_o, H)}_{\text{model parameters}})$$

Techniques for Model Calibration (Material Characterization)

	Traditional	Advanced, Full-Field
Specimen Geometry	Tensile dog bones; torsion cylinders	Arbitrary
Type of Experimental Data	Global data → engineering stress and extensometer strain	Full-field data → DIC data over the entire specimen surface
Stress State	Uniaxial (tension only; shear only)	Multi-axial
Advantages	• Simple experiments • Data easier to interpret	• Loading conditions of calibration specimen reflect real-world • Reduced number of experiments
Disadvantages	• Uniaxial stress state does not reflect real-world conditions • Multiple experiments required to fit complex model	• Experiments more complicated • Data analysis more complicated

Parameter set is effectively not unique.

$$\text{Flow Stress Difference} = \frac{\sigma_f(p, \dot{p}, \xi_{\text{VFM}}) - \sigma_f(p, \dot{p}, \xi_{\text{traditional}})}{\sigma_f(p, \dot{p}, \xi_{\text{traditional}})}$$

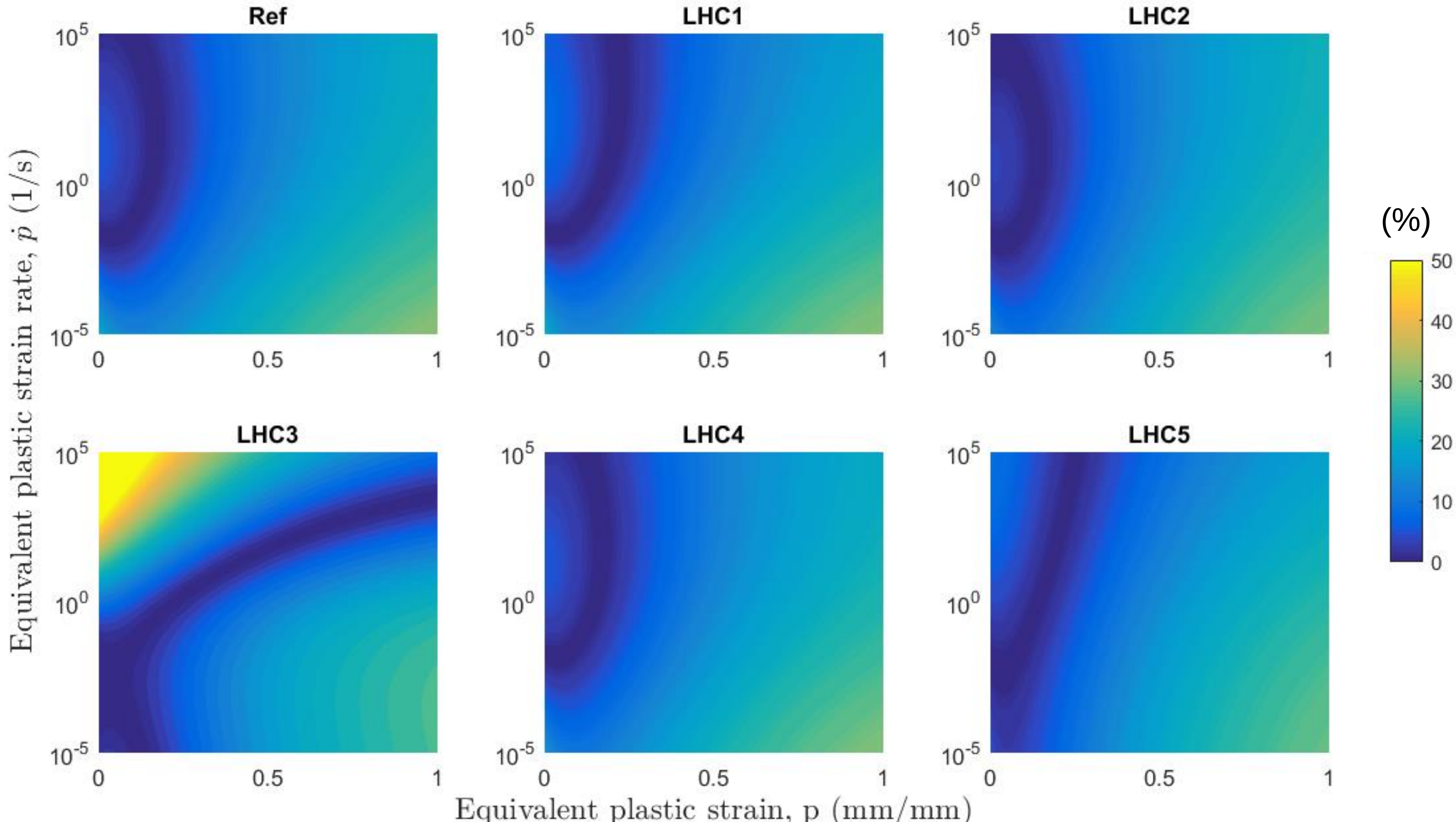

Backwards-difference strain rate approximation

Parameter set is effectively not unique.

$$\text{Flow Stress Difference} = \frac{\sigma_f(p, \dot{p}, \xi_{\text{VFM}}) - \sigma_f(p, \dot{p}, \xi_{\text{traditional}})}{\sigma_f(p, \dot{p}, \xi_{\text{traditional}})}$$

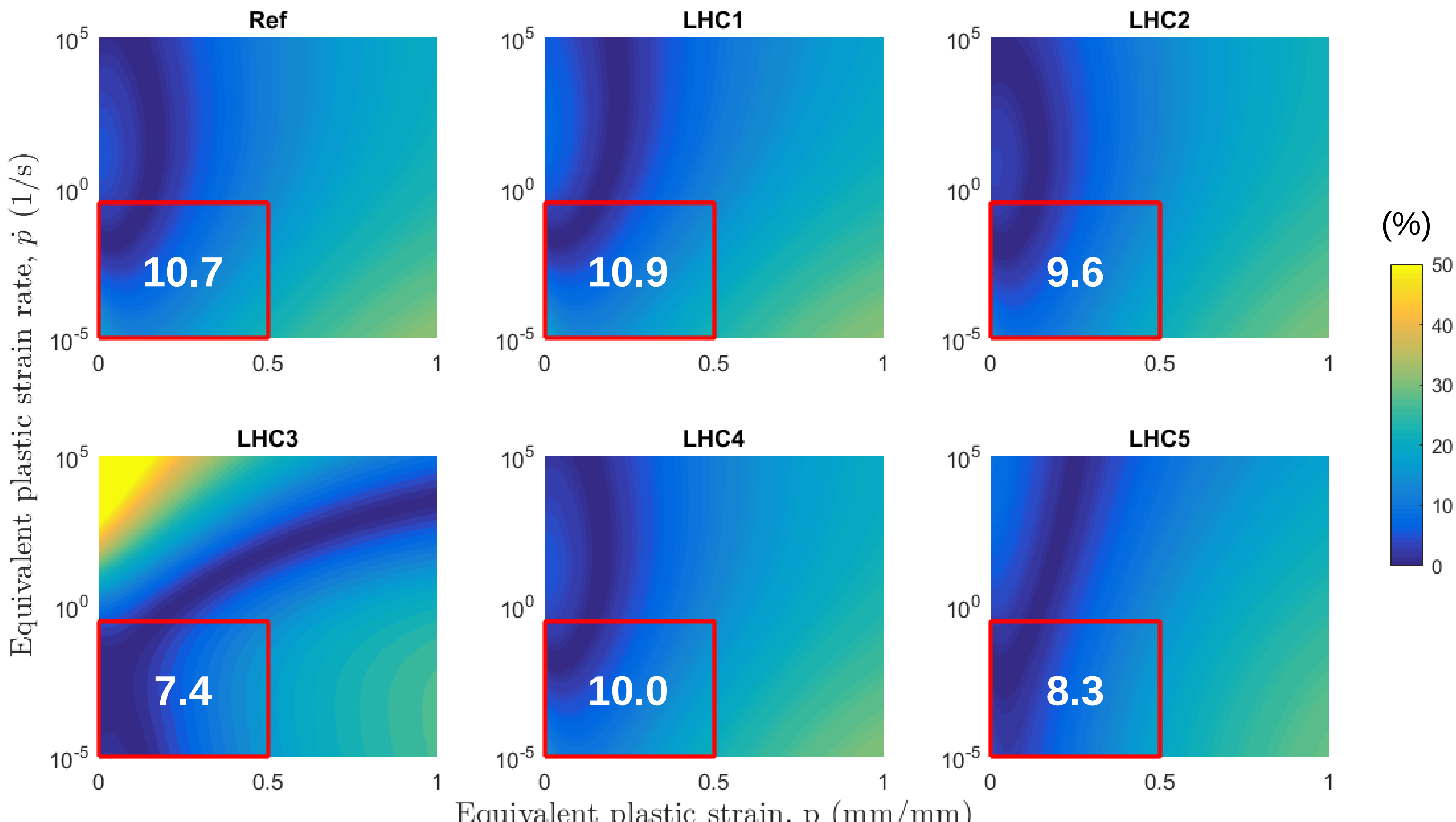

Backwards-difference strain rate approximation

Stereo DIC provides locations and displacements in three dimensions.

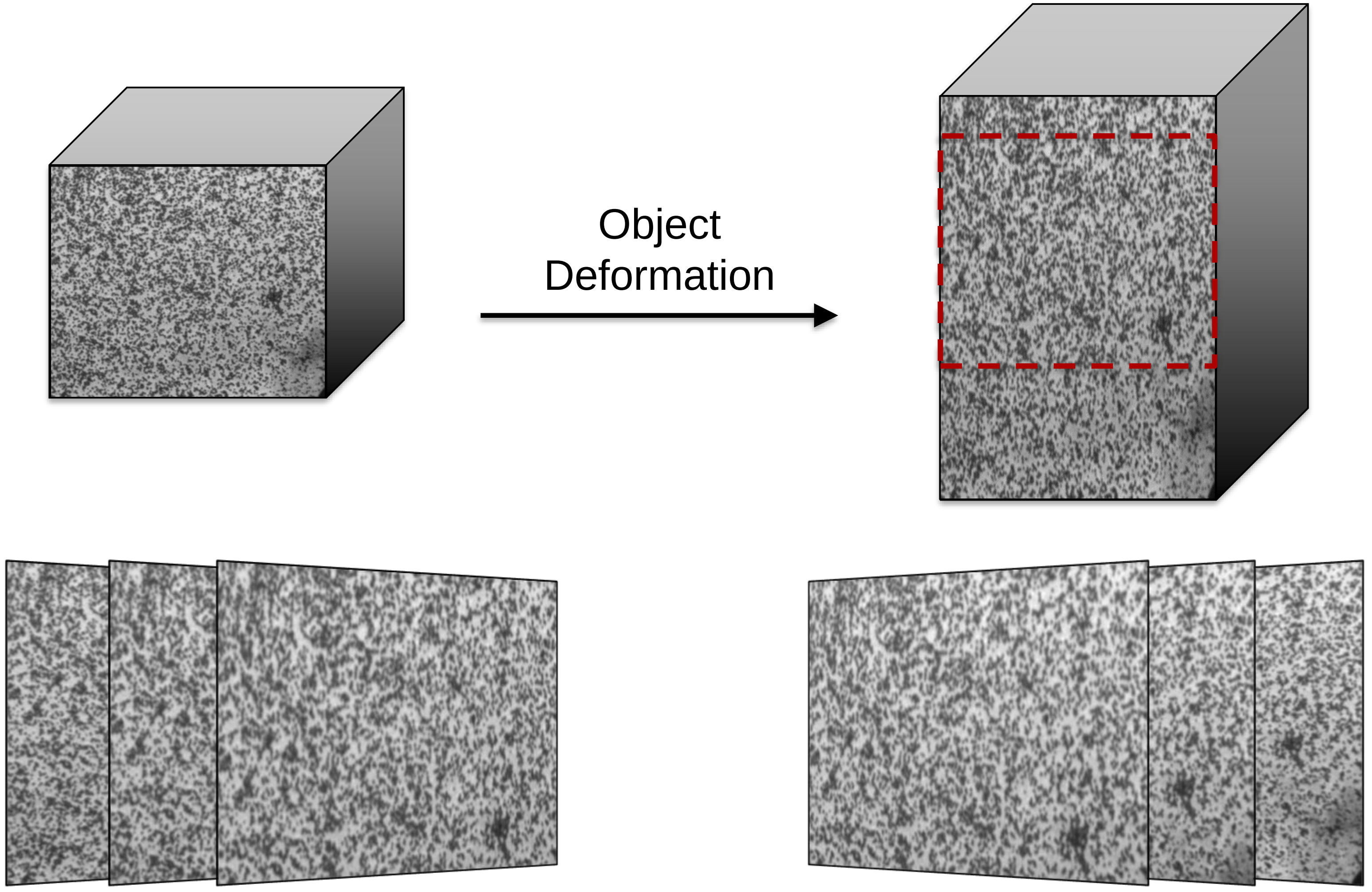

Complex specimen geometry induces stress and strain rate heterogeneity in sample.

Stress Distribution

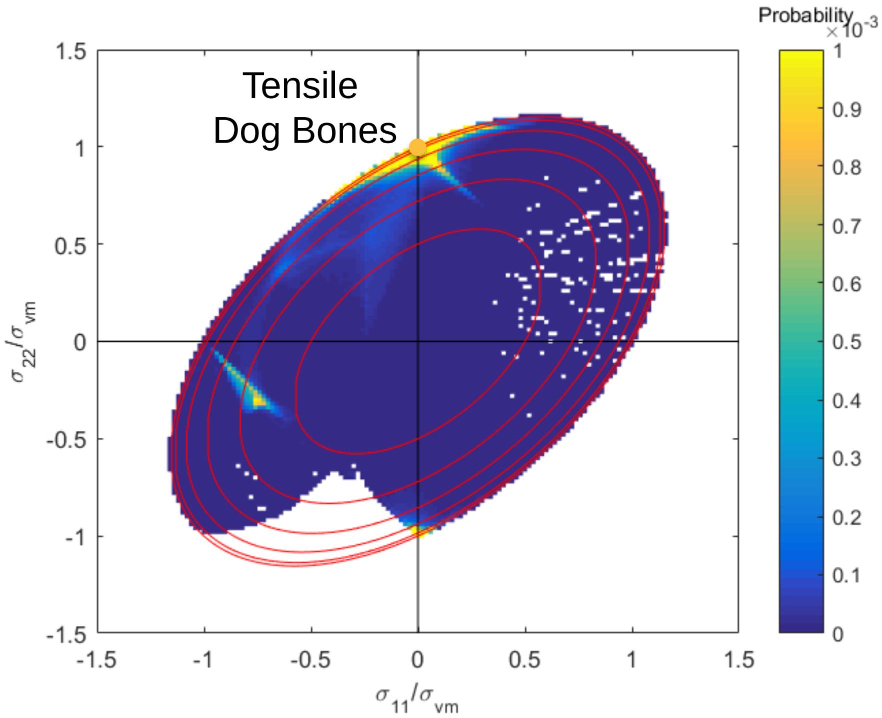

Strain/Strain Rate Distribution